

From the Institute of Medical Biochemistry and Molecular Biology

Directed by Prof. Elke Krüger

University Medicine of the University of Greifswald

**Functional characterisation of de novo mutations in the *PSMC5* gene carried by patients  
with the syndromic form of intellectual disability**

Inaugural - Dissertation

to

the attainment of the academic degree

**Doctor of Medicine**  
(Dr. med.)

of the

University Medicine

of the

University of Greifswald

2021

submitted by:

Anna Marta Hajdukowicz

born on the 26<sup>th</sup> October 1994

in Szczecin, Poland

Dean: Prof. Karlhans Endlich, PhD  
1. Reviewer: Prof. Angela Kaindl, PhD  
2. Reviewer: Prof. Elke Krüger, PhD  
Supervisor: PD Frédéric Ebstein, PhD  
Place: Greifswald, Germany  
Day of Disputation: 08.08.2022

*Vere scire est per causas scire*

## Table of Contents

Table of Contents .....	4
Abbreviations .....	6
List of Figures .....	9
List of Tables.....	10
Abstract .....	11
1. Introduction .....	13
1.1. The ubiquitin proteasome system (UPS).....	13
1.1.1. The structure of ubiquitin and its molecular functions .....	13
1.1.2. The ubiquitination pathway .....	14
1.1.3. The ubiquitin-proteasome system and its cellular functions.....	16
1.1.4. The structure of proteasome.....	16
1.1.5. The proteasome – its types and function.....	18
1.1.6. The proteasome activator PA28.....	20
1.2. Endoplasmic reticulum (ER) key quality control systems .....	20
1.2.1. Endoplasmic reticulum - associated degradation pathway (ERAD).....	21
1.2.2. Unfolded Protein Response (UPR) .....	23
1.3. TCF 11/Nrf1 and its role in the autoregulatory feedback mechanism of proteostasis .	27
1.4. The mTOR protein and its signalling pathway.....	28
1.5. Dysregulation of proteostasis and its clinical significance.....	30
1.5.1. Proteasome-Associated Autoinflammatory Syndromes (PRAAS).....	33
1.5.2. Neurodevelopmental syndromes .....	34
2. Aim of the Study.....	36
3. Materials and Methods .....	38
3.1. Materials .....	38
3.1.1. Chemicals.....	38
3.1.2. Enzymes .....	39
3.1.3. Kits .....	39
3.1.4. Primers .....	40
3.1.5. Buffers.....	40
3.1.6. Antibodies .....	42
3.2. Methods .....	47
3.2.1. Ethics statement .....	47
3.2.2. Sample preparation .....	48

3.2.3. Protein extraction and quantification for SDS-PAGE .....	48
3.2.4. Sodium dodecyl sulphate–polyacrylamide gel electrophoresis (SDS-PAGE) ...	48
3.2.5. Protein extraction and quantification for Native PAGE .....	50
3.2.6. Native polyacrylamide gel electrophoresis (Native PAGE) and proteasome in-plate peptidase activity assay.....	51
3.2.7. RNA isolation .....	52
3.2.8. cDNA synthesis through reverse transcription (RT) from RNA extracted from expanded T-cells.....	52
3.2.9. Real-Time Quantitative Polymerase Chain Reaction (RT-qPCR).....	53
3.2.10. Polymerase Chain Reaction (PCR) for XBP1 splicing and agarose gel electrophoresis .....	55
3.2.11. Data representation and statistical analysis .....	56
3.2.12. Flow cytometry (FCM) procedure.....	56
3.2.13. Flow cytometric analysis .....	58
4. Results .....	59
4.1. Clinical features of two subjects carrying <i>de novo</i> missense variants in the <i>PSMC5</i> gene and suffering from a syndromic form of ID .....	59
4.2. Impact of the identified <i>PSMC5</i> genomic alterations on proteasome function in patient T cells .....	62
4.3. Impact of the identified <i>PSMC5</i> variants on ER stress .....	65
4.4. Impact of the <i>PSMC5</i> variants on the TCF11/Nrf1 compensatory pathway.....	66
4.5. Impact of the <i>PSMC5</i> variants on the mTOR pathway .....	67
4.6. Impact of the <i>PSMC5</i> gene mutations on T cell subpopulations.....	68
5. Discussion.....	71
5.1. Patient T cells with <i>PSMC5</i> variants exhibit severe signs of proteasome dysfunction	71
5.2. <i>PSMC5</i> variants dysregulate mTORC1 signalling in patient T cells .....	71
5.3. Both <i>PSMC5</i> variants promote receptor-mediated mitophagy in patient T cells.....	73
5.4. <i>PSMC5</i> gene mutations in the context of interferonopathies .....	74
5.5. Conclusion and outlook.....	76
6. Bibliography .....	79
Affidavit .....	91
Curriculum Vitae.....	92
Acknowledgments .....	94

## Abbreviations

4E-BP1	eukaryotic initiation factor 4E (eIF4E)-binding protein 1	CNS	central nervous system
AAA+	ATPases associated with various cellular activities	CP	20S proteasome core particle
AD	Alzheimer's disease	CRE	cAMP responsive element
ADHD	attention-deficit hyperactivity disorder	CREB	cyclic AMP responsive element binding protein
AMPK	AMP-activated protein kinase	CRP	C-reactive protein
APC	allophycocyanin	DC	dendritic cells
APS	ammonium persulfate	DDI2	DNA Damage Inducible 1 Homolog 2
ARE	antioxidant response elements	DGV	Database of Genomic Variants
ASD	autism spectrum disorder	dH <sub>2</sub> O	distilled /deionized water
ATF	activating transcription factor	DMSO	dimethyl sulfoxide
ATP	adenosine triphosphate	DN	double negative [T cells]
BCA	bicinchoninic acid	DNA	deoxyribonucleic acid
BiP	binding immunoglobulin protein	DNMs	de novo mutations
bp	base pair	dNTP	deoxyribonucleoside triphosphate
BPF	bandpass filter	(D)PBS	(Dulbecco's) Phosphate-Buffered Saline
BSA	bovine serum albumin	DQ	digital intelligence quotient
BTZ	bortezomib	DTT	dithiothreitol
b-ZIP	basic region-leucine zipper	DUBs	deubiquitinating enzymes
CANDLE	chronic atypical neutrophilic dermatosis with lipodystrophy and elevated temperature	E1	ubiquitin-activating enzyme
CD	cluster of differentiation	E2	ubiquitin-conjugating enzyme
CDKs	cyclin-dependent kinases	E3	ubiquitin-protein ligase
cDNA	complementary deoxyribonucleic acid	EDTA	ethylenediaminetetraacetic acid
C/EBP	CCAAT-enhancer-binding protein	eEF2K	eukaryotic elongation factor 2 kinase
CHOP	transcriptional factor C/EBP homologous protein	eIF2 $\alpha$	eukaryotic translation initiation factor-2
		eIF4E	eukaryotic initiation factor 4E

ER	endoplasmic reticulum	LOF	loss-of-function
ERAD	endoplasmic reticulum associated degradation	MHC	major histocompatibility complex
ESR	erythrocyte sedimentation rate	MHC I	major histocompatibility complex class I
FACS	fluorescence-activated cell sorting (TM), syn. FCM	MHC II	major histocompatibility complex class II
FC	fold change	mM	milli molar
FCM	flow cytometry	MOM	mitochondrial outer membrane
FMO	fluorescence minus one	mtDNA	mitochondrial deoxyribonucleic acid
FSC	forward scatter	mTOR	mammalian target of rapamycin
GADD34	growth arrest and DNA damage-inducible protein 34	mTORC	mTOR complex
GRP94	glucose-regulated protein 94	n/a	not applicable
GWASs	genome-wide association studies	NC	nitrocellulose
h	hour	ND	not determined
HIF-1 $\alpha$	hypoxia-inducible transcription factor 1 $\alpha$	NDDs	neurodevelopmental disorders
HO-1	haem oxygenase 1	NGS	next generation sequencing
HPRT1	hypoxanthine phosphoribosyltransferase 1	NI	not indicated
HRP	horse radish peroxidase	NIR	near infrared fluorescence
ID	intellectual disability	NIX	NIP3-like protein X
IFI	Interferon Alpha Inducible Protein /Coding Gene	NPP	naphthyl pyridyl pyrazole
IFN	interferon	OFC	occipital frontal circumference
IgG	immunoglobulin G	OMIM	Online Mendelian Inheritance in Man
IL	interleukin	OPTN	optineurin
iPSC	induced-pluripotent stem cells	PA	phosphatidic acid
IRE1	inositol requiring enzyme 1	PAC	proteasome assembly chaperone proteins
IRF	interferon regulatory factor	PAHs	polycyclic aromatic hydrocarbons
ISGs	IFN-stimulated genes	PB	peripheral blood
ISR	integrated stress response	PBDEs	polybrominated diphenyl ethers
JAK	Janus kinase		
LBD	Lewy-body dementia		
LIR	LC3 interacting region		

PBMCs	peripheral blood mononuclear cells	S1P	site-1 protease
PBS	phosphate-buffered saline	S2P	site-2 protease
PBST	phosphate-buffered saline with Tween 20	S6K1	S6 kinase 1
PCBs	polychlorinated biphenyls	SCZ	schizophrenia
PCR	polymerase chain reaction	SD	standard deviation
PD	Parkinson's disease	SDS	sodium dodecyl sulphate
PDI	protein disulphide - isomerase	SDS-PAGE	sodium dodecyl sulphate–polyacrylamide gel electrophoresis
PERK	protein endoplasmic reticulum RNA-like kinase	SNPs	single nucleotide polymorphism
PHA	phytohemagglutinin	SREBP	sterol response element binding protein
PI3K	phospho-inositide 3-kinase	SSC	side scatter
PINK 1	PTEN-induced kinase 1	sXBP1	spliced X-box binding protein 1
PNG	peptide N-glycosidase	TAE	Tris base, acetic acid, EDTA
POMP	proteasome maturation protein	TBST	mixture of tris-buffered saline (TBS) and Tween 20
PPAR $\gamma$	peroxisome proliferator-activated receptor- $\gamma$	TCR	T-cell antigen receptor
PRAAS	proteasome-associated autoinflammatory syndromes	TEMED	tetramethylethylenediamine
PVDF	polyvinylidene fluoride	TF	transcription factor
Rictor	rapamycin-insensitive companion of mTOR	TNF	tumour necrosis factor
RIDD	regulated IRE1-dependent decay	TSC	tuberous sclerosis complex
RNase	ribonuclease	Ub	ubiquitin
ROS	reactive oxygen species	uORF1	upstream Open Reading Frame
RP	19S proteasome regulatory particle	UPR	unfolded protein response
rpm	rounds per minute	UPS	ubiquitin - proteasome system
Rpn	regulatory particle of non-ATPase	uXBP1	unspliced X-box binding protein 1
Rpt	regulatory particle of triple-ATPase	VCP	valosin-containing protein
RT	room temperature	v/v	volume per volume
RT-qPCR	real-time quantitative polymerase chain reaction	w/v	weight per volume
		XBP 1	X-box binding protein 1



## List of Figures

Figure 1. Molecular structure of ubiquitin with the highlight on its secondary structure.....	14
Figure 2. The ubiquitination pathway .....	15
Figure 3. The structure of the 30S proteasome .....	17
Figure 4. The structure of the proteasome and the main functions of its subunits.....	19
Figure 5. Two key ER quality control systems in mammals .....	21
Figure 6. Key steps in ERAD.....	22
Figure 7. Branches of the UPR.....	24
Figure 8. TCF11/Nrf1 and its role in the autoregulatory feedback loop of proteostasis.....	28
Figure 9. mTOR signalling pathway .....	30
Figure 10. Schematic depiction of the proteasome subunits affected by pathogenic loss-of-function mutations.....	32
Figure 11. Example of a TruCount image.....	57
Figure 12. The standardized procedure conducted at the beginning of each data analysis.....	58
Figure 13. Identification of two <i>PSMC5</i> variants in two unrelated subjects with a syndromic form of ID.....	59
Figure 14. Subjects carrying <i>PSMC5</i> variants exhibit no major changes in proteasome subunit expression and/or composition.....	63
Figure 15. <i>PSMC5</i> variants cause proteasome assembly defects in patients with a syndromic form of ID.....	64
Figure 16. Subjects with a syndromic form of ID carrying <i>PSMC5</i> variants exhibit reduced proteasome chymotrypsin-like activity .....	65
Figure 17. Subjects carrying <i>PSMC5</i> variants exhibit no obvious signs of ER stress .....	66
Figure 18. Subjects carrying <i>PSMC5</i> variants express higher levels of NGLY1 which do not result in increased TCF11/Nrf1 processing.....	67
Figure 19. <i>PSMC5</i> variants exhibit distinct effects on mTORC1 signalling and autophagy/ mitophagy.....	68
Figure 20. The p.(Pro320Arg) <i>PSMC5</i> variant alters T cell subpopulations in Subject 1 .....	69
Figure 21. The p.(Arg201Trp) <i>PSMC5</i> variant alters T cell subpopulations in Subject 2.....	70
Figure 22. The <i>PSMC5</i> variants augment the frequency of CD4/CD8-double negative (DN) T cells .....	70

## List of Tables

Table 1. Summary of the genetic and clinical features of two <i>PSMC5</i> variants.....	62
---	----

## Abstract

Despite the extensive ongoing research, there still exist plenty of diseases whose mechanisms have not yet been fully understood, one such example being proteasome-related disorders. Over the last few years, an increasing number of studies have been initiated to elucidate their driving pathophysiological mechanisms. Determining the systematic effects of genomic alterations occurring in genes encoding 19S proteasome subunits is a key to comprehend the molecular basis of syndromic intellectual disability (ID) pathogenesis and the subsequent design of new targeted therapies. Therefore, the main objective of my research was to contribute to the identification of potential drivers of syndromic ID, and thereby pave the way for the development of new targeted therapy approaches. In this regard, my aim was to characterize tissue, proteomic and metabolomic changes in cells from patients with *PSMC5* mutations and uncover a potential dysregulation of various biochemical and/or inflammatory pathways.

To this end, I undertook a comparative examination of control and patient T cells expanded from peripheral blood mononuclear cells (PBMCs). First, I assessed the proteasome composition in these samples (both in its denatured and native form), by means of SDS-PAGE, native PAGE and western-blotting. Moreover, I determined proteasome chymotrypsin-like activity by measure of Suc-LLVY-AMC peptidase activity assay. In addition, I analysed the activation status of the ER stress and mTOR pathway by RT-PCR and SDS-PAGE /western-blotting prior to a subsequent analysis of T-cell markers.

The data show that the investigated p.(Pro320Arg) and p.(Arg201Trp) *de novo* heterozygous missense mutations in the *PSMC5* gene do not cause haploinsufficiency as the steady-state expression level of the PSMC5/Rpt6 full-length protein does not vary between control and patient cells. Further analysis of control and patient T cells under non-reducing conditions revealed that PSMC5/Rpt6 mutants were less efficiently incorporated into 26S proteasome complexes than their wild-type counterparts. The failure to assemble PSMC5/Rpt6 into fully mature proteasomes was associated with a reduced proteasome chymotrypsin-like activity in patient T cells, as determined by in-plate assays. These data unambiguously demonstrate that both of the p.(Pro320Arg) and p.(Arg201Trp) *PSMC5* mutations identified in patients suffering from syndromic ID are loss-of-function mutations. Interestingly, my data further show that proteasome dysfunction in these patients was accompanied by abnormalities in mTOR

signalling and T-cell differentiation, as determined by western-blotting and flow cytometry, respectively.

Altogether, our data identified for the first time *PSMC5* as a disease-causing gene for a syndromic form of ID. How proteasome dysfunction caused by *PSMC5* variants contributes to disease pathogenesis, remains to be fully determined.

## 1. Introduction

### 1.1. The ubiquitin proteasome system (UPS)

#### 1.1.1. The structure of ubiquitin and its molecular functions

Ubiquitin is a small highly conserved ubiquitously expressed protein present in all tissues and eukaryotic cells, hence its name [1; 2; 3]. It is synthesized as a precursor protein comprising multiple ubiquitin moieties in tandem or a single ubiquitin fused to an unrelated protein and needs to undergo proteolytic processing to produce a mature 76-amino acid-long molecule that folds properly to form a compact globular structure [4], symbolically depicted in **Figure 1**.

Ubiquitin chains may have a variety of different functions depending on how the ubiquitin monomers forming the chains are linked with each other. Specifically, the topology and length of polyubiquitin chains determine the fate of the modified protein. The ubiquitin molecule contains seven internal lysine residues (symbolised by Lys or K): Lys6, Lys11, Lys27, Lys29, Lys33, Lys48 or Lys63 (**Figure 1**), which forms an isopeptide bond with the carboxy-terminal glycine, thereby generating ubiquitin chains [5]. However, only polyubiquitination on particular lysine residues, mostly K48 and K29, signifies degradation by the UPS, and is even referred to as the molecular kiss of death. Moreover, it is known that a minimum of four ubiquitin moieties (forming the tetraubiquitin chain) are required to provide efficient proteasomal degradation [6]. Ubiquitination on other lysine residues (e.g. on K63, K11, K6) or on the N-terminal methionine of the previous ubiquitin molecule (M1) may have non-proteolytic functions and is involved in the regulation of cellular processes such as endocytic trafficking, inflammation, translation and DNA repair [7; 8; 9]. The role of ubiquitin linkages through K6, K11, K27, K29 and K33 is less understood, but recent evidence suggests that these may be associated with DNA repair [10; 11; 12; 13], human cell cycle control [14], DNA damage response and innate immunity [15; 16], and regulation of both T-cell antigen receptor (TCR) and AMP-activated protein kinase (AMPK)-related protein kinases [17; 18; 19], embryogenesis as well as tumorigenesis and manifold other diseases [20]. Linear M1-linked ubiquitin chains constitute a key regulator in cytokine signalling and play pivotal roles in inflammatory and immune responses by regulating the activation of the transcription factor NF- $\kappa$ B [21; 22; 23]. Altogether, the vast number and variety of functions makes it increasingly clear that different ubiquitin linkages convey different information to the cell and are involved in numerous processes.

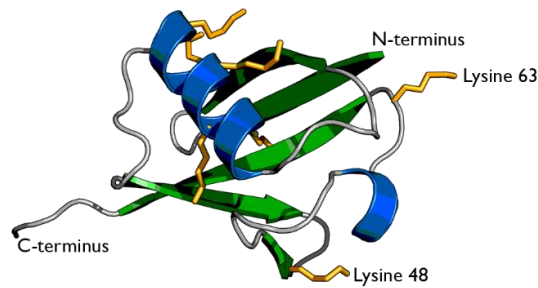


**Figure 1. Molecular structure of ubiquitin with the highlight on its secondary structure.**  $\alpha$ -helices are coloured in blue and  $\beta$ -strands in green. Orange sticks depict the sidechains of the 7 lysine residues. The two best-characterised attachment points for further ubiquitin molecules in polyubiquitin chain formation (Lys 48 & Lys 63) are labelled.

Credits to: Rogerdodd, <https://commons.wikimedia.org/w/index.php?curid=4771409>.

### 1.1.2. The ubiquitination pathway

The functional versatility of ubiquitin resides in its ability to covalently mark target proteins or itself to generate polyubiquitin chains. Both processes are multistep reactions that require the sequential action of three ubiquitin enzymes known as ubiquitin-activating enzyme (E1), ubiquitin-conjugating enzyme (E2), and ubiquitin-protein ligase (E3). The enzymatic cascade of ubiquitination begins with the ATP-dependent activation of ubiquitin by the E1 and the formation of an E1-ubiquitin thioester. After that, ubiquitin is transferred from the E1 to the E2, where it binds to the active site cysteine of E2, forming an E2-ubiquitin thioester-linked intermediate. Finally, transfer of ubiquitin from the E2 usually to an internal lysine (K) residue on the target protein is mediated by E3 enzymes which attach its C-terminal carboxyl group (Gly76) via an isopeptide bond to the substrate. The above described process is depicted in **Figure 2**.

The ubiquitination of target proteins is a reversible and dynamic process. Ubiquitin molecules can be removed from the modified proteins, a process facilitated by deubiquitinating enzymes (DUBs), specific cysteine proteases and (more seldom) metalloproteases that hydrolyse the isopeptide bond between the ubiquitin C-terminus and the amino group of the lysine residues [5]. DUBs are able to protect proteins from degradation, by removing the ubiquitin chain from the substrate, or in case of proteasome-associated DUBs, enable degradation events as they cleave precursor proteins to produce mature ubiquitin molecules and release ubiquitin moieties

from free or unanchored polyubiquitin chains [24; 25]. They determine neuronal cell fate, synaptic plasticity, axonal growth, and thereby proper function of the nervous system [26]. DUBs are also part of the ubiquitin-conjugation system, and through cleavage and recycling of ubiquitin ensure a certain level of free ubiquitin in the cell that is required for rapid adjustment to changes within the cellular environment [27; 28].

The specificity and selectivity of the ubiquitin-conjugation system is determined by two distinct and unrelated groups of proteins: (1) E3s and (2) ancillary proteins such as molecular chaperones that act as recognition elements and serve as a link to the appropriate ligase [29].

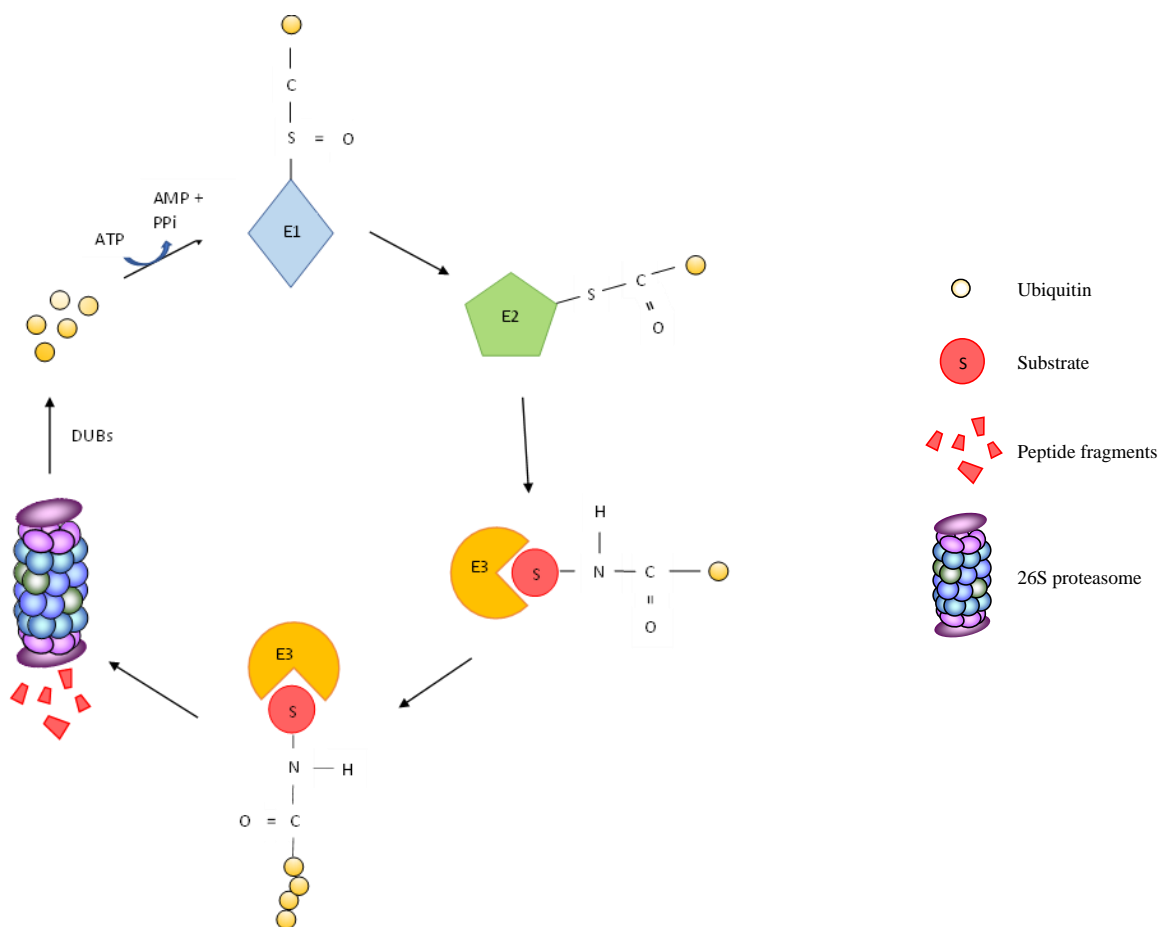


**Figure 2. The ubiquitination pathway.** In the first step ubiquitin is activated by the E1 enzyme in an ATP-dependent manner and forms an E1-ubiquitin thioester. In the second step, it is transferred from the E1 to the E2, where it binds to the active site cysteine of E2, forming an E2-ubiquitin thioester-linked intermediate. In the final step, it is transferred from the E2 usually to an internal lysine (K) residue on the target protein, a process mediated by the E3 which attaches its C-terminal carboxyl group (Gly76) via an isopeptide bond to the substrate. Next, ubiquitin particles can be attached forming the polyubiquitin chains. DUBs can remove the ubiquitin particles, ensuring the reversibility of the process.

### **1.1.3. The ubiquitin-proteasome system and its cellular functions**

The ubiquitin-proteasome system (UPS) plays an essential role in the maintenance of proteostasis in eukaryotes, as it secures degradation of most short-lived intracellular proteins. Responsible also for the quality control, it ensures that misfolded or aberrant proteins which may originate directly from defective mRNAs in the cytoplasm, as well as nascent polypeptides, do not accumulate nor aggregate inside of the cell [30]. Proteins destined for destruction, including regulatory, misfolded or oxidized ones, are typically labelled with K48-linked ubiquitin chains, making them targets for degradation by the 26S proteasome [31], a function that may be influenced by the regulatory complexes PA28 and PA200. Controlling the vast numbers of intracellular regulators, including I $\kappa$ B or IRF3, both standard and immunoproteasomes are actively involved in the regulation of numerous signalling pathways, such as mTOR, the unfolded protein response (UPR) and innate and adaptive immune response.

Beside proteostasis, the UPS performs regulatory functions, including cell cycle regulation through the modification of the cyclins' levels – regulatory proteins responsible for cell cycle progression [32]. While degradation of cell cycle mediators warrants proliferation, the UPS is also involved in the programmed and strictly-controlled cell death known as apoptosis via degradation of key regulatory proteins. Though various apoptotic pathways can be targeted by the UPS, it is the p53 protein that plays the crucial role both as a cell fate regulator and a tumour suppressor, a function revealed by the growing number of discovered E3s responsible for its proteasomal degradation or functional regulation [33]. Other remarkable anchor point is the NF- $\kappa$ B family of transcription factors, especially because of proteasome's involvement in activation of the inhibitory I $\kappa$ B kinase and processing of the NF- $\kappa$ B-precursor [34]. The list of cellular proteins that are targeted by ubiquitin is still expanding [29]. Altogether, the UPS holds a vast number of essential tasks, providing proteostasis and playing a major mechanistic role in regulating cell proliferation as well as cell death, and therefore constituting a prerequisite for cell viability, integrity, and proper functioning.

### **1.1.4. The structure of proteasome**

Mammalian 26S proteasome is a barrel-shaped hollow structure that consists of one 20S core particle (CP), inside of which proteins undergo degradation, and one or two 19S regulatory particles (RP) which contain multiple ATPase active sites and ubiquitin binding sites,



recognizing polyubiquitinated proteins, catalysing their deubiquitination and unfolding, before their translocation into the catalytic core [35; 36]. Since the proteolytic active sites reside in the inner chamber, and its cylindrical form allows only unfolded and threaded proteins to enter through the narrow axial pores, high substrate specificity and selectivity can be guaranteed. Dependent on configuration, it forms either a 19S-20S or 19S-20S-19S structure, creating a 26S and 30S proteasome, respectively, both commonly referred to as 26S proteasome [37]. The structure of the 30S proteasome is schematically illustrated in **Figure 3**.

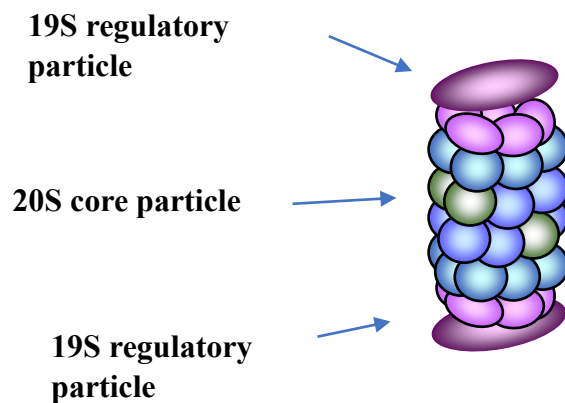


**Figure 3. The structure of the 30S proteasome.** A cylinder – shaped 20S core is made of four hetero-heptameric rings creating a 28-subunit  $\alpha 1-7-\beta 1-7-\beta 1-7-\alpha 1-7$  conformation. It is capped on both sides with 19S regulatory particles, each of them comprised of 2 subcomplexes, called the base and the cap.

The 20S CP is composed of four hetero-heptameric rings, of which the two outer ones are formed by  $\alpha$ -subunits ( $\alpha 1-\alpha 7$ ) and the inner ones by  $\beta$ -subunits ( $\beta 1-\beta 7$ ), creating a 28-subunit  $\alpha 1-7-\beta 1-7-\beta 1-7-\alpha 1-7$  conformation. Each of the monomers is encoded by a distinct gene [31]. The proteasome assembly starts with the synthesis of  $\alpha$  and  $\beta$  subunits, followed by the maturation of the proteasome through the assembly of the  $\alpha$ -rings, facilitated by proteasome assembly chaperone proteins (PAC1-PAC4) in the cytoplasm [38; 39]. After that, the  $\alpha$ -ring is targeted and bound to the ER-membrane via the proteasome maturation protein POMP, so that the  $\beta$ -subunits can be incorporated in the following sequence:  $\beta 2, \beta 3, \beta 4, \beta 5, \beta 6, \beta 1$  and  $\beta 7$ , forming the  $\beta$ - rings [40]. The  $\beta 1, \beta 2$  and  $\beta 5$  subunits are located in the inside of the cavity and display caspase-like, trypsin-like and chymotrypsin-like proteolytic activity, respectively, depending on their ability to cleave peptide bonds after acidic, basic and hydrophobic remnants, accordingly. As soon as the assembly is finished, POMP is degraded by the nascent proteasome complex [41; 42].

The 20S proteasomal core is capped on both sides with 19S regulatory particles, each of them comprised of 2 subcomplexes, called the base and the cap. They are formed by approximately 20 different subunits that can be subclassified into two main groups: regulatory particle of triple-ATPase (Rpt) and regulatory particle of non-ATPase (Rpn). Both functions – channel opening and unfolding of the substrate – require metabolic energy, and indeed the 19S RP contains ATPase subunits [29]. The base subcomplex is composed of six homologous AAA-ATPase subunits (Rpt1–Rpt6) and four non-ATPase subunits (Rpn1, Rpn2, Rpn10 and Rpn13) and has three functional roles: (1) capturing client proteins via ubiquitin recognition, (2) promoting substrate unfolding, and (3) opening the channel in the  $\alpha$ -ring to allow the entry of a substrate into the catalytic centre [36]. The lid subcomplex consists of at least nine non-ATPase subunits: Rpn3, Rpn5, Rpn6, Rpn7, Rpn8, Rpn9, Rpn11, Rpn12 and Rpn15, and its main function is the deubiquitylation of the captured substrates. While it is the metalloisopeptidase Rpn11 that is known for recycling the ubiquitin particles, since they are not degraded along with the substrate by the proteasome [43], the role of most of the other subunits in the lid is yet to be discovered [36].

### **1.1.5. The proteasome – its types and function**

Being a compartmental protease of the ATPases associated with various cellular activities (AAA+) family, the proteasome uses ATP hydrolysis to unravel spatial structures of its substrates and translocate the unfolded polypeptides to the inside of the degradation chamber for proteolytic cleavage. This ability to disrupt native structures enables the proteasome not only to degrade damaged or misfolded polypeptides, but also numerous regulatory proteins, thus playing an essential role as a modulator of the eukaryotic proteome. Therefore, it remains crucial for the maintenance of protein homeostasis and control of myriad essential cellular processes, such as the cell cycle and division, differentiation and development, and involvement in the cellular response to stress and extracellular effectors, but also morphogenesis of neuronal networks, modulation of cell surface receptors, ion channels and the secretory pathway, DNA repair, replication, transcriptional regulation, transcriptional silencing, signal transduction, long-term memory, circadian rhythms, regulation of the immune and inflammatory responses, and biogenesis of organelles [29; 44]. The structure of the proteasome as well as the main functions of its subunits are summarized in **Figure 4**.

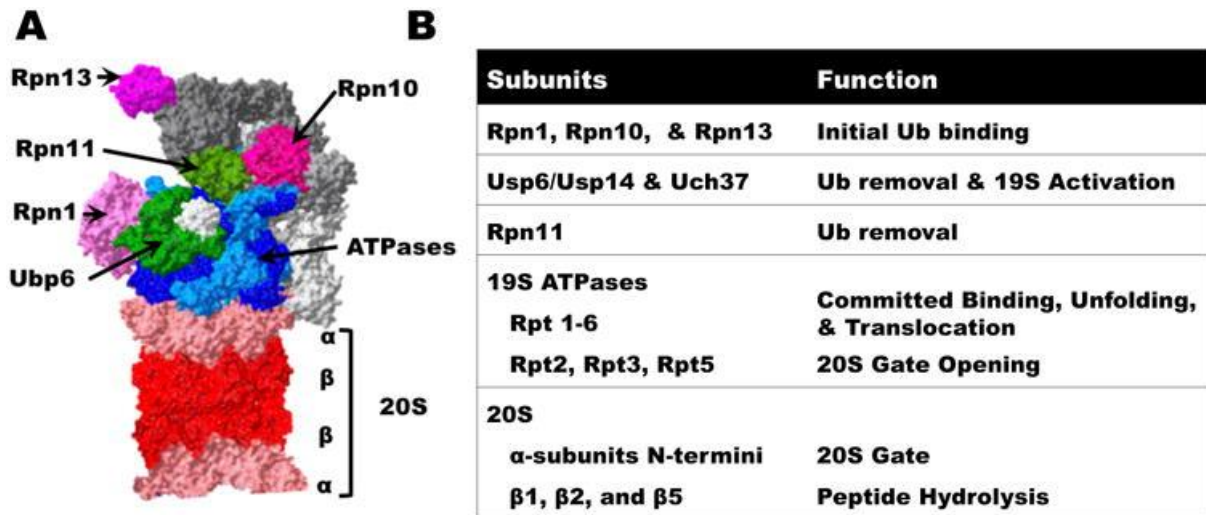


**Figure 4. The structure of the proteasome and the main functions of its subunits.** Source: Collins GA, Goldberg AL. The Logic of the 26S Proteasome. Cell. 2017 [45].

Notably, at least two forms of proteasomes can be distinguished: first, the standard one, widely present in all cells, and second, its isoform, the so-called immunoproteasome which is constitutively expressed in immune cells such as dendritic cells (DC) or whose expression can be induced in other cell types by interferon (IFN)- $\alpha/\beta$  or  $-\gamma$ , or by viral infections [46; 47; 48; 49]. IFN-signalling exposes cells to additional oxidative stress with concomitant production of nascent-oxidant damaged poly-ubiquitylated proteins, contributing to the generation of unfolded protein response – a topic that will be described in detail further on in this work.

Immunoproteasomes differ from the standard ones through the substitution of the  $\beta$ 1,  $\beta$ 2, and  $\beta$ 5 constitutive subunits by the three inducible  $\beta$ -type subunits:  $\beta$ 1i (LMP2),  $\beta$ 2i (MECL1), and  $\beta$ 5i (LMP7), respectively [50; 51]. It was long assumed that the main function of immunoproteasomes was merely restricted to the regulation of MHC class I antigen presentation. Yet, in recent studies it emerged clear that it was solely the tip of the iceberg and that their function reaches far beyond that, encompassing practically all aspects of cell physiology and development [52; 53; 54]. Nonetheless, the subject becomes even more perplexing with the insight on the latest findings, where the identification of so called intermediate-type proteasomes occurred. Bearing one or two out of three inducible or tissue-specific subunits such as  $\beta$ 5t in the thymus [55; 56; 57; 58] and possessing the ability of standard and immunoproteasomes to destroy ubiquitin-modified proteins, they can additionally be vastly influenced by their association with regulatory complexes such as PA28 and PA200 [59; 60;

61]. Altogether, by controlling the broad spectrum of intracellular regulators (e.g. such as I $\kappa$ B or IRF3), both standard- and immunoproteasomes actively participate in the regulation of numerous signalling pathways, including the unfolded protein response (UPR), mTOR, NF- $\kappa$ B, as well as the modulation of both innate and adaptive immune responses [62; 63; 64; 65], thereby exerting a significant impact on cell homeostasis, integrity, viability and functioning.

### **1.1.6. The proteasome activator PA28**

The activity of the 20S proteasome is regulated by protein complexes that bind to its one or both ends in an ATP-independent manner [66]. One of these regulatory complexes, PA28 (which is also known as REG or the 11S regulator), stimulates proteasome peptidase activity and enhances the production of antigenic peptides for presentation by class I molecules of the major histocompatibility complex (MHC I). There are three PA28 subunits that have been identified: two homologue heteropolymeric complexes PA28 $\alpha$  and PA28 $\beta$  [67], which are mainly present in the cytoplasm of immune cells, and a third, slightly different, homopolymeric complex PA28 $\gamma$  (also called the Ki antigen) with its highest abundance in the nuclei of brain cells [68]. The binding of PA28 regulatory particle leads to conformational changes that open a gate in the proteasome  $\alpha$ -subunits through which substrates and products can pass [69]. Moreover, the PA28 $\alpha\beta$  regulatory protein is inducible by interferon- $\gamma$  [70], a cytokine excreted by the lymphocytes, which is an important activator of macrophages and inducer of MHC II molecule expression [71], playing an important role both in the innate and adaptive immune response, including the inhibition of the viral replication, immunostimulation and immunomodulation. Still, aberrant IFN- $\gamma$  secretion can be associated with numerous autoinflammatory and autoimmune diseases. PA28 $\gamma$  on the other hand is rather involved in cell cycle progression and apoptosis, and its levels decrease under the influence of IFN- $\gamma$  [68].

## **1.2. Endoplasmic reticulum (ER) key quality control systems**

There are two major security-ensuring pathways in the ER responsible for providing the proteostasis; properly folded proteins are secreted from the ER, whereas the terminally unfolded or misfolded ones are either recruited to the ERAD complex via the activity of various ER chaperones for cytosolic proteasomal degradation, or start the UPR through the stimulation of one of the sensors: IRE1 $\alpha$ , PERK or ATF6 [72], as symbolically depicted below in **Figure 5**.

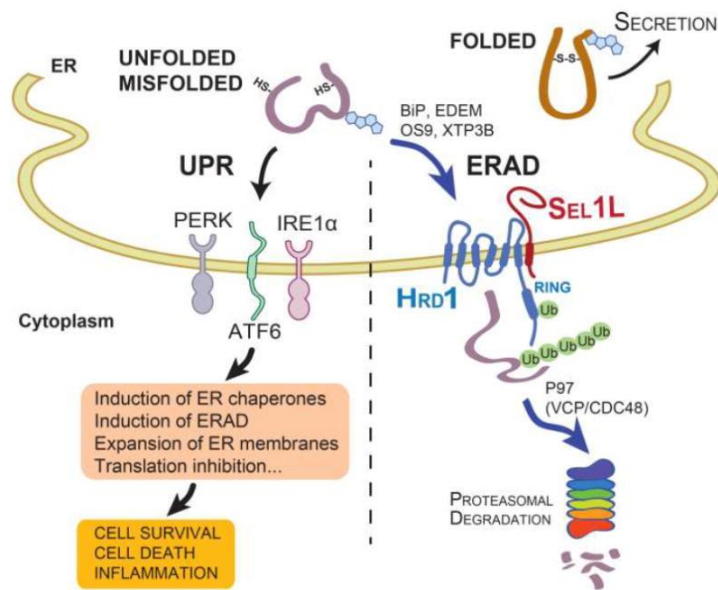


**Figure 5. Two key ER quality control systems in mammals.** While folded proteins exit the ER, terminally unfolded or misfolded proteins in the ER activate UPR via three sensors: IRE1 $\alpha$ , PERK and ATF6. In addition, misfolded proteins can be recruited to the ERAD complex via the activity of various ER chaperones such as BiP, EDEM, OS9 and XTP3B for cytosolic degradation. The Sel1L-Hrd1 protein complex represents the most conserved ERAD complex in mammals. Following retrotranslocation into the cytosol, substrates are ubiquitinated and, with the help of p97 (VCP/CDC48), degraded by the proteasome in the cytosol. Credits to: Qi L, Tsai B, Arvan P. New Insights into the Physiological Role of Endoplasmic Reticulum-Associated Degradation. Trends in Cell Biology. 2017 [73].

### 1.2.1. Endoplasmic reticulum - associated degradation pathway (ERAD)

It is estimated that as much as one-third of the mammalian genome encodes proteins destined for the secretory pathway, thereby implying that the ER folding apparatus must be able to accommodate substrates highly diverse in terms of structure, oligomeric state or folding rate [74; 75]. This diversity necessitates rigorous quality control systems which ensure the maintenance of the biosynthetic fidelity and prevent from the accumulation or deployment of misfolded proteins, therefore concurrently averting proteotoxicity. ER contains a specialized oxidative environment in which nascent polypeptides fold and assemble into native structures with the help of a unique set of molecular chaperones, folding catalysts, and posttranslational modifications [76]. The failure to meet these conformational standards results in degradation in a complex, temporally and spatially coordinated process [74], called endoplasmic reticulum - associated degradation pathway, known under the acronym ERAD.

ERAD is a process comprised of four tightly coupled steps including (1) substrate recognition and selection, (2) dislocation (retrotranslocation) across the ER membrane to the cytosol, (3) ubiquitination, and (4) proteasomal degradation, depicted in **Figure 6**.

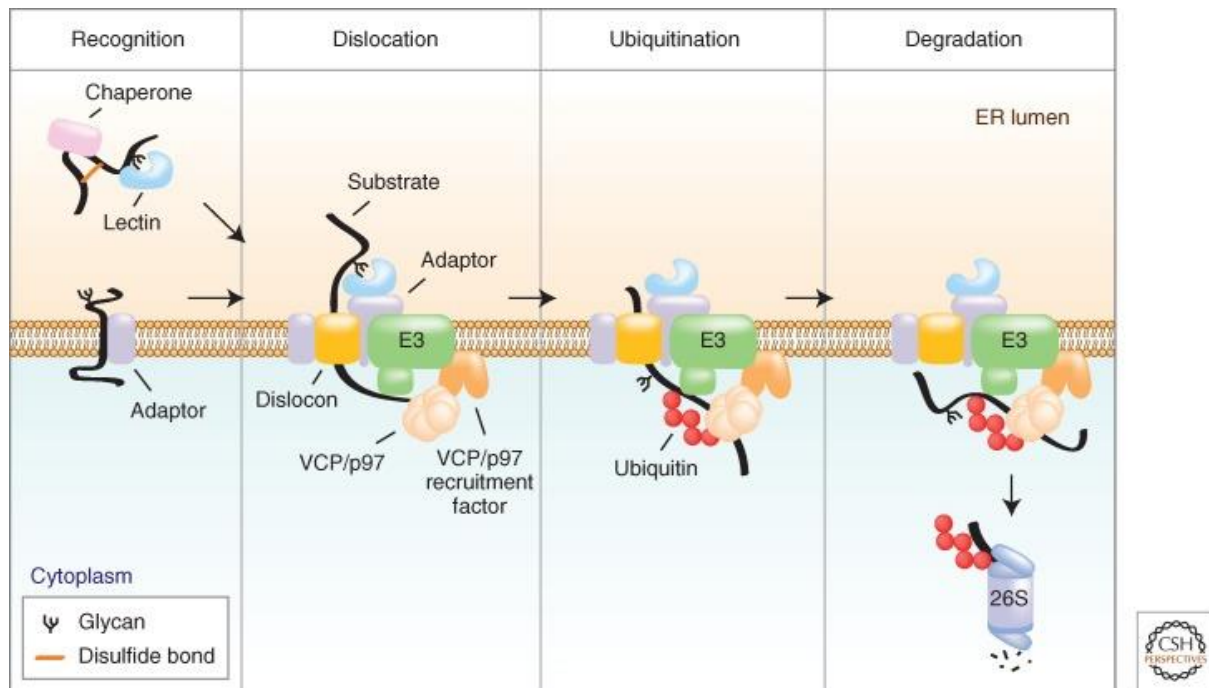


**Figure 6. Key steps in ERAD.** (1) Substrate recognition: Molecular chaperones and lectins within the ER lumen interact with incompletely folded or unassembled proteins and enable binding to membrane-embedded adaptors. (2) Dislocation: Substrates are retrotranslocated across the membrane through proteinaceous pores called dislocons (translocons) in the process requiring ATP energy gained through its hydrolysis by VCP/p97 – transitional endoplasmic reticulum ATPase (TER ATPase). (3) Ubiquitination: After reaching the cytosol, substrates are polyubiquitinated by E3 ligases. (4) Degradation: Ubiquitinated proteins can enter the cytosolic 26S proteasomes, where they encounter the degradation process.

Credits to: Olzmann JA, Kopito RR, Christianson JC. The mammalian endoplasmic reticulum-associated degradation system. Cold Spring Harbor Laboratory Press, 2013 [74].

ERAD substrates include proteins that have failed to achieve a native structure due to mutations, translational misincorporation or stochastic inefficiency in gaining native structure or assembly into protein complexes, as well as ER proteins controlled by regulatory pathways in response to metabolic signals [77; 78; 79]. Recognition of misfolded or misassembled proteins triggers the formation of dislocons, assembled among others by Herp and BiP proteins [80]. Herp is believed to facilitate oligomerization of the membrane-integrated Hrd1 ligase – one of the E3 - enzymes responsible for polyubiquitination, and hence for marking as a target for the proteasome [81]. BiP – binding immunoglobulin protein (also known as GRP-78 or HSPA5) – binds to a number of glycosylated and non-glycosylated ERAD substrates and provides a barrier

on the ER luminal side of the translocon, opening or closing the Sec61 channel for substrate passage into the cytosol [80]. After retrotranslocation, BiP protein seals the luminal side of the translocon which may then be disassembled prior to engagement of a new substrate, whereas the ERAD substrates undergo the process of deglycosylation executed by the peptide N-glycosidase (PNGase) and become exposed to cytosolic E1, E2 and E3 enzymes, resulting in the attachment of the polyubiquitin chain, and then via interaction of p97 (a hexameric ATPase of the AAA family, also known as VCP – valosin-containing protein) with the 19S proteasome cap [82] being targeted for the subsequent proteasomal degradation.

### **1.2.2. Unfolded Protein Response (UPR)**

Despite the vigour of the ER, cells often work close to the limits of their secretory capacity. The effectiveness of protein folding in the ER can be disrupted by a wide range of cellular disturbances, leading to the accumulation of unfolded or misfolded proteins within this organelle – a state known as ER stress [83]. Furthermore, many proteins containing disease-associated mutations are structurally incapable of reaching native conformations and become ‘permanently’ entrapped in the ER, accumulating inside of it and disrupting its proper function [73]. Various conditions may provoke the ER stress, among others hypoxia, nutrient deprivation, point mutations in secreted proteins that stabilize intermediate folding forms or cause aggregation, loss of calcium homeostasis with its detrimental effects on ER-inhabiting calcium-dependent chaperones, etc. [84]. Moreover, the secretory capacity of a cell is continuously confronted with varying physiological demands and pathological perturbations, making it essential to adjust and match the protein-folding capacity of the ER to fluctuating secretory needs [85]. In order to maintain this balance, cells constantly monitor the amount of misfolded proteins in the ER lumen and, if they accumulate above a critical level, employ a dynamic intracellular signalling pathway known as the unfolded protein response, aimed to restore the homeostasis [86].

The unfolded protein response, referred to as UPR, consists of three principal branches which operate parallelly and use unique mechanisms of signal transduction. Each of these branches is defined by a class of signalling components residing in the ER membrane, called as follows: (1) IRE1 – inositol requiring enzyme 1, (2) PERK – protein endoplasmic reticulum kinase or, more precisely, double-stranded RNA-activated protein kinase (PKR-like ER kinase), and

(3) ATF6 – activating transcription factor 6. They are depicted in **Figure 7**. Activation of the UPR triggers two distinct cellular mechanisms to mitigate protein misfolding: an initial reaction to reduce protein synthesis and enhance degradation of misfolded proteins, and a second wave of transcriptional upregulation of numerous target genes involved in global proteostasis control, all in all leading to the induction of ER chaperones and ERAD, expansion of ER membranes and translation inhibition [87; 88; 89].

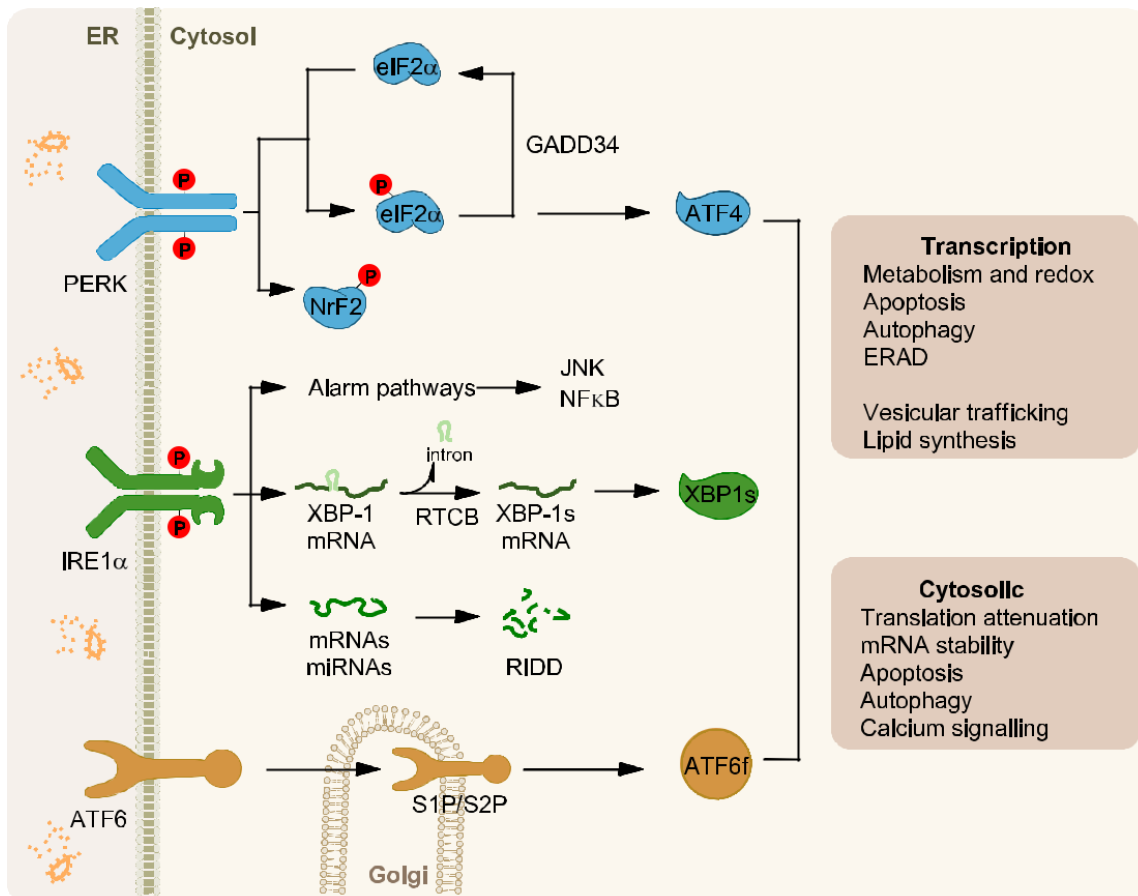


**Figure 7. Branches of the UPR.** All three ER stress sensors – PERK, IRE1 and ATF6 – initially activate signalling mechanisms aimed to increase protein-folding capacity and reduce protein load on the ER. These transcriptional and translational outputs are likely to re-establish protein-folding homeostasis in the ER and promote cell survival. Credits to: Hetz C, Papa FR. The Unfolded Protein Response and Cell Fate Control. Mol Cell, 69(2):169-181, 2018 [86].

IRE1 defines the most conserved and, because of its presence in yeast, best-explored branch of the UPR. It is a bifunctional transmembrane serine/threonine kinase / endoribonuclease which uses a unique mechanism of nonconventional mRNA splicing to transmit the UPR signal. In response to unfolded protein accumulation in the ER, the protein kinase domain located on its cytoplasmic part self-associates, undergoing oligomerization and subsequent trans-



autophosphorylation, leading to its activation [90; 91]. Conformational changes following lateral IRE1 oligomerization in the ER membrane activate its ribonuclease (RNase) function leading to the cleavage of the mRNA [92] encoding a UPR-specific transcription factor, called X-box binding protein 1 (XBP1), responsible for excising an intron in two specific positions. The severed exons are then ligated, giving rise to a spliced mRNA that is translated to the active forms of the transcription factor XBP1s, where 's' indicates that it is the product of the spliced mRNA. XBP1s appears to have a special role in a number of processes, including regulating lipid biosynthetic enzymes and ER-associated degradation components, as well as activating gene expression of chaperones and promoting the development of an intricate ER characteristic for active secretory cells [83; 93]. Moreover, IRE1 also promotes the degradation of mRNAs encoding mostly ER-targeted proteins leading to their decay, and thereby reducing the load of incoming ER client proteins during the ER stress, an activity termed regulated IRE1-dependent decay (RIDD) [94; 95]. This additional output of IRE1 has been associated with the degradation of a multitude of ER-localized and cytosolic mRNAs, ribosomal RNA, and microRNAs, and plays a crucial biological function in the control of glucose metabolism, inflammation, and apoptosis [96].

Another sensor of ER stress – PERK – is a type I transmembrane kinase that after oligomerization and autophosphorylation in response to ER stress phosphorylates eukaryotic translation initiation factor-2 (eIF2 $\alpha$ ) at serine 51 position, inhibiting the recycling of eIF2 $\alpha$  to its active GTP-bound form, which is required for the initiation of the 5'cap-dependent protein translation, in other words of the general polypeptide chain synthesis [83; 97; 98]. This event not only reduces the overload of proteins entering the ER during cellular stresses, but also elicits gene expression designed to ameliorate the underlying cellular disturbance. In non-stressed cells, where eIF2-GTP is abundant, ribosomes scanning downstream the upstream Open Reading Frame 1 (uORF1) reinitiate at the next coding region, upstream Open Reading Frame 2 (uORF2), an inhibitory element that blocks activating transcription factor 4 (ATF4) expression. However, under stress conditions, phosphorylation of eIF2 and the complementary reduction in the levels of eIF2-GTP prolong the time required for the scanning ribosomes to become capable of reinitiating translation. This delay allows ribosomes to scan through the inhibitory uORF2 and reinitiate at the ATF4-coding region instead, promoting the selective translation of the mRNA encoding ATF4. Increased expression of ATF4 is contributing to the expression of genes involved in remediation of cellular stress damage, reinforcement of the antioxidant response, enhancement of the folding capacity of the ER, and upregulation of

macroautophagy [86; 99; 100; 101]. ATF4 belongs to the ATF/CREB (activating transcription factor / cyclic AMP response element binding protein) family of basic region-leucine zipper (b-ZIP) transcription factors which possess the consensus binding site cAMP responsive element (CRE) [102]. Critical targets driven by ATF4 comprise CHOP (transcriptional factor C/EBP homologous protein) [103], GADD34 (growth arrest and DNA damage-inducible protein 34) [104], and ATF3 [105]. While CHOP and ATF3 are induced upstream by the ATF4, GADD34 expression is, in contrast, induced downstream by phosphorylated eIF2 $\alpha$  and ATF4 during the later stages of the ISR, thus, leading to the significant increase in eIF2 $\alpha$  dephosphorylation and acting as an important negative feedback loop to restore protein synthesis once the ER stress has been resolved, contributing to the cell survival [106; 107; 108]. Moreover, recent studies have shown that GADD34 may also play an independent role in apoptosis induction [109]. Sustained ATF4 expression which occurs under chronic stress conditions, in turn, contributes to the induction of apoptosis. Notably, eIF2 $\alpha$  phosphorylation represents a convergence point of different stress pathways known as the integrated stress response (ISR) which is governed by specific kinases that are activated by inflammation, viral infections, nutrient deprivation, and haem deficiency. Being primarily a pro-survival, homeostatic mechanism, under the severe stress it can also drive the signalling towards the cell death [110]. Apart from eIF2 $\alpha$ , PERK can also phosphorylate nuclear erythroid p45-related factor 2 (NRF2), contributing to the dissociation of the NRF2-Keap1 complex and promoting the expression of genes (e.g. such as haem oxygenase 1 (HO-1)) that contain antioxidant response elements (ARE), and thereby diminishing oxidative stress [98; 111].

The third branch of UPR is formed by the activating transcription factor-6 (ATF6) which is initially synthesized as an ER-resident transmembrane precursor glycoprotein with a large ER-luminal b-ZIP domain reaching into the cytoplasm (p90ATF6) and containing intra- and intermolecular disulphide bonds that may monitor the ER environment as redox sensors [83]. In a normal state, ATF6 is retained in the ER by association with the chaperone BiP (binding immunoglobulin protein, also known as GRP78) [112]. Upon accumulation of unfolded proteins, the BiP chaperone cannot be bound to ATF6. As a result, ATF6 is packed into transport vesicles that detach from the ER, and thus delivered to the Golgi apparatus, where it encounters two proteases, S1P and S2P (site-1 and site-2 protease), that consecutively remove the luminal domain and the transmembrane anchor, respectively [112; 113; 114]. Proteolytically cleaved into a smaller protein (p50ATF6) with the liberated N-terminal cytosolic fragment (ATF6(N)), it is further translocated to the nucleus, where it activates UPR

target genes, such as BiP (a chaperone of the HSP70 family), protein disulphide isomerase, and GRP94 (glucose-regulated protein 94 – a chaperone of the HSP90 family) – all in all, prominent ER-resident proteins involved in protein folding. What is more, it also contributes to the stimulation of the transcription factor NF- $\kappa$ B [115; 116]. Notably, ATF6 processing resembles the mechanism by which sterol response element binding protein (SREBP) – the transcription factor that controls sterol biosynthesis – is regulated, and uses even the same proteases on top of that [83; 114; 117].

To sum up, activation of each of the branches leads in the end to the production of b-ZIP transcription factors, which work alone or together to activate UPR target genes. All in all, the UPR's transcriptional programs work collectively as a complex signalling network that enforces various outputs to impose adaptive events and under surveillance re-establish ER proteostasis, thereby preserving proper cellular function.

### **1.3. TCF 11/Nrf1 and its role in the autoregulatory feedback mechanism of proteostasis**

As previously mentioned, a coordinated regulation of the UPS is crucial for the cell to adjust its protein degradation capacity to changing proteolytic requirements. One of the important transcription factors regulating the formation of 26S proteasome in order to compensate for cell's diminished proteolytic activity is the basic-leucine zipper (bZIP) transcription factor 11 – TCF11 (long isoform of Nrf1). Under normal conditions, TCF11/Nrf1 resides in the ER membrane, where it is targeted to ER-associated protein degradation with the help of the E3 ubiquitin ligase HRD1 and the AAA ATPase p97 [118]. Proteasome inhibitors prompt the accumulation of oxidant-damaged proteins and promote the nuclear translocation of TCF11/Nrf1 from the ER. With the help of DNA Damage Inducible 1 Homolog 2 (DDI2) – a ubiquitin-directed endoprotease that binds to the highly poly-ubiquitylated TCF11/Nrf1-protein, it comes to the cleavage of TCF11/Nrf1 factor which subsequently enters the nucleus and binds to the antioxidant response elements (ARE) in their promoter regions. As a result, proteasome gene expression is activated [119]. This transcriptional control loop regulates human proteasome-dependent protein degradation to counteract proteotoxic stress caused by proteasome inhibition. To sum up, human proteasome homeostasis is controlled by an autoregulatory feedback mechanism that allows the compensation of reduced proteasome activity, symbolically depicted in the following figure (**Figure 8**) [118; 120].

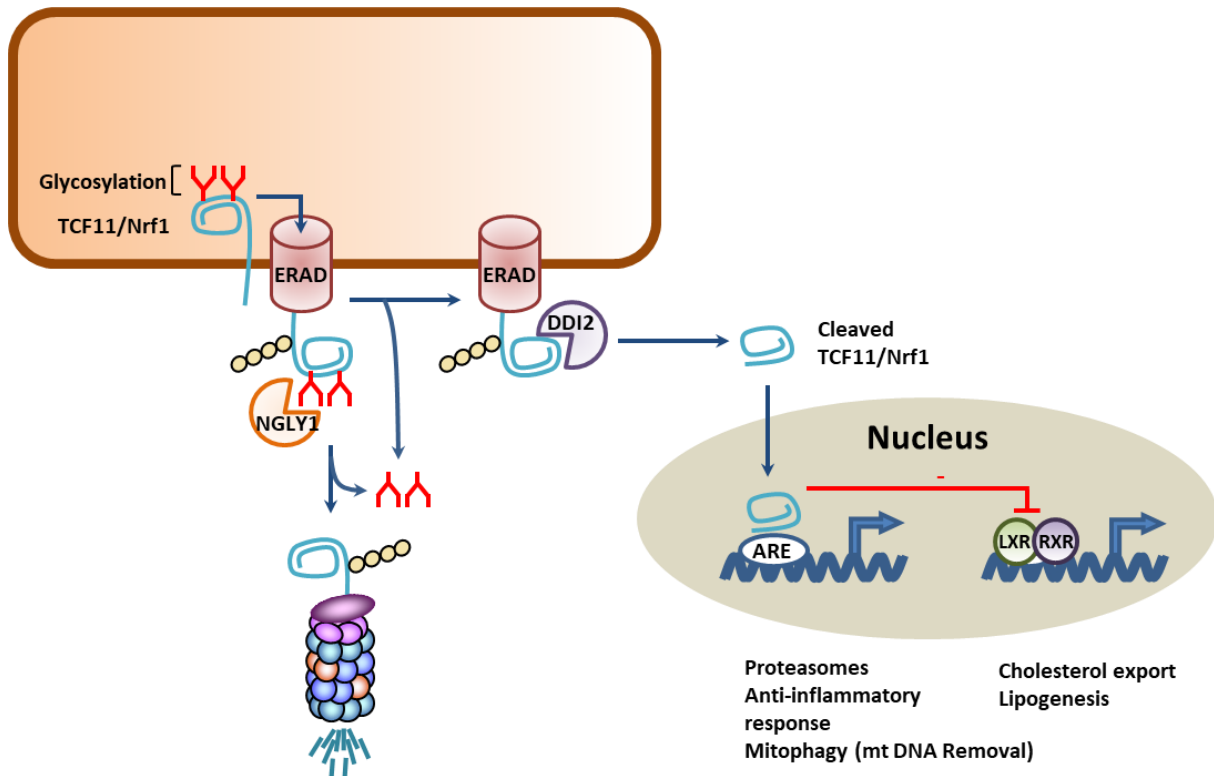


**Figure 8. TCF11/Nrf1 and its role in the autoregulatory feedback loop of proteostasis.** Glycosylated TCF11/Nrf1 factor enters the ERAD pathway. When bound with NGLY1 (de-N-glycosylating enzyme) it undergoes deglycosylation and can either be directed to the cytoplasmic proteasomal degradation, or, if bound with DDI2, undergo the cleavage and enter the cell nucleus. Inside, it binds to the antioxidant response elements (ARE) in their promoter regions, resulting in the activation of proteasome gene expression. In this way, it forms a transcriptional control loop which regulates proteasome-dependent protein degradation. Source: Frédéric Ebstein's own materials.

#### 1.4. The mTOR protein and its signalling pathway

The mammalian target of rapamycin, known as mTOR protein, is a highly conserved serine/threonine kinase ubiquitously expressed in eukaryotic cells. It belongs to the phosphoinositide 3-kinase (PI3K)-related family, consists of a couple of structural domains, and nucleates at least two different multi-protein complexes: the first, mTOR complex 1 (mTORC1) located in the lysosomal membrane and serving as a regulator of cell growth and metabolism, and the second, cytosolic, mTOR complex 2 (mTORC2) [121; 122; 123]. Their structure and main functions are symbolically depicted in **Figure 9**.

Integrating both intracellular and extracellular signals, the mTOR signalling pathway plays a pivotal role as a central regulator of cell metabolism, growth, proliferation, and survival. The

enormous spectrum of cellular processes in which it is actively involved, varying from tumour formation and angiogenesis, through insulin resistance, adipogenesis, to T-lymphocyte activation, attract broad scientific and clinical interest due to its huge potential in understanding the mechanisms of various diseases as well as in serving as prospective targets of therapy, some of which being already in use in pathological settings [124; 125; 126].

During embryonic development, mTOR regulates neuronal progenitor proliferation and differentiation, as well as neurite outgrowth and elongation, crucial processes that appear to be coordinated via mRNA translation and regulation of cell cycle progression and exit [127]. In the mature brain, mTOR participates in further key processes, such as adult neurogenesis, learning, memory, circuit refinement, and synaptic plasticity [128]. mTOR combines inputs from three signalling sources: 1) the growth factor pathway, which comprises the PI3K-AKT-TSC complex, 2) the energy-sensing arm, which responds to low concentrations of ATP through the AMPK-TSC complex, and 3) the amino acid-sensing arm, which controls the activation of mTORC1 directly through Rag GTPases [127].

In this context also the process of autophagy (autophagocytosis) is worth mentioning. Deriving from Ancient Greek *αὐτόφαγος* (*autóphagos*) which means *self-devouring* [129] – it constitutes, in short, a process in which eukaryotic cells destroy their own components through the lysosomal apparatus. Autophagy is a tightly-regulated cellular mechanism describing the chaperone- or vesicle-mediated reprocessing of excessive or damaged proteins, protein complexes and organelles, conducted by enzymes stemming from the same cell [130; 131; 132]. This recycling system has several crucial functions, such as nutrient acquisition [133], maintenance of cellular homeostasis [130; 134], adaptivity [131], immunity and differentiation [135], playing also a pivotal role in its growth, ageing and development [136]. Responsible for maintaining the balance between synthesis and degradation, it recycles the cellular products, ensuring the protein turnover and compensating the energy influx oscillation. When nutrient accessibility is restricted, the degradation of organelles and protein complexes through autophagy provides biological material to maintain anabolic processes such as protein synthesis and energy production [137]. It is known that stimulation of mTORC1 reduces autophagy, whereas inhibition of mTORC1 increases this process, assigning mTOR the role of an amino-acid sensor [121; 137]. Thereby it is not surprising that multiple variants affecting negative regulators of the growth factor and amino acid-sensing arms are known to cause hyperactivation of mTORC1 and have been reported in individuals with NDDs.

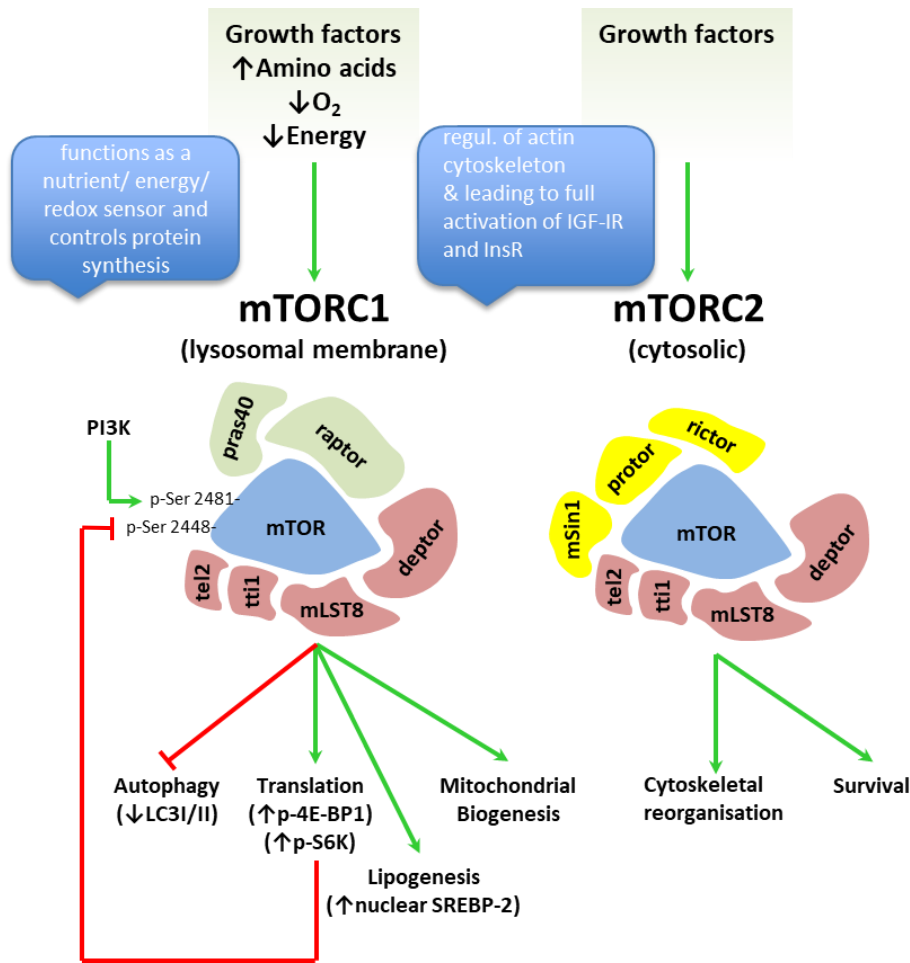


**Figure 9. mTOR signalling pathway.** The insight to the structure and main functions of the mTOR protein with regard to its both complexes – mTORC1 and mTORC2.  
Source: Frédéric Ebstein’s own materials edited for the need of this work.

### 1.5. Dysregulation of proteostasis and its clinical significance

Throughout innate immune responses, proteostasis is significantly influenced by the synthesis of pathogen proteins and by the tissue damage resulting from the omnipresent inflammation, with released free radicals and phagocytic destructive molecules. The resulting protein overload requires an adequate adaptation of cellular clearance pathways and plays a pivotal role in preventing protein aggregation, inclusion-body formation, and – in the end – also cell death. Dysregulation of this fine-tuning is therefore likely to induce cell death and – at the same time – to boost inflammation. The relationship between proteostasis impairment and inflammation may be an essential factor in the process of autoinflammation as well as in many age-related or neurodegenerative diseases (such as Alzheimer’s disease, Parkinson’s disease,

Huntington's disease), all in all, 'gain-of-toxic-function' diseases [138], as well as other pathologies (like cystic fibrosis – which would be a 'loss-of-function disease'), and malignant transformations [139] or other yet uncharacterized illnesses [140; 141].

Within the broad spectrum of autoinflammatory diseases, type I interferonopathies are a phenotypically heterogeneous group of rare genetic diseases including the newly described proteasome-associated autoinflammatory syndromes (PRAAS). By definition, PRAAS are caused by inherited and/or de novo loss-of-function (LOF) mutations in genes encoding proteasome subunits, such as *PSMB8*, *PSMB9*, *PSMB7*, *PSMA3*, *PSMB10* or proteasome assembly factors including *POMP* and *PSMG2*, respectively [31]. Disruption of any of these subunits leads to perturbation of intracellular protein homeostasis, in particular regarding the accumulation of ubiquitinated proteins associated with the generation of a type I interferon (IFN) signature. Interestingly, proteasome dysfunctions, similarly to pathogens, are potent type I IFN inducers – a process of which underlying molecular mechanisms remain up to now largely unknown. Hypothetically, it is the UPR initiated in response to the ER stress that may be a key factor in its induction and the crosstalk between the proteasome impairment and interferonopathy onset, elucidating the potential pathogenesis of PRAAS [31].

Analysis of de novo mutations (DNMs) from sequencing data of nuclear families has pinpointed risk genes for numerous complex diseases, including multiple neurodevelopmental and psychiatric disorders. Genome-wide association studies (GWASs) have proven that mutations important to human diseases can lie both in protein-coding sequences as well as in the non-coding regions. Sequencing studies of parent-proband trios with intellectual disability (ID), autism spectrum disorder (ASD), schizophrenia (SCZ), and epilepsy have all advocated that de novo point mutations play a significant role in paediatric and adult disorders affecting brain development. Biologically, 75–80% of de novo point mutations arise paternally, most probably due to increasing numbers of cell divisions in the male germline lineage when compared to the female one [142].

Recently, an increasing number of loss-of-function (LOF) mutations have been identified in genes encoding proteasome subunits. Fascinatingly, depending on the subunit affected, such genomic alterations result in the development of two apparently distinct phenotypes, namely: (1) systemic autoinflammation (PRAAS) and (2) cognitive impairment [31]. Mutations in the *PSMB8*, *PSMB9*, *PSMB10*, *PSMB4*, *PSMA3*, *POMP* or *PSMG2* subunits are typically

associated with a group of autoinflammatory syndromes sharing the same clinical signs and symptoms, commonly referred to as chronic atypical neutrophilic dermatosis with lipodystrophy and elevated temperature (CANDLE). On the contrary, genetic disruption of the *PSMD12*, *PSMC3* or *PSMB1* subunits mostly leads to neurodevelopmental syndromes. However, the most recent studies have shown that this division is non-binary, as *PSMC3* variants were detected to cause neurosensory syndrome combining deafness and cataract [143], while biallelic variants in *PSMB1* – an impairment of proteasome function, microcephaly, intellectual disability, developmental delay and short stature [144]. In short, no clear cut line between 19S RP and 20S CP mutants can be drawn, as mutations may result in symptoms that combine diverse pathological aspects. The way the pathogenic LOF mutations affect the proteasome subunits is depicted in **Figure 10**.

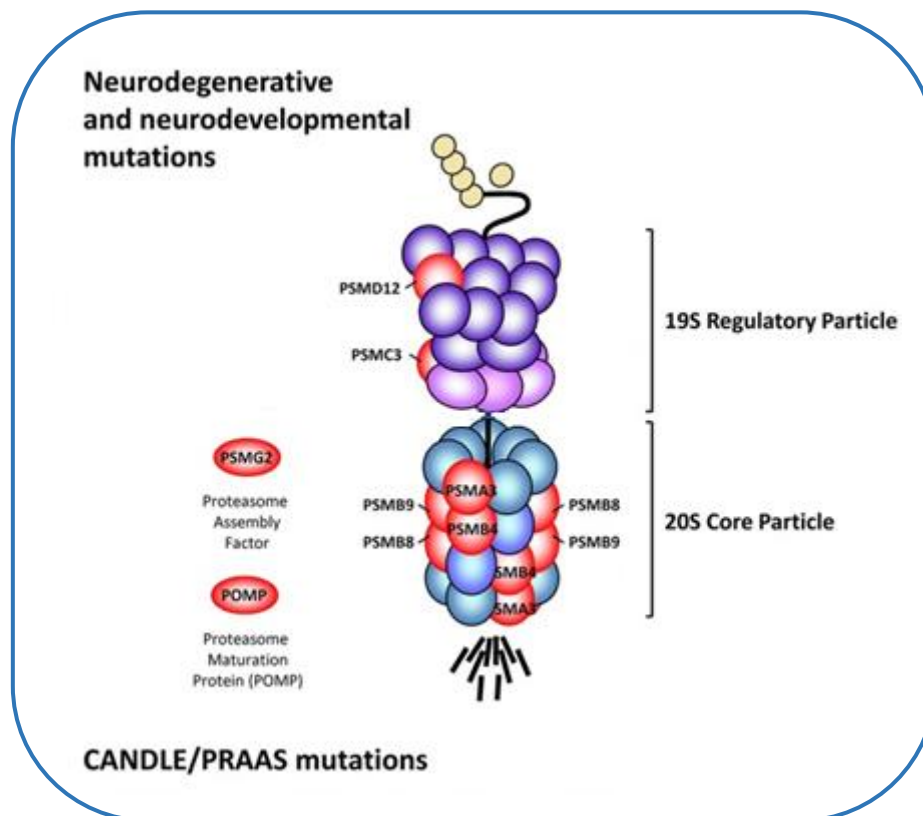


**Figure 10. Schematic depiction of the proteasome subunits affected by pathogenic loss-of-function mutations.** The various proteasome loss-of-function mutations described so far (red) are localized in genes encoding subunits of the 20S core particle (PSMB8, PSMB9, PSMA3, PSMB4), 19S regulatory particle (PSMC3 and PSMD12) and the proteasome assembly factors POMP and PSMG2. Diverse mutations result in different clinical manifestation of the disorder. Credits to: Ebstein, Poli Harlowe, Studencka-Turski and Krüger. Contribution of the Unfolded Protein Response (UPR) to the Pathogenesis of Proteasome-Associated Autoinflammatory Syndromes (PRAAS). *Front Immunol*, 2019 [31], updated and edited for the need of this work.



### **1.5.1. Proteasome-Associated Autoinflammatory Syndromes (PRAAS)**

Proteasome-Associated Autoinflammatory Syndromes (PRAAS) are rare (exact frequency unknown) autosomal-recessively inherited diseases present within different ethnical groups, including the Caucasian, Hispanic, Japanese and South African ones [145]. Their onset is dated at birth or in infancy, with progressive damage resulting from chronic inflammation noted parallel to the child's growth [145; 146]. The main disease manifestations consist of chronic-frequent fevers with inflammatory flares, often present before the age of 6 months, and a plethora of symptoms affecting different organs, such as cutaneous, neurologic, auditory, ophthalmic, cardiopulmonary, abdominal, and lymphatic ones, or another concerning joints, bones, muscles or cartilage, as well as additional abnormal laboratory findings [145; 146].

To the skin symptoms belong annular cutaneous plaques with residual purpura, lipodystrophy (first noted on the face and around joints and limbs), swollen lips with flares and persistently swollen, violaceous (purple-red) eyelids. From the neurological side aseptic meningitis and systemic inflammation can be observed, with common growth delays, low height and weight, and developmental delays noted. The sensory nervous system can also be affected, manifested in auditory changes such as frequent otitis and/or recurrent sinusitis, as well as ophthalmic ones, such as nodular episcleritis, conjunctivitis, keratitis, periorbital oedema and chronically swollen, violaceous (purple-red) eyelids. Cardiopulmonary symptoms may be comprised of clubbing of the fingers and/or toes induced by chronically low blood oxygen levels. Higher risk of cardiac arrhythmias and dilated cardiomyopathy is also present. Abdominal symptoms include diarrhoea and inflammatory intestinal diseases. Hepatosplenomegaly with elevated liver enzymes can also be observed. Moreover, the patients suffer from growth retardation and are at risk for being underweight and fail to thrive, in the worst scenario leading to the multi-organ failure and death. Lymphatic system may be affected through splenomegaly and lymphadenopathy. Also, musculoskeletal system may be perturbed, resulting in joint contractures, muscle atrophy, panniculitis-induced lipodystrophy, myositis, fatigue, and malaise. Inflamed nose and ear cartilage (chondritis) can be present. As mentioned, short stature and delayed growth are common as well. Symptoms such as vasculitis or amyloidosis have not been noted. Within the laboratory results following abnormalities can be found: hypochromic, microcytic or normocytic anaemia, elevated C-reactive protein (CRP) levels, higher erythrocyte sedimentation rate (ESR) and excessive levels of triglycerides (TG). Sometimes elevated platelets, TSH, and/or LDL can also be observed [145; 146].

### **1.5.2. Neurodevelopmental syndromes**

Neurodevelopmental disorders (NDDs) are a class of disorders that affect brain development and function, characterized by wide genetic and clinical variability [147; 148]. These disabilities are associated primarily with the functioning of the neurological system and include disorders like attention-deficit/hyperactivity disorder (ADHD), autism, learning disabilities, intellectual disability (ID), conduct disorders, epilepsy, or impairments in vision and hearing. Epitomized by an inability to reach cognitive, emotional, and motor developmental milestones, they are typically associated with the disruption of the tightly coordinated events that lead to brain development [149]. The most frequently used definitions of ID accentuate subaverage intellectual functioning before the age of 18, usually defined as an IQ less than 70, and deficiencies in life skills such as communication, self-care, home living, social or interpersonal skills. Various severity categories, ranging from mild to severe retardation, are defined on the basis of IQ scores, as stated by the American Association on Intellectual and Developmental Disabilities and various published works [150; 151]. Children with NDDs may encounter difficulties with language and speech, motor skills, behaviour, memory, learning, or other neurological functions. While some symptoms and behaviours of neurodevelopmental disabilities often change or evolve as a child grows older, other disabilities are permanent. Diagnosis and treatment of these disorders can be challenging and often involves a combination of professional therapy, pharmaceuticals, as well as home- and school-based programs [147]. Notably, NDDs constitute a serious health problem in our society, affecting around 3% of children worldwide [149].

Diverse causes of ID have been identified, such as genetic disorders, traumatic injuries, and prenatal events like maternal infection or exposure to alcohol; however, in 30–50% of all cases they remain unknown [152]. The triggers are more commonly recognized for cases of severe retardation (IQ less than 50), whereas the origin of mild retardation (IQ between 50 and 70) remains unknown in over 75% of cases [153; 154]. Exposures to environmental contaminants such as lead, mercury, PCBs, organophosphate pesticides, PBDEs, phthalates, and PAHs could contribute to mild retardation or be the reason for its deterioration to more severe stadiums. Nonetheless, recent studies stress more and more the importance of genetical imprint and shared molecular pathways that could account for the multiple clinical signs characterizing NDDs [155; 156]. Despite their heterogeneous aetiology that includes chromosomal rearrangements, copy number variations, small indels, and point mutations, the awareness of their shared

pathogenic mechanisms could contribute to the establishment of an effective treatment. Factors such as varying gene sensitivity, with highly vulnerable genes categorized as rare variants associated with significant disease risk and high penetrance, and physical or functional interactions between affected genes (i.e. epistasis), contribute to the higher mutational load and may be associated with more severe phenotypes. Most NDDs' cases most likely have a multifactorial and/or polygenic nature, hence confirming the broad heterogeneity of these disorders at both clinical and molecular level. Importantly, the clinical outcome might also be influenced at various levels by nongenetic factors.

## 2. Aim of the Study

Beginning with the Nobel Prize in Chemistry awarded in 2004 for the discovery of ubiquitin-mediated protein breakdown, through the following Nobel Prizes in Physiology or Medicine: 2011 for discoveries concerning the activation of innate immunity, 2016 for discoveries of mechanisms for autophagy, 2018 for discovery of cancer therapy by inhibition of negative immune regulation, finishing with 2019 for discoveries of how cells sense and adapt to oxygen availability, we can observe that unveiling the mechanisms regulating the cellular homeostasis is of a great importance for science and, as Alfred Nobel stated himself, with the greatest benefit of humankind. The only way to understand the disease pathology and apply the most successful treatment, which will not only be addressed at the visible symptoms, but at the real initial cause, is the knowledge of its driving mechanisms. Since, as already Aristotle claimed, *vere scire est per causas scire* (lat. to know truly is to know the causes).

Despite the extensive ongoing research, there are still plenty diseases whose cellular and molecular mechanisms have not yet been fully understood, one such example being the above-mentioned proteasome-associated autoinflammatory syndromes (PRAAS) and neurodevelopmental syndromes (NDDs). Over the last few years, an increasing number of studies has been initiated to elucidate their driving pathophysiological mechanisms. Defining the systematic effects of genomic alterations occurring in genes encoding 19S proteasome subunits will be a key to comprehend the molecular basis of syndromic intellectual disability (ID) pathogenesis and the subsequent design of new targeted therapies. Therefore, the main objective of my research was to contribute to these studies by identifying syndromic ID drivers, and thereby pave the way for the development of new targeted therapy approaches.

Our geneticist collaborators from the Dept. of Genetics of the University of Nantes undertook a comparative examination of the entire exome in various patients diagnosed with syndromic ID using next-generation sequencing (NGS). Trio-exome sequencing allowed them to identify heterozygous missense *de novo* mutations in the *PSMC5* gene encoding the Rpt6 subunit of the 19S regulatory particle in these subjects. Herein, my objective was to characterize cells isolated from these patients at the biochemical level. Specifically, I aimed to analyse their proteasome compositions under denaturing and non-denaturing conditions using SDS- and native-PAGE / western-blotting techniques. In addition, I wanted to check the impact of the mutations on the ER-stress and mTOR pathway, examine the mitochondrial integrity and mitophagy, as well as

its stimulation through TCF11/Nrf1 factor [118]. Moreover, I intended to determine the proteasomes' activity using the proteasome in-plate peptidase activity assay (Suc-LLVY-AMC Assay) [157]. I also inspected the presence of XBP1 splicing, an indicator of the ER stress, using the semi-quantitative PCR [158; 159]. Subsequently, I assessed the gene expression of markers suggesting the presence of ER-stress, using the RT-qPCR. Last, but not least, I conducted the flow cytometry in order to take a closer look on the lymphocyte subpopulations and their characteristics. On the whole, all collected data were objected to deepen the understanding of the pathogenesis of the syndromic ID, identify the disease drivers, and contribute to the ongoing studies, thereby paving the way for the development of new targeted therapy approaches.

### 3. Materials and Methods

#### 3.1. Materials

##### 3.1.1. Chemicals

Chemical	Supplier	Reference number
BSA	Roth	2834.3
Clarity™ Western ECL Substrate	Bio-Rad	Cat. # 170-5060, Control 102031040, Exp.: 2019-08-30
Developer for CP 1000/ Curix 60 for medical X-ray processing	AGFA	REF HT536
DMSO	Applichem	A3672.0250
Page Ruler™ Prestained Protein Ladder	Thermo Scientific	LOT#00627819, 8159680747
Rapid fixer for medical X-ray film processing, G354	AGFA	G354
Roti®-Block	Roth	A151.1
Suc-LLVY-AMC	Bachem	4011369 0100
TaqMan® Gene Expression Assays	Applied Biosystems	RR390W
10xreaction buffer with MgCl <sub>2</sub> and 50mM EDTA	Thermo Fisher	cat# EN0521
M-MLV reverse transcriptase	Promega	cat#M1701
M-MLV RT 5x buffer	Promega	cat#M531A
RNasin® Plus RNase Inhibitor	Promega	cat#N261A
FcR Blocking Reagent, human (diluted 1:50 in FACS buffer)	Miltenyi Biotec	130-059-901

### 3.1.2. Enzymes

Enzyme	Company
innuTaq DNA polymerase	Analytik Jena AG
M-MLV Reverse transcriptase	Promega
MyTaq <sup>TM</sup> HS Mix	Bioline
Premix Ex Taq <sup>TM</sup> (Probe qPCR)	TaKaRa
RNase A	Roth
RNasin <sup>®</sup> Plus	Promega
T4-ligase	Fermentas
TB Green <sup>®</sup> Premix Ex Taq <sup>TM</sup> II	TaKaRa

### 3.1.3. Kits

Kit	Company	Reference number
Pierce <sup>TM</sup> BCA Protein Assay Kit, LOT TI270915	Thermo Scientific	REF 23225
Centrifuge 5415 R	Eppendorf	n/a
Electrophoresis System	Bio Rad	1658005
Immobilon <sup>®</sup> – P Transfer Membrane	Milipore	CAT. NO. IPVH00005 LOT. NO. R7BA7795E, pore size: 4,5 µm)
Micro tube 1,5ml	Sarstedt AG & Co.KG	REF 72.690.001
RP new / UV, medical X-ray screen film blue sensitive	CEA	XC63P
Whatman <sup>®</sup> Cellulose Filter Papers (Blotting Paper, 703)	VWR	REF: VWR European Cat. No. 732-0591, LOT: Batch No. 16898654),

### 3.1.4. Primers

Name	Sequence (5' to 3')
hPSMC5_for	AAG ATG GCG CTT GAC GGA
hPSMC5_rev	GGC AAT TGG GTG TCA CAT CAT
hXBP1_for	GGG AAT GAA GTG AGG CCA GTG
hXBP1_rev	GAC TGG GTC CAA GTT GTC CA

### 3.1.5. Buffers

#### Lysis buffer for protein extraction for SDS PAGE

Lysis buffer ingredients	Volume
RIPA buffer (including 1x complete EDTA)	5 ml
NaF (1M)	50 µl
Na <sub>4</sub> P <sub>2</sub> O <sub>7</sub> (preheated in 60°C water)	20 µl
Na <sub>3</sub> VO <sub>4</sub>	50 µl
MG-132 (melted in the room temperature)	5 µl
NEM (melted in the room temperature)	50 µl

#### 10 x PBS buffer

Salt	Amount
NaCl	80 g
KCl	2 g
Na <sub>2</sub> HPO <sub>4</sub> + 2 H <sub>2</sub> O	18 g
KH <sub>2</sub> PO <sub>4</sub>	2.4 g
Dissolved in dH <sub>2</sub> O ad 1000 ml and autoclaved. pH 7.4	

#### PBST buffer

1x PBST-buffer ingredients	Volume
10x PBS buffer	200 ml
Milli-Q <sup>®</sup> dH <sub>2</sub> O	1800 ml
Tween 20	8 ml



### 10x SDS-PAGE running buffer

10 x SDS-PAGE running buffer ingredients	Amount
SDS (powder or pellets)	10 g
Tris	30,3 g
Glycine	144,1 g
Milli-Q® dH <sub>2</sub> O	815,6 g

### 1x transfer buffer

1 x blot buffer ingredients	Amounts for the volume of 2 litres
Glycine	5,8 g
Tris	11,6 g
SDS	0,74 g
Methanol	400 ml
Adjusted with dH <sub>2</sub> O to the end volume of 2 litres and stored in 4°C.	

### TDSG buffer for Native PAGE

TDSG buffer ingredients	Volume
TDSG	5 ml
DTT 0,2M	50 µl
ATP 200µM	50 µl

### FACS buffer

FACS-buffer components
2% FCS
0,02% NaN <sub>3</sub>
2 mM EDTA
BD FACS Flow™ sheath fluid

### 3.1.6. Antibodies

#### Western Blot primary antibodies

Primary antibody	Dilution	Diluting agent	Secondary antibody	Volume /well	Resolving gel
<b>Rpn 5</b>	1:2000	TBST/BSA 5% + 0,03% NaN <sub>3</sub>	Anti- mouse IgG HRP - linked	10 µl	12,5%
<b>Rpt 6</b>	1:6000	1x Roti Block	Anti- mouse IgG HRP - linked	10 µl	12,5%
<b>LMP2</b>	1:20000	1x Roti Block	Anti- rabbit IgG HRP - linked	10 µl	12,5%
<b>LMP7</b>	1:100000	TBST/BSA 5% + 0,03% NaN <sub>3</sub>	Anti- mouse IgG HRP - linked	10 µl	12,5%
<b>Rpt5</b>	1:2000	TBST/BSA 5% + 0,03% NaN <sub>3</sub>	Anti- rabbit IgG HRP - linked	10 µl	12,5%
<b>Rpt1</b>	1:1000	1x Roti Block	Anti- rabbit IgG HRP - linked	10 µl	12,5%
<b>MECL1</b>	1:3000	1x Roti Block	Anti- goat IgG (H+L)	10 µl	12,5%
<b>β1</b>	1:4000	TBST/BSA 5% + 0,03% NaN <sub>3</sub>	Anti- mouse IgG HRP - linked	10 µl	12,5%
<b>α-tubulin</b>	1:50000	TBST/BSA 5% + 0,03% NaN <sub>3</sub>	Anti- mouse IgG HRP - linked	10 µl	12,5%
<b>β5</b>	1:2000	TBST/BSA 5% + 0,03% NaN <sub>3</sub>	Anti- rabbit IgG HRP - linked	10 µl	12,5%
<b>USP14</b>	1:1000	TBST/BSA 5% + 0,03% NaN <sub>3</sub>	Anti- mouse IgG HRP - linked	10 µl	12,5%
<b>β2</b>	1:5000	1x Roti Block	Anti- mouse IgG HRP - linked	10 µl	12,5%
<b>Rpn10</b>	1:1000	1x Roti Block	Anti- mouse IgG HRP - linked	10 µl	12,5%
<b>α2</b>	1:1000	1x Roti Block	Anti- mouse IgG HRP - linked	10 µl	12,5%
<b>GADD34</b>	1:2000	TBST/BSA 5% + 0,03% NaN <sub>3</sub>	Anti- rabbit IgG HRP - linked	10 µl	12,5%
<b>PA28α</b>	1:100000	TBST/BSA 5% + 0,03% NaN <sub>3</sub>	Anti- rabbit IgG HRP - linked	10 µl	12,5%
<b>Rpt3</b>	1:1000	1x Roti Block	Anti- mouse IgG HRP - linked	10 µl	12,5%

<b>LC3b</b>	1:1000	1x Roti Block	Anti- rabbit IgG HRP - linked	10 µl	12,5%
<b>Rpt4</b>	1:1000	1x Roti Block	Anti- mouse IgG HRP - linked	10 µl	12,5%
<b>Casp3</b>	1:1000	1x Roti Block	Anti- rabbit IgG HRP - linked	10 µl	12,5%
<b>STAT1</b>	1:1000	1x Roti Block	Anti- mouse IgG HRP - linked	20 µl	12,5%
<b>p-STAT1</b>	1:1000	TBST/BSA 5% + 0,03% NaN <sub>3</sub>	Anti- rabbit IgG HRP - linked	20 µl	12,5%
<b>EIF2α</b>	1:2000	1x Roti Block	Anti- rabbit IgG HRP - linked	20 µl	12,5%
<b>p-EIF2α</b>	1:1000	TBST/BSA 5% + 0,03% NaN <sub>3</sub>	Anti- rabbit IgG HRP - linked	20 µl	12,5%
<b>IRF3</b>	1:1000	TBST/BSA 5% + 0,03% NaN <sub>3</sub>	Anti- rabbit IgG HRP - linked	20 µl	12,5%
<b>p-IRF3</b>	1:1000	TBST/BSA 5% + 0,03% NaN <sub>3</sub>	Anti- rabbit IgG HRP - linked	20 µl	12,5%
<b>4-EBP1</b>	1:1000	TBST/BSA 5% + 0,03% NaN <sub>3</sub>	Anti- rabbit IgG HRP - linked	20 µl	12,5%
<b>p-4-EBP1</b>	1:1000	1x Roti Block	Anti- rabbit IgG HRP - linked	20 µl	12,5%
<b>p62</b>	1:2000	1x Roti Block	Anti- rabbit IgG HRP - linked	30 µl	12,5%
<b>GβL (mLST8)</b>	1:1000	TBST/BSA 5% + 0,03% NaN <sub>3</sub>	Anti- rabbit IgG HRP - linked	30 µl	12,5%
<b>NDP-52</b>	1:1000	1x Roti Block	Anti- rabbit IgG HRP - linked	30 µl	12,5%
<b>LMP2</b>	1:20000	1x Roti Block	Anti- rabbit IgG HRP - linked	30 µl	12,5%
<b>mTOR</b>	1:1000	1x Roti Block	Anti- rabbit IgG HRP - linked	20 µl	10%
<b>ATF4</b>	1:1000	TBST/BSA 5% + 0,03% NaN <sub>3</sub>	Anti- rabbit IgG HRP - linked	20 µl	10%
<b>mTOR pSer2448</b>	1:1000	1x Roti Block	Anti- rabbit IgG HRP - linked	20 µl	10%
<b>BIP (GRP78)</b>	1:1000	TBST/BSA 5% + 0,03% NaN <sub>3</sub>	Anti- rabbit IgG HRP - linked	20 µl	10%
<b>Raptor</b>	1:1000	1x Roti Block	Anti- rabbit IgG HRP - linked	20 µl	10%

<b>Bnip3</b>	1:1000	1x Roti Block	Anti- rabbit IgG HRP - linked	20 µl	10%
<b>Bnip3L</b>	1:1000	1x Roti Block	Anti- rabbit IgG HRP - linked	20 µl	10%
<b>TCF11</b>	1:1000	1x Roti Block	Anti- rabbit IgG HRP - linked	20 µl	10%
<b>mTOR p2481</b>	1:1000	1x Roti Block	Anti- rabbit IgG HRP - linked	20 µl	10%
<b>Parkin</b>	1:1000	TBST/BSA 5% + 0,03% NaN <sub>3</sub>	Anti- mouse IgG HRP - linked	20 µl	10%
<b>Rictor</b>	1:1000	1x Roti Block	Anti- rabbit IgG HRP - linked	20 µl	10%
<b>PINK1</b>	1:1000	1x Roti Block	Anti- rabbit IgG HRP - linked	20 µl	10%
<b>Rictor</b>	1:1000	1x Roti Block	Anti- rabbit IgG HRP - linked	20 µl	10%
<b>Optineurin</b>	1:1000	1x Roti Block	Anti- rabbit IgG HRP - linked	20 µl	10%
<b>mTOR pSer2481</b>	1:1000	1x Roti Block	Anti- rabbit IgG HRP - linked	20 µl	10%
<b>ATF6</b>	1:1000	TBST/BSA 5% + 0,03% NaN <sub>3</sub>	Anti- mouse IgG HRP - linked	20 µl	10%
<b>Raptor</b>	1:1000	1x Roti Block	Anti- rabbit IgG HRP - linked	20 µl	10%
<b>p62</b>	1:500	1x Roti Block	Anti- rabbit IgG HRP - linked	20 µl	10%
<b>TCF11</b>	1:500	1x Roti Block	Anti- rabbit IgG HRP - linked	20 µl	10%
<b>Bnip3</b>	1:500	1x Roti Block	Anti- rabbit IgG HRP - linked	20 µl	10%
<b>SREBP2</b>	1:1000	1x Roti Block	Anti- mouse IgG HRP - linked	20 µl	10%
<b>GRP94</b>	1:5000	TBST/BSA 5% + 0,03% NaN <sub>3</sub>	Anti- rabbit IgG HRP - linked	20 µl	10%
<b>NGLY1</b>	1:2000	1x Roti Block	Anti- rabbit IgG HRP - linked	20 µl	10%
<b>PKR</b>	1:1000	TBST/BSA 5% + 0,03% NaN <sub>3</sub>	Anti- rabbit IgG HRP - linked	20 µl	12,5%
<b>II-24</b>	1:10000	TBST/BSA 5% + 0,03% NaN <sub>3</sub>	Anti- goat IgG (H+L)	20 µl	12,5%

<b>LC3b</b>	1:1000	1x Roti Block	Anti- rabbit IgG HRP - linked	20 µl	12,5%
<b>TCF11 (Nrf 1)</b>	1:500	1x Roti Block	Anti- rabbit IgG HRP - linked	30 µl	10%
<b>Rpt6</b>	1:6000	TBST/BSA 5% + 0,03% NaN <sub>3</sub>	Anti- mouse IgG HRP - linked	30 µl	10%
<b>S6K</b>	1:1000	1x Roti Block	Anti- rabbit IgG HRP - linked	15 µl	12,5%
<b>4E-BP1</b>	1:1000	TBST/BSA 5% + 0,03% NaN <sub>3</sub>	Anti- rabbit IgG HRP - linked	15 µl	12,5%
<b>pS6K</b>	1:1000	TBST/BSA 5% + 0,03% NaN <sub>3</sub>	Anti- rabbit IgG HRP - linked	15 µl	12,5%
<b>p4E-BP1</b>	1:1000	1x Roti Block	Anti- rabbit IgG HRP - linked	15 µl	12,5%

#### Western Blot secondary antibodies

<b>Name</b>	<b>REF</b>	<b>LOT</b>	<b>Company</b>
Anti- mouse IgG HRP – linked antibody	7076S	35	Cell-Signalling Technology 7076S
Anti- rabbit IgG HRP – linked antibody	7074S	29	Cell-Signalling Technology 7074S
Anti- goat antibody, diluted 1:1 in glycine	Sc-2020	G0208	Santa Cruz Biotechnology
Cy3-AffiniPure F(ab') <sub>2</sub> Fragment Rabbit Anti-Goat IgG (H+L), diluted 1:1 in glycerol	A11034	1812166	Life Technologies

## Native PAGE antibodies

Primary antibody	Supplier	Dilution	Diluting buffer	Secondary antibody	Volume/well
<b>Rpt 6</b>	Enzo Life Sciences	1:6000	TBST/BSA 5% + 0,03% NaN <sub>3</sub>	Anti- mouse IgG HRP - linked	20 µl
<b>α6</b>	Enzo Life Sciences	1:10000	1x Roti Block	Anti- mouse IgG HRP - linked	20 µl
<b>Rpn 5</b>	Santa Cruz Biotechnology Inc	1:2000	TBST/BSA 5% + 0,03% NaN <sub>3</sub>	Anti- mouse IgG HRP - linked	20 µl
<b>PA28α</b>	Laboratory stock	1:50000	TBST/BSA 5% + 0,03% NaN <sub>3</sub>	Anti- rabbit IgG HRP - linked	20 µl

## Flow cytometry fluorophore-conjugates

Fluorophore conjugate	Excitation wavelength [nm]	Excitation max [nm]	Emission max [nm]	Laser	Power [mW]	Channel	Bandpass filter
<b>APC</b>	640	652	660	Trigon	40	R670	670/14
<b>FITC</b>	488	495	520	Trigon	100	B525	525/50
<b>PerCP-Vio700</b>	488	482	704	Trigon	100	B710	710/50
<b>VioBlue</b>	405	400	452	Octagon	100	V450	525/50
<b>PE</b>	561	565	578	Octagon	50	YG582	582/12
<b>PE-Vio770</b>	561	565	775	Octagon	50	B4	750 LP
<b>A700</b>	640	702	723	Trigon	40	R710	710/50
<b>BV650</b>	405	405	645	Octagon	100	V670	660/20

## Flow cytometry fluorophore-conjugated primary antibodies

Marker	Conjugate	Channel	Host	Iso-type	Clone	Conc. [mg/ml]	Dil.	Producer	Cat. No.	LOT
<b>CD3</b>	APC	R670	human	IgG1	REA613	NI	1:25	Miltenyi	130-113-697	5190516638
<b>CD4</b>	FITC	B525	mouse	IgG1k	SK3	0,1	1:10	Biolegend	344604	B183664
<b>CD8</b>	PerCP-Vio700	B710	human	IgG1	REA734	NI	1:25	Miltenyi	130-110-820	5190603542
<b>CD45 RA</b>	Vio Blue	V450	human	IgG1	REA1047	NI	1:25	Miltenyi	130-117-854	5190531153
<b>CD62L</b>	PE	YG582	human	IgG1	REA615	NI	1:25	Miltenyi	130-114-151	5190509565
<b>CD19</b>	PE-Vio770	YG780	human	IgG1	REA675	NI	1:25	Miltenyi	130-114-173	5190603498
<b>CD197</b>	A700	R710	mouse	IgG2a, k	G043H7	0,4	1:10	Biolegend	353244	B238923
<b>CD45 R0</b>	BV650	V660	mouse	IgG2a, k	UCHL1	0,1	1:10	Biolegend	304232	B239720

## 3.2. Methods

### 3.2.1. Ethics statement

The approval from ethics committee for all experimental procedures on human samples conducted at the University Medicine of Greifswald within the project entitled '*Unravelling the molecular pathogenesis of proteasome-related disorders*' was obtained under the Human Ethics registration number BB 209/18. Informed consent forms from the parents of the patients were acquired before the onset of the research. The present study includes 2 patients with clinical disease manifestations who were diagnosed with mutations in the *PSMC5* gene and their respective mothers serving as controls. Research was conducted using multiple cell biological, protein biochemical and molecular biological methods which are described in detail below.

### **3.2.2. Sample preparation**

Cryopreserved peripheral blood mononuclear cells (PBMC) formerly isolated by our partners from Boston Children's Hospital, Harvard, USA and the UPMC Children's Hospital of Pittsburgh, USA from blood drawn from patients and related healthy controls (mothers of the probands) were used for the study. They were then expanded using phytohemagglutinin (PHA) and interleukin 2 (IL2) cocktail to stimulate the T cell culture by my supervisor PD Frédéric Ebstein, PhD.

### **3.2.3. Protein extraction and quantification for SDS-PAGE**

To extract the proteins out of the cell pellets, both chemical and physical lysis methods were used. First, the cell pellets were resuspended in 200-500  $\mu$ l of RIPA lysis buffer prior to four freeze-and-thaw cycles in liquid nitrogen and lukewarm water, to guarantee rupture of the cell membranes. The lysates were then centrifuged for 15 min at the speed of 13.000 rpm, and the supernatant re-pipetted to the new Eppendorf tubes, and used for bicinchoninic acid assay (BCA- assay) or stored at  $-80^{\circ}\text{C}$ .

Total protein concentrations in cell lysates were determined using the bicinchoninic acid protein assay (BCA Protein Assay) conducted according to the protocol. In a 96-well microplate, bovine serum albumin (BSA) in the amount of 10  $\mu$ l/well in decreasing concentrations was pipetted as a control and the protein lysates were diluted with dH<sub>2</sub>O in a 1:5 ratio. To each well 200  $\mu$ l of the resolution was added and incubated for 30 min at  $37^{\circ}\text{C}$ , prior to the photometrical determination of the protein concentrations. Absorbance was measured at 562 nm.

### **3.2.4. Sodium dodecyl sulphate–polyacrylamide gel electrophoresis (SDS-PAGE)**

The samples were vortexed with the loading buffer (625 ml Tris–HCl (pH 6.8), 20% sodium dodecyl sulphate (SDS), 0.5% bromophenol blue, 10% glycerol, 0.5%  $\beta$ -mercaptoethanol and dH<sub>2</sub>O, centrifuged, and heated to  $95^{\circ}\text{C}$  for the min. time of 5 min, to ensure denaturation of the proteins and inactivation of the present proteases. The resolving and stacking gels for electrophoresis were prepared as follows:



Resolving gel ingredients	Gel concentration	
	12,5%	10%
Acrylamide 30%	8,33 ml	6,7 ml
Milli-Q® dH <sub>2</sub> O	6,27 ml	7,9 ml
Tris 1,5M pH 8,8	5 ml	5 ml
10% SDS	0,2 ml	0,2 ml
10% APS	0,2ml	0,2ml
TEMED	0,02 ml	0,02 ml
	Volumes for 2 gels á 80x75x1,5mm. End substance volume of 20 ml.	

Stacking gel ingredients	Volume
Acrylamide 30%	2 ml
Milli-Q® dH <sub>2</sub> O	9 ml
Tris 1M pH 6,8	1 ml
10% SDS	0,12 ml
10% APS	0,12 ml
	Volumes for 2 gels á 80x75x1,5mm. End substance volume of 12 ml.

Protein lysates in the volume ranging from 5 to 50  $\mu$ l (adjusted to the protein concentration and antibody used) were loaded along with the 5  $\mu$ l of Page Ruler™ Prestained Protein Ladder. SDS-PAGE was run in the 1 x SDS-PAGE running buffer diluted from the concentrate, for 2h, under 120-150 V and 0.4 A. The polyvinylidene difluoride (PVDF) membrane was activated with methanol for approximately 10 seconds, as recommended in the manufacturer's protocol.

The wet blot procedure was applied to transfer proteins onto a PVDF membrane. Blotting was performed in a Bio-Rad Mini-Protean® tetra system filled with the transfer buffer solution cooled to 4°C. The ice blot was put inside, to assure stable low temperature. Wet blot was run under 200 V and 0.4 A for 1 h.

Transfer efficiency was assessed by the visualization of the total protein with Amido Black staining. The membrane was incubated with Amido Black for approx. 5 min under constant shaking, washed 3 times with dH<sub>2</sub>O, and scanned.

<b>Amido Black ingredients diluted in dH<sub>2</sub>O</b>	<b>Amount for the end volume of 50 ml</b>
9% MeOH (v/v)	4,5 ml
2% Acetic acid (100%) (v/v)	1 ml
0,02% Amido Black 10 B (m/v)	0,01 g

Subsequently, the membrane was blocked with 1x Roti®-Block for 30 min at RT under constant shaking to reduce unspecific binding sites and eliminate false positive results, and then incubated with the primary antibodies (see materials, antibodies) diluted in antibody-solution (10 ml/membrane) overnight at 4°C with constant shaking. After the incubation, the membranes were washed 3 times for 5 min with 1x PBST-buffer (10ml for a membrane) under constant shaking.

Next, the membranes were incubated with the horse-radish-peroxidase-coupled (HRP-linked) anti-mouse or -rabbit or -goat secondary antibodies diluted in 1x Roti Block 1:5000 for approx. 1 h at room temperature under constant shaking. After that, the membranes were washed again 3 times for approx. 5 min with 10ml of PBST solution a time. Proteins were then visualized using an enhanced chemiluminescence detection kit (ECL, Biorad), with Clarity™ Western ECL Substrate used for detection. Both digital and film-based imaging was tried out, but since the film-based imaging provided far better-quality results, it was the method chosen for the experiments performed. The film incubation time was adjusted to the antibodies used and the proteins investigated, and ranged from 3 sec. to 24 h. The imaging included the usage of the developer, dH<sub>2</sub>O, and fixator (see materials – chemicals).

### **3.2.5. Protein extraction and quantification for Native PAGE**

Cell pellets from resting T cells isolated from patients and related controls were lysed in 50 to 400 µl ice-cold homogenization TSDG buffer and subsequently treated with the liquid nitrogen for 4 freeze-and-thaw cycles, ensuring the breakage of the membranes, and centrifuged at 13.000 rpm for 15 min in 4°C. The supernatant with extracted proteins was re-pipetted into a fresh Eppendorf tube. Protein quantification of the soluble lysates was determined using the Bradford Assay (Coomassie dye-based assay) according to the manufacturer's protocol. 0,2 x Bovine Serum Albumin (BSA) Standard mixed with 1 µl lysis buffer and dH<sub>2</sub>O was used for calibration and obtaining the standard curve. 1 µl of each of the protein extracts was diluted

with 19  $\mu$ l of the dH<sub>2</sub>O and added to the 280  $\mu$ l of the Bradford reagent pre-pipetted to the wells on the 96-well microplate and incubated under constant shaking and light-protection for 5 min prior to the photometrical determination of their concentrations. Absorbance was measured at 595 nm and data exported and analysed to determine the protein concentration.

### 3.2.6. Native polyacrylamide gel electrophoresis (Native PAGE) and proteasome in-plate peptidase activity assay

5x NPP was used as a dye and next diluted with dH<sub>2</sub>O to the total volume of 50  $\mu$ l based on the protein concentration determined via Bradford assay.

Ingredients	Amount
Bis-Tris pH 6.8	250 mM
NaCl	250 mM
Bromophenol blue	0.5 mg/10 ml
50% glycerol	v/v

Twenty micrograms of whole-cell lysates were run on precast 3-12% gradient Bis-Tris gel (Thermo Fisher Scientific) at 45 V overnight at 4°C using an electrophoresis buffer consisting of 1 M Bis-Tris, 1 M tricine (pH 6,8). Subsequently, the blotting with the transfer at the PVDF membrane was performed, with further steps like Amido Black staining, Roti Block blocking, incubation with primary and secondary antibodies (see materials, antibodies), detection and visualization same as described in detail in Western Blot technique. Proteasome bands were subsequently visualized by exposing the gel to UV light at 360 nm and detected at 460 nm using an Imager.

Following separation, peptidase activity of the proteasome was measured via a Proteasome Activity Assay Kit with 0.1 mM of the Suc-LLVY-AMC fluorogenic peptide (Bachem) at 37°C for 20 min in an overlay buffer (20 mM Tris, 5 mM MgCl<sub>2</sub>, pH 7,0) in a light-protective microplate. The excitation was set up for 470 nm, whereas the emission measurement was done at 570 nm. Within the first hour, the activity was measured every 15 min, while within the second hour – every 30 min. The mean of 4 measurements for each probe was taken and placed on the curve, thereby representing the changes in proteasome's activity in time.

### **3.2.7. RNA isolation**

Total RNA was isolated from expanded T cells using the kit from Analytic Jena AG following the manufacturer's instructions. The cell pellets were incubated for 2 min with 400 µl of Lysis Solution RL at room temperature, resuspended and incubated for another 3 min at room temperature. All Eppendorf tubes and pipette tips used for this experiment were RNase free. The lysed samples were transferred onto the Spin Filter D placed into described Receiver Tubes and centrifuged at 11.000 rpm for 2 min, and Spin Filter D was discarded. Spin Filters R were placed into new described Receiver Tubes. 400 µl of 70% ethanol was added to each of the filtrates and the samples were mixed through re-pipetting. The samples were transferred to the Spin Filters R and centrifuged at 11.000 rpm for 2 min. The Receiver Tube with filtrate was discarded and the Spin Filter R placed into a new Receiver Tube. 500 µl of Washing Solution HS was added to the Spin Filter R and centrifuged at 11.000 rpm for 1 min. The Receiver Tube with filtrate was again discarded and the Spin Filter R placed into a new Receiver Tube. 700 µl of Washing Solution LS was added to the Spin Filter R and centrifuged at 11.000 rpm for 1 min. The Receiver Tube with filtrate was once more discarded and the Spin Filter R placed into a new Receiver Tube, which was subsequently centrifuged at 11.000 rpm for 3 min to remove the traces of ethanol. The Spin Filter R was placed into an Elution Tube and 30-80 µl of RNase-free water (volume depending on the size of the cell pellet) were added. The solution was incubated for 1 min at room temperature, centrifuged at 11.000 rpm for 1 min, taken out and placed directly on ice. Thermo Scientific™ NanoDrop 2000 spectrophotometer was used to quantify and assess purity of extracted RNA, using 1 µl of RNase-free water as a blank measurement.

### **3.2.8. cDNA synthesis through reverse transcription (RT) from RNA extracted from expanded T-cells**

100-500 ng of the isolated total RNA was reverse transcribed using the M-MLV reverse transcriptase (Promega). Following components were mixed and spinned briefly in the PCR tubes:

Component	Amount
total RNA	1 µg
DNase I (RNase-free, 1U/µl)	1 µl
10x reaction buffer with MgCl <sub>2</sub>	1 µl
Milli-Q® dH <sub>2</sub> O	up to 10 µl of the total volume

and incubated for 30 min at 37°C in the cycler. Next, 1 µl of 50mM EDTA was added to each tube and incubated for 10 min at 65°C. After DNase I treatment, mix primer consisting of 1 µl of oligo-dT primers and 1.5 µl of Milli-Q® dH<sub>2</sub>O was added to each sample, spinned briefly and incubated in the cycler for 5 min in 65°C. The M-MLV RT mix was prepared as follows:

Component	Volume [µl] per tube
M-MLV RT 5x buffer	4
10 mM dNTP	1
M-MLV RT enzyme	1
RNasin	0.5

whereas for NRT control, M-MLV RT was substituted by Milli-Q® dH<sub>2</sub>O.

The PCR program was run in the Bio-Rad C1000 Touch Thermal Cycler with the following parameters:

Duration time	Temperature
1:00:00	42°C
0:10:00	70°C
HOLD	10°C

The samples were diluted 10 times with Milli-Q® dH<sub>2</sub>O and transferred to 1.5 ml Eppendorf tubes. Obtained cDNA template was stored at -20°C.

### 3.2.9. Real-Time Quantitative Polymerase Chain Reaction (RT-qPCR)

Quantitative PCR was performed using one of two methods: SYBR Green and the Premix Ex Taq™ (probe qPCR purchased from TaKaRa). Following mix for qPCR was prepared:

For SYBR Green:

Component	Volume per well [ $\mu$ l]
2x TB Green Premix Ex Taq II	7.5
5 $\mu$ M primer pairs	1.5
Milli-Q <sup>®</sup> dH <sub>2</sub> O	2.5

For TaqMan:

Component	Volume per well [ $\mu$ l]
ExTaq Probe qPCR	7.5
Gene 20x	0.75
Milli-Q <sup>®</sup> dH <sub>2</sub> O	3.25

11.5  $\mu$ l of mix was pipetted to each well of the 96-well microplate and 3.5  $\mu$ l of cDNA was added. The qPCR was run in the Bio-Rad C1000 Touch Thermal Cycler using following program:

Duration time [min]	Temperature
00:30	95°C
00:05	95°C
00:30	60°C + acquire
GO TO 2	39-44 repeats
Melting curve	65-95°C, 0.5°C/step

The procedures were conducted according to the manufacturer's instructions (TaqMan™ Gene Expression Assays obtained from Thermo Fisher Scientific). TaqMan™ probes were used in this study for quantification of DDIT3 (CHOP), GRP94 and HSPA5 (BIP). Logarithmic changes in the fluorescence of the product enabled us to estimate the initial amount of the product and visualize the differences in the gene expression levels. The data were analysed either automatically using BioRad CFX Manager computer program or independently via the quantitation cycle (Cq) values for target genes converted to values of relative expression using the relative quantification (RQ) method ( $2^{-\Delta\Delta Cq}$ ). Target gene expression was calculated relative to Cq values for the HPRT control housekeeping gene.

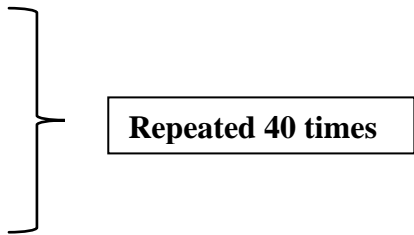
### 3.2.10. Polymerase Chain Reaction (PCR) for XBP1 splicing and agarose gel electrophoresis

Following components were mixed in the Eppendorf tube:

Component	Volume [ $\mu$ l] per tube ( $\Sigma$ 10 $\mu$ l)
Milli-Q <sup>®</sup> dH <sub>2</sub> O	5.3
10x buffer	1
Mg (25mM)	0.6
dNTP	0.2
XBP1-span26_for (10 $\mu$ M)	0.4
XBP1-span26_rev (10 $\mu$ M)	0.4
vortex before adding the Taq-Polymerase	
Taq-Pol. (5U/ $\mu$ l)	0.1
cDNA template	2

and 8  $\mu$ l of the mixture added to each of the Eppendorf tubes. Following cDNA templates were added: patient, parent, NRT, SH-SY5Y + Tun, NTC. The PCR programme was run as follows:

No.	Step	Temp. [ $^{\circ}$ C]	Time
1.	<b>Initial denaturation</b>	95	2 min
2.	<b>Denaturation</b>	95	15 s
3.	<b>Annealing</b>	56	20 s
4.	<b>Elongation</b>	72	30 s
5.	<b>Final elongation</b>	72	5 min
6.	<b>Final holding</b>	8	$\infty$



PCR products were analysed on 0.8 % - 2.0 % agarose gels to verify the correct product size and product abundance. The gel was supplemented with 12  $\mu$ l/100 ml RedSafe<sup>TM</sup> to label the nucleic acid (diluted 1:10 with 1 x TAE-buffer). DNA were taken up in 1x DNA loading buffer (6 x Loading dye: 50 % (v/v) glycerol, 50 mM EDTA (pH 8.0), 0.25 % (w/v) bromophenol blue). Gel electrophoresis was run at 100 V for 60 min in 1 x TAE-buffer (40 mM Tris, 20 mM

acetic acid, 1 mM EDTA). DNA ladders with fragment lengths of 100 bp and 500 bp (Invitrogen, Darmstadt, Germany) were used as control. The evaluation was done with a transilluminator (Nippon Genetics Europe, Düren) at 400 nm wavelength. For documentation, the gels were photographed in the UV transilluminator at 312 nm (Herolab Laborgeräte, Wiesloch).

### **3.2.11. Data representation and statistical analysis**

Data are typically mean  $\pm$  SEM and are analysed by pair ratio t-test between two groups. Charts and statistical analyses were generated using Microsoft Excel or GraphPad version Prism 8. A p value  $<0.05$  was considered significant.

### **3.2.12. Flow cytometry (FCM) procedure**

The activation status of human T cells was measured by flow cytometry as outlined below. Frozen cells (see section methods – sample preparation) were thawed, washed twice in Phosphate-Buffered Saline (PBS) (300 g, 8 min, 4 °C) and counted using BD Trucount™ tubes according to the manufacturer's protocol. The differentiation between living and dead cells was based on the cell phenotype in an FSC-A/SSC-A plot, as shown in **Figure 11**.  $1 \times 10^6$  live cells were transferred into 5 ml round-bottom polypropylene tubes (FACS tubes) and used for further staining.



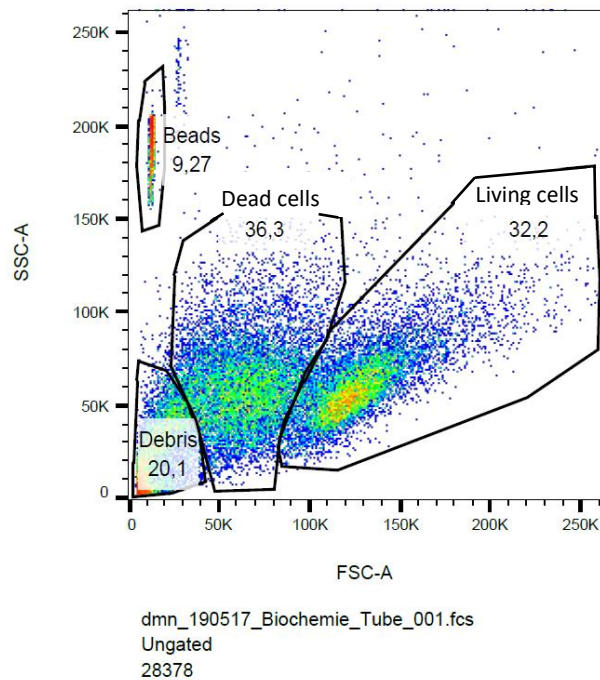


**Figure 11. Example of a TruCount image** where the dead cells can be ignored in the cell number determination. The proportion of living cells here equals:  $0.322/(0.322+0.363) = 0.47$  (47 %).

Cells were washed once again with 2 ml PBS (300 g, 8 min, 4 °C) and the supernatant was decanted afterwards. 50 µ of NIR™ dye (diluted 1:150 in PBS) were pipetted onto the cells and after vortexing incubated for 30 min at room temperature (RT) in the dark. Cells were washed with FACS buffer (see section: materials, flow cytometry) (300 g, 8 min, 4 °C), then 50 µl of ‘FcR Blocking Reagent, human’ diluted 1:50 in FACS buffer were added, and incubated for 5 min at 4 °C in the dark. Afterwards, 50 µl of staining solution containing antibodies against lineage and activation markers (see Materials, Flow cytometry fluorophore-conjugated primary antibodies) were added without washing and incubated for 20 min at 4 °C in the dark. Finally, the cells were washed twice using 1 ml FACS-buffer (300 g, 8 min, 4 °C), resuspended in 180 µl FACS-buffer and measured on an LSR II.

### 3.2.13. Flow cytometric analysis

The flow cytometric data were acquired at a BD™ LSR II (BD Biosciences) using the software FACSDiva (BD Biosciences). Data were analysed with FlowJo version 10.7.1 (Treestar, Ashland, USA). The results were presented as a histogram or dot plot, where the numbers within the gates correspond to the percentage of cells included. Following gating scheme was applied (**Figure 12**):

1. Doublet exclusion
2. Live dead discrimination
3. Lymphocyte gate
4. T cell gate
5. CD4 vs. CD8 positive T cells
6. Other specific cell markers such as CD45R0, CD45RA, CD62L, CD197 followed.

Fluorescence minus one (FMO) controls were used to set positive gates for CD45RA, CD62L, CD197, CD45R0.

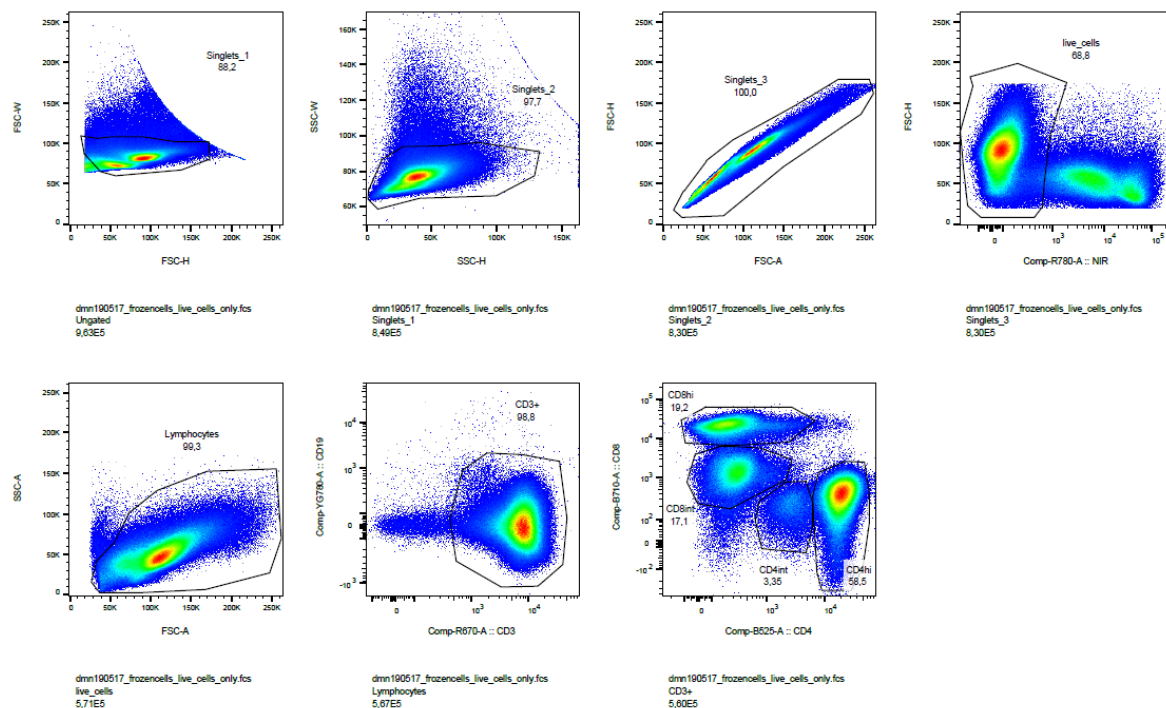


**Figure 12.** The standardized procedure conducted at the beginning of each data analysis consisted of following steps: 1) Doublet exclusion (pictures 1-3), 2) Live dead discrimination (picture 4), 3) Lymphocyte gate (picture 5), 4) T cell gate (picture 6), 5) CD4 vs. CD8 positive T cells (picture 7). Other specific cell markers such as CD45R0, CD45RA, CD62L, CD197 followed.

## 4. Results

### 4.1. Clinical features of two subjects carrying *de novo* missense variants in the *PSMC5* gene and suffering from a syndromic form of ID

In this work, the clinical data relating to two subjects suffering from a syndromic form of ID were meticulously examined. Both subjects have healthy parents and carry heterozygous missense mutations in the *PSMC5* gene at different loci, as depicted in **Fig. 13A**. As illustrated in **Fig. 13B**, the *PSMC5* gene encodes the AAA (ATPase Associated with diverse cellular Activities) Rpt6, a subunit of the 19S regulatory particle of the 26S proteasome complex which participates in substrate unfolding before translocation into the 20S core particle [44]. The clinical anamnesis and examination was collected by our partners: Siddharth Srivastava from Boston Children's Hospital, Harvard, USA, for Subject 1, and by Damara Ortiz from the UPMC Children's Hospital of Pittsburgh, USA, for Subject 2.

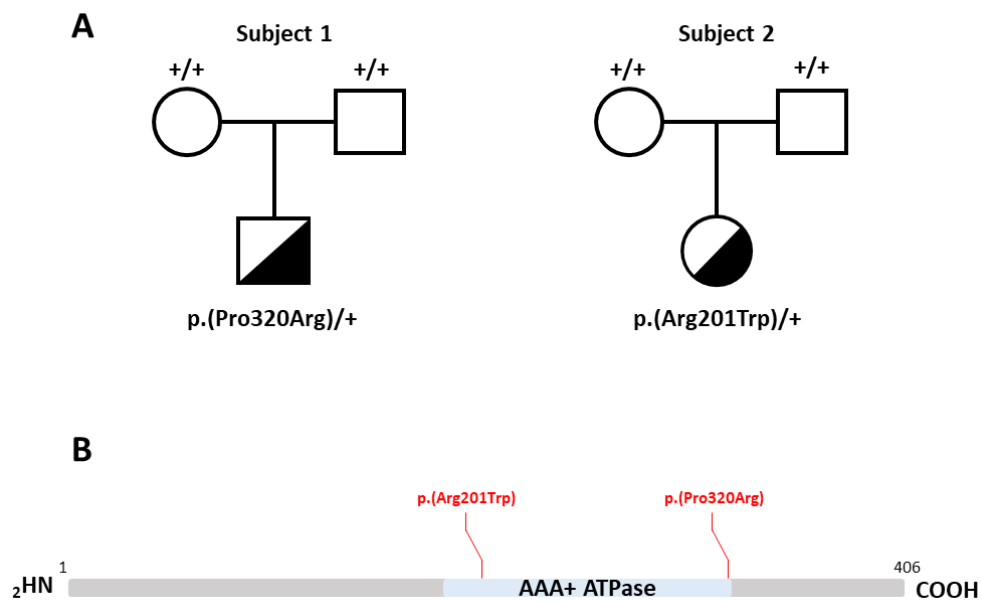


**Figure 13. Identification of two *PSMC5* variants in two unrelated subjects with a syndromic form of ID.** (A) Syndromic ID pedigrees of two families carrying genomic alterations in the *PSMC5* gene. (B) The localization of the two missense variants in the *PSMC5* (i.e. Rpt6) protein are indicated in red. The AAA-ATPase domain of the Rpt6 proteasome subunit of the 19S regulatory particle is depicted in blue in the schematic representation.

As indicated in **Table 1**, Subject 1, carrying the p. (Pro320Arg) *de novo* heterozygous *PSMC5* mutation is a 3.5-year-old boy (data for the time of assessment) with the following observed clinical abnormalities:

- malformations: bilateral ear pits and craniofacial abnormalities such as broad nasal root, bulbous nose,
- cardiovascular: mildly elongated distal transverse aortic arch and hypotonia,
- developmental regression: motor developmental delay (retarded walking – first with 18-20 months), speech delay (with only 5-10 words by 18-24 months which were gradually lost; currently mute, operating with only a few signs),
- intellectual disability: cognitive Digital Intelligence Quotient (DQ)~40%,
- abnormal behaviour and psychosomatic disorders: autism,
- feeding difficulties: dysphagia,
- ophthalmological findings: optic nerve hypoplasia, left ptosis,

and following findings in medical examinations:

- in magnetic resonance imaging of the brain: visible thinning of the corpus callosum, particularly in the region of the splenium, decreased posterior periventricular white matter volume, minimally smaller optic nerves and chiasm.

Subject 2, carrying the p. (Arg201Trp) *de novo* heterozygous *PSMC5* mutation is a 10-year-old girl (data for the time of assessment) with the following clinical abnormalities observed:

- malformations: decreased muscle bulk, pes cavus, skin anomalies,
- cardiovascular: hypotonia,
- renal: increased echogenicity of the medullary pyramids bilaterally,
- neurological: epilepsy (both generalized and partial seizures), sensory hypersensitivity, sleep apnoea,
- developmental regression: motor developmental delay (retarded sitting – at 14 months, slightly retarded walking – alone at 15 months), speech delay (spoke at 4 years old),
- intellectual disability: learning difficulties, failure to thrive,
- abnormal behaviour and psychosomatic disorders: ADHD, disruptive behaviour, tics,
- feeding difficulties: dysphagia,
- ophthalmological findings: mild convergence insufficiency in 2013, blue sclera,

with no mentioned additional findings in medical examinations such as magnetic resonance imaging of the brain.

Interestingly, while it was clear that the mutation in *PSMC5* gene emerged *de novo* (heterozygous) in Subject 1, the inheritance in the case of Subject 2 was a little more questionable, as both parents are diagnosed with intellectual disability and the mother additionally with attention deficit hyperactivity disorder (ADHD). However, despite these clinical symptoms observed in parents, it was proven to be as well a heterozygous *de novo* mutation. Importantly, while Subject 2 exhibits a normal 46XX female karyotype, Subject 1 carries a likely benign deletion of 7q11.23 from 55 to 234 kB, as detected in chromosomal microarray [160].

	Subject 1	Subject 2
Chromosomal localization (GRCh37)	Chr17:g.61908775C>G	Chr17:g.61908217C>T
Variant in <i>PSMC5</i>	c.959C>G	c.601C>T
Reference sequence NM_002805.5 according to NCBI	p.(Pro320Arg)	p.(Arg201Trp)
Inheritance	<i>de novo</i> (heterozygous)	<i>de novo</i> (heterozygous)
Family history	negative	negative
Gender	male	female
Age at last assessment	3 years 7 months	10 years
Birth weight (grams/SD)	3520/-0.07	2860/-1.19
Birth length (cm/SD)	53.34/+1.21	ND
OFC at birth (cm/SD)	ND	ND
Weight at assessment (kg/SD)	16/+0.30	22.3/-2.21
Length at assessment (cm/SD)	96/-0.80	129.5/-1.31

OFC at assessment (cm/SD)	51/+0.62	51/-0.94 SD
Karyotype	ND	normal 46XX
Chromosomal microarray	likely benign deletion of 7q11.23 from 55 to 234 KB in range; the genes within the copy number variant are pseudogenes and are not listed in OMIM as being associated with any known syndrome; there are overlapping deletions listed in DGV	normal female (no SNPs)

**Table 1. Summary of the genetic and clinical features of two *PSMC5* variants.** Nomenclature HGVS V2.0 according to mRNA reference sequence NM\_002805.5. Nucleotide numbering uses +1 as the A of the ATG translation initiation codon in the reference sequence, with the initiation codon as codon 1. ND: not determined; SD: standard deviation; OFC: occipital frontal circumference.

#### 4.2. Impact of the identified *PSMC5* genomic alterations on proteasome function in patient T cells

Given that recent studies have shown that genomic alterations in genes encoding proteasome subunits may result in proteasome loss-of-function, as initially described for *PSMB8* (encoding the  $\beta 5i/LMP7$  subunit of the 20S core particle) or lately for *PSMA3* (encodes  $\alpha 7$ ), *PSMB4* (encodes  $\beta 7$ ), *PSMB9* (encodes  $\beta 1i/LMP2$ ), and *PSMB10* (encodes  $\beta 2i/MECL1$ ) [161; 162], we first sought to determine the impact of our two *PSMC5* variants on proteasome subunit composition. To this end, T cells isolated from both subjects were assessed for their contents in various proteasome subunits by means of SDS-PAGE and western-blotting. As shown in **Fig. 14**, the steady-state expression levels of *PSMC5/Rpt6* were lower in Subject 1 than in its respective control, and similar in control and patient T cells in the case of Subject 2, indicating that the p.(Pro320Arg) missense mutation had an impact on *PSMC5/Rpt6* protein half-life, but p.(Arg201Trp) not. Likewise, apart from the  $\beta 5$  standard subunit which was downregulated in Subject 2 (**Fig. 14**), the expression profile of most of the 20S and 19S

proteasome subunits did not substantially vary between patient and control T cells. These suggest that proteasome expression and composition was not severely compromised in subjects with *PSMC5* variants.

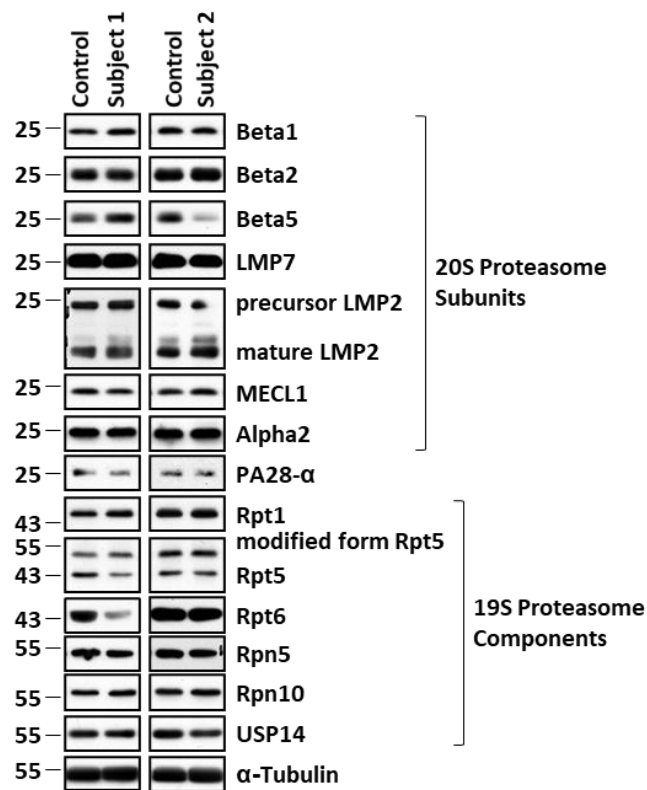


**Figure 14. Subjects carrying *PSMC5* variants exhibit no major changes in proteasome subunit expression and/or composition.** Five to twenty micrograms of RIPA lysates from T cells isolated from Subjects 1 and 2 as well as their related controls were separated by SDS-PAGE followed by western-blotting using antibodies directed against Beta1, Beta2, Beta5, LMP7, LMP2, MECL1, Alpha2, PA28- $\alpha$ , Rpt1, Rpt5, Rpt6, Rpn5, Rpn10 and USP14, as indicated. Equal protein loading was ensured by probing the membrane with an anti- $\alpha$ -tubulin antibody.

To ascertain whether proteasome assembly was affected by either one of the two identified *PSMC5* missense mutations, whole-cell lysates from control and patient T cells were separated by native-PAGE prior to western-blotting analysis. As expected, staining with an antibody directed against the  $\alpha 6$  subunit revealed two major bands corresponding to the 20S and 26S proteasome complexes (**Fig. 15**). Interestingly, our data revealed a decreased signal for both of the *PSMC5*/Rpt6 and *PSMD12*/Rpn5 subunits in the 26S region (**Fig. 15**), suggesting that the incorporation of these subunits into 26S proteasomes was defective in patient T cells. Likewise,

as illustrated in **Fig. 15**, the signals for PA28- $\alpha$  were slightly weaker in the 26S area in both patient T cells, pointing for a decreased assembly of PA28-20S-19S hybrid proteasomes.

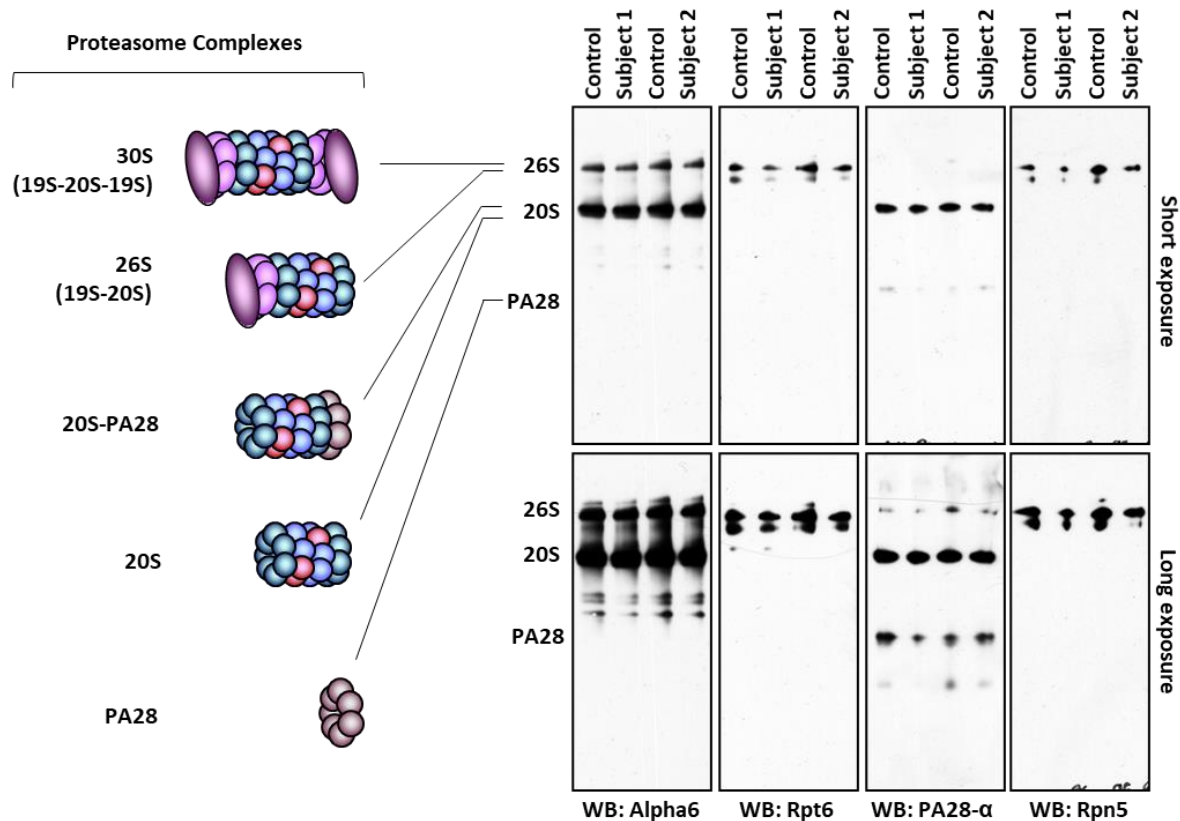


**Figure 15. *PSMC5* variants cause proteasome assembly defects in patients with a syndromic form of ID.** Twenty micrograms of native whole-cell lysates derived from T cells isolated from Subjects 1 and 2 as well as related controls were separated by 3-12% native-PAGE prior to transfer to PVDF membranes and probed with antibodies specific for Alpha6, Rpt6, PA28- $\alpha$  and Rpn5, as indicated. Two exposure times are shown.

Taken together, these data indicate that patient T cells with *PSMC5* variants exhibit an assembly defect primary affecting 26S proteasomes. To address the question whether this dysfunction resulted in a proteasome loss-of-function, we next monitored the proteasome chymotrypsin-like activity of control and patient T cells by exposing them to the Suc-LLVY-AMC fluorescent peptide. As shown in **Fig. 16**, the peptide turnover in both patients was significantly decreased overtime when compared to control cells, indicating that the chymotrypsin-like activity of proteasomes was substantially reduced following incorporation of either one of the two *PSMC5* variants.



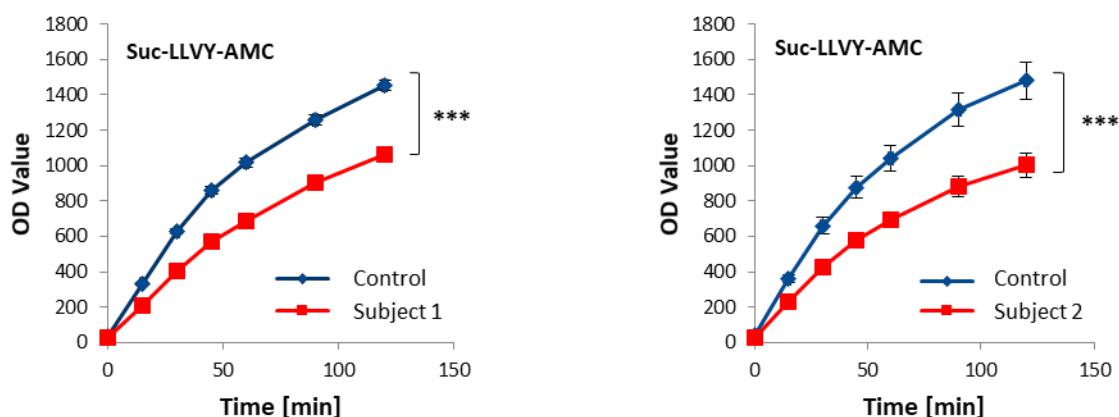


**Figure 16. Subjects with a syndromic form of ID carrying *PSMC5* variants exhibit reduced proteasome chymotrypsin-like activity.** Ten micrograms of TSDG-cell lysates from T cells isolated from Subjects 1 and 2 as well as their related controls were assessed for their ability to cleave the Suc-LLVY-AMC proteasome substrate on 96-well plates, as indicated. Peptide turnover was detected by measuring fluorescence AMC at 360/460 nm over a 2-h period of time. Statistical significance was assessed by ratio paired t test, \*\*\* $p < 0.0001$ .

Altogether, these data unambiguously identify the *PSMC5* p.(Pro320Arg) and p.(Arg201Trp) alterations as proteasome loss-of-function mutations.

#### 4.3. Impact of the identified *PSMC5* variants on ER stress

Because proteasome loss-of-function mutations have been shown to result in the propagation of ER stress [31], we next compared control and patient T cells carrying *PSMC5* variants for their contents in ER stress-related markers by western-blotting. With the exception of ATF6 whose cleavage was upregulated in Subject 2 (Fig. 17A), our data reveal no signs of ER stress, as evidenced by the steady-state expression of GRP94, which remained unaffected in both subjects. The notion that both of the *PSMC5* variants failed to engage a strong UPR is further supported by the observation that patient T cells do not upregulate CHOP, a downstream target of the ER stress sensor PERK [100], as determined by RT-qPCR (Fig. 17B). Likewise, T cells from both subjects did not splice XBP1 (Fig. 17C), an mRNA substrate of the ER stress sensor IRE1 [163]. Altogether, these data suggest that the identified *PSMC5* variants are not strong inducers of ER stress /UPR in patient T cells.

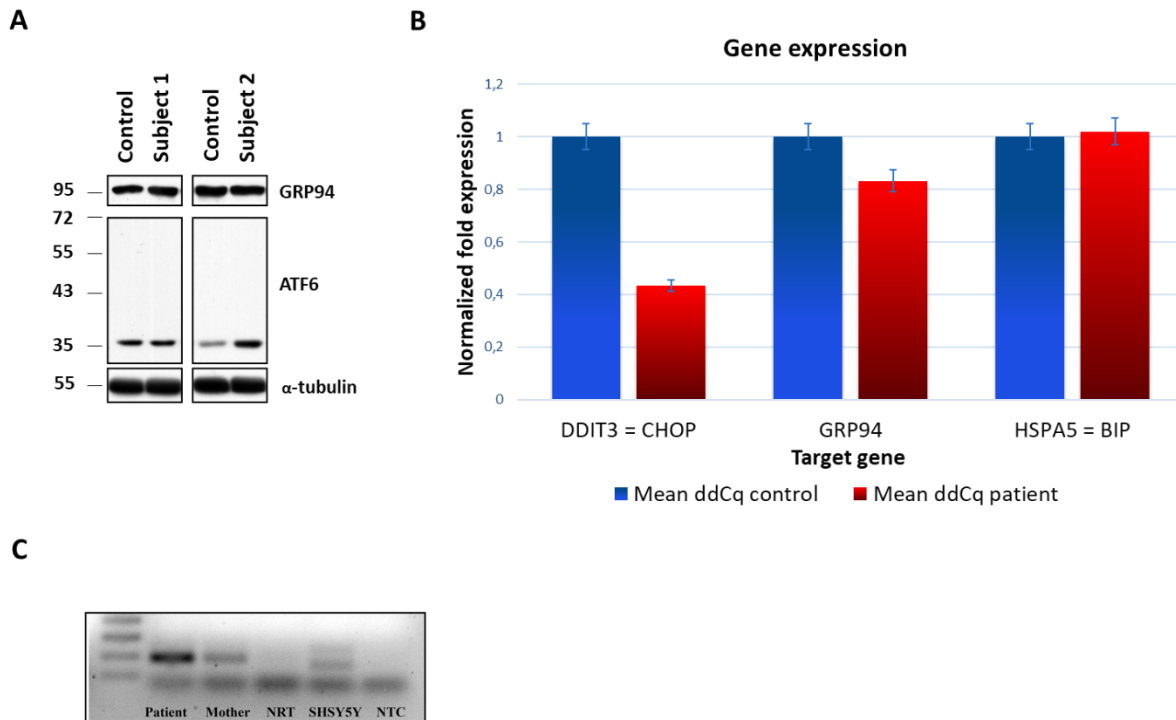


**Figure 17. Subjects carrying *PSMC5* variants exhibit no obvious signs of ER stress.** (A) Five to twenty micrograms of RIPA lysates from T cells isolated from Subjects 1 and 2 as well as their related controls were separated by SDS-PAGE followed by western-blotting using antibodies directed against GRP94 and ATF6, as indicated. Equal protein loading was ensured by probing the membrane with an anti- $\alpha$ -tubulin antibody. (B) Gene expression of DDIT3 (i.e. CHOP), GRP94 and HSPA5 (i.e. BIP) was assayed by RT-qPCR on T cells derived from Subject 1 as well as his respective control (parent). Expression levels were normalized to GAPDH and relative quantifications (RQ) are presented as fold change over controls. (C) XBP1 splicing in T cells from Subject 2 and her related control (mother) was assessed by semi-quantitative PCR. Depiction shows as follows: patient, mother, NRT – no reverse transcriptase control, tunicamycin-stimulated SHSY5Y cell line serving as a positive control, NTC – no template control. Upper band depicts XBP1, lower band – sXBP1.

#### 4.4. Impact of the *PSMC5* variants on the TCF11/Nrf1 compensatory pathway

ER-associated protein degradation (ERAD) designates a cellular pathway which targets misfolded proteins of the ER for ubiquitination and subsequent degradation by proteasomes and is transcriptionally controlled by TCF11/Nrf1 [118]. In response to proteasome inhibition, TCF11/Nrf1 translocates into the nucleus following its de-glycosylation and cleavage by NGLY1 and DDI2, respectively [164; 165]. Interestingly, it was recently observed that mutations in the *NGLY1* gene cause neuromotor impairment, intellectual disability, neuropathy, etc., forming a multisystemic neurodevelopmental disorder [166; 167], thereby supporting the notion that a dysregulation of the TCF11/Nrf1-NGLY1-DDI2 pathway might contribute to

disease pathogenesis in subjects carrying *PSMC5* variants. To answer this question, whole cell lysates from control and patient T cells were monitored for their expression of TCF11/Nrf1 and NGLY1 by western-blotting. As illustrated in **Fig. 18**, even though an upregulation of NGLY1 could be detected in both subjects, the expression and/or processing of TCF11/Nrf1 did not substantially vary between control and patient T cells.

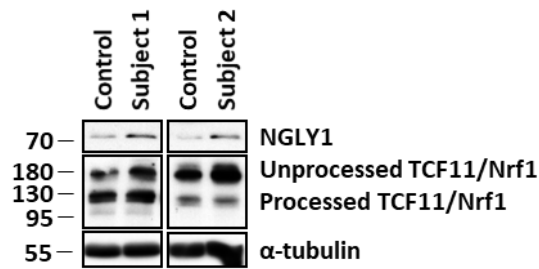


**Figure 18. Subjects carrying *PSMC5* variants express higher levels of NGLY1 which do not result in increased TCF11/Nrf1 processing.** Five to twenty micrograms of RIPA lysates from T cells isolated from Subjects 1 and 2 as well as their related controls were separated by SDS-PAGE followed by western-blotting using antibodies directed against NGLY1, TCF11/Nrf1 and  $\alpha$ -tubulin (loading control), as indicated.

#### 4.5. Impact of the *PSMC5* variants on the mTOR pathway

Because proteasomes generate intracellular peptides which are further degraded into free amino acids which are normally sensed by the mTORC1 complex [168], we hypothesized that the proteasome dysfunction detected in subjects with *PSMC5* variants might result in decreased mTOR signalling. To address this point, we examined the activation status of mTORC1 by monitoring its phosphorylation at Ser2448 as well as the phosphorylation of its downstream target 4E-BP1, both of which being associated with active mTOR signalling [169]. Interestingly, our data show that phosphorylation of mTORC1 and 4E-BP1 was increased in Subject 1 but decreased in Subject 2 (**Fig. 19**), suggesting that the *PSMC5* variants exert opposing effects on mTORC1. Since mTORC1 represses autophagy under normal conditions [170], we further reasoned that this process might be differentially affected by the *PSMC5* variants. To verify this assumption, T cells from Subjects 1 and 2 as well as related controls were assessed for their contents in autophagy-related proteins by western-blotting. In line with its ability to upregulate mTORC1 activity, the p.(Pro320Arg) *PSMC5* variant had a negative

impact on autophagy, as evidenced by decreased levels of LC3b-II in Subject 1 (**Fig. 19**). By contrast, autophagy was increased in Subject 2 carrying the p.(Arg201Trp) variant, whereby the LC3b-II steady-state expression levels were heightened, when compared to her mother (**Fig. 19**). Importantly, autophagy is also involved in the elimination of intracellular organelles including damaged mitochondria, a process commonly referred to as mitophagy [171; 172]. To gain insight into the impact of the *PSMC5* variants on mitophagy, both Subjects 1 and 2 as well as their related controls were assessed for their contents in the Bnip3L/NIX and NDP-52 proteins, involved in receptor- and ubiquitin-mediated mitophagy, respectively [173]. As shown in **Fig. 19**, while NDP-52 was equally expressed in control and patient T cells, Bnip3L/NIX was consistently upregulated in both Subjects 1 and 2, indicating that receptor-mediated mitophagy was increased in these cells.

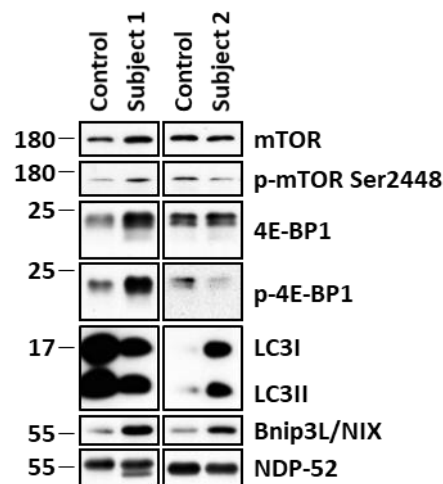


**Figure 19. *PSMC5* variants exhibit distinct effects on mTORC1 signalling and autophagy/mitophagy.** Five to twenty micrograms of RIPA lysates from T cells isolated from Subjects 1 and 2 as well as their related controls were separated by SDS-PAGE followed by western-blotting using antibodies directed against mTOR, phosphor(p)-mTOR (Ser2448), 4E-BP1, phosphor(p)-4E-BP1, Bnip3L/NIX, NDP52, as indicated.

#### 4.6. Impact of the *PSMC5* gene mutations on T cell subpopulations

We next asked the question how proteasome dysfunction caused by *PSMC5* variants affects T cell differentiation. To address this issue, T cells isolated from Subjects 1 and 2 as well as related controls were subjected to phenotypic analysis by flow cytometry. Interestingly, as depicted in **Fig. 20**, our data show a decreased amount of CD3<sup>+</sup> CD8<sup>+</sup> cells in Subject 1 (6.66% CD3<sup>+</sup> CD8<sup>hi</sup> and 5.7% CD3<sup>+</sup> CD8<sup>int</sup> vs. 40.9% CD3<sup>+</sup> CD8<sup>hi</sup> and 14.4% CD3<sup>+</sup>

CD8int) and a concomitant increased amount of CD3+ CD4+ cells (62.6% CD3+ CD4hi and 20.0% CD3+ CD4int vs. 33.8% CD3+ CD4hi and 8.42% CD3+ CD4int) when compared to its relative control. Hence, the p.(Pro320Arg) *PSMC5* variant was characterized by a substantial difference in the relative amount of CD8+ T cells (55.3% control vs. 12.36% p.(Pro320Arg)) and CD4+ T cells (42.22% control vs. 82.6% p.(Pro320Arg)), inducing a shift in CD4/CD8 ratio from 0.76 (control) to 6.68 (Subject 1), the latter being far from the expected standard CD4/CD8 ratio of 1.5-2.5 [174].

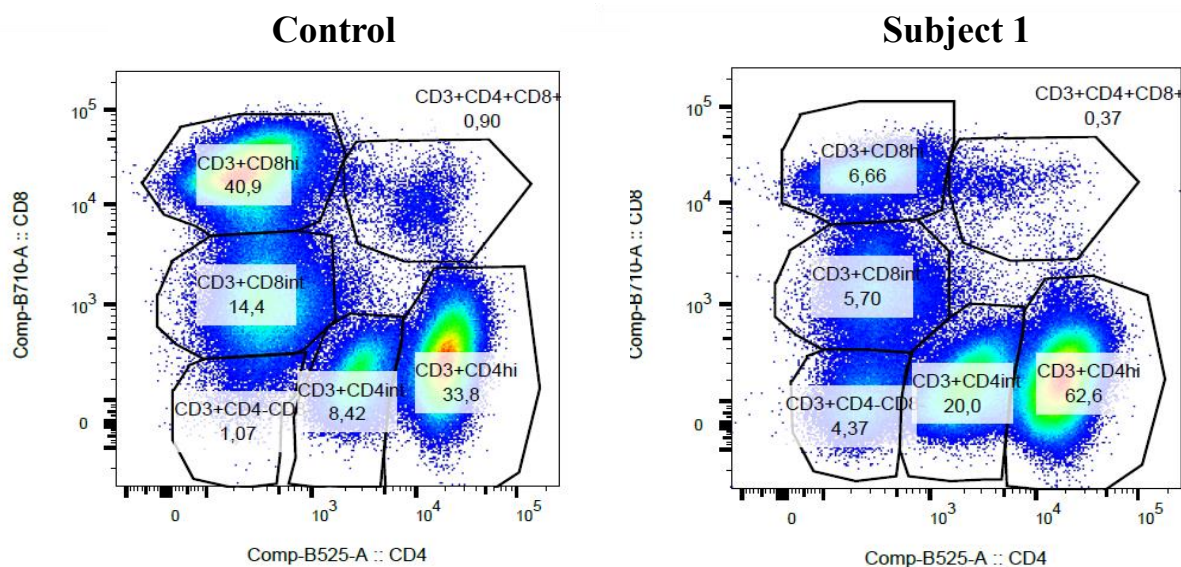


**Figure 20. The p.(Pro320Arg) *PSMC5* variant alters T cell subpopulations in Subject 1.** Dot plots based on flow cytometric results depicting the T cell subpopulations of the examined subjects. The figure in the right panel represents Subject 1 with the p.(Pro320Arg) *PSMC5* variant, while the related control is depicted in the left panel. The numbers within the gates correspond to the percentage of included cells. The gating strategy is described in the Materials & Methods section.

By contrast, in Subject 2 carrying the p.(Arg201Trp) substitution, opposing effects were observed. Indeed, as shown in **Fig. 21**, the relative amount of CD8+ T cells increased from 43.1% in control to 52.7% in Subject 2 (16.8% CD3+ CD8hi and 26.3% CD3+ CD8int vs. 35.3% CD3+ CD8hi and 17.4% CD3+ CD8int, respectively). Accordingly, the relative amount of CD4+ T cells decreased from 53.64% in control to 40.22% in Subject 2 (49.3% CD3+ CD4hi and 4.34% CD3+ CD4int vs. 35.6% CD3+ CD4hi and 4.62% CD3+ CD4in, respectively). Altogether, our data indicate that the CD4/CD8 ratio of Subject 2 was 0.76, namely lower than that of 1.24 detected in control T cells, and lower than the expected standard CD4/CD8 ratio of 1.5-2.5 [174].

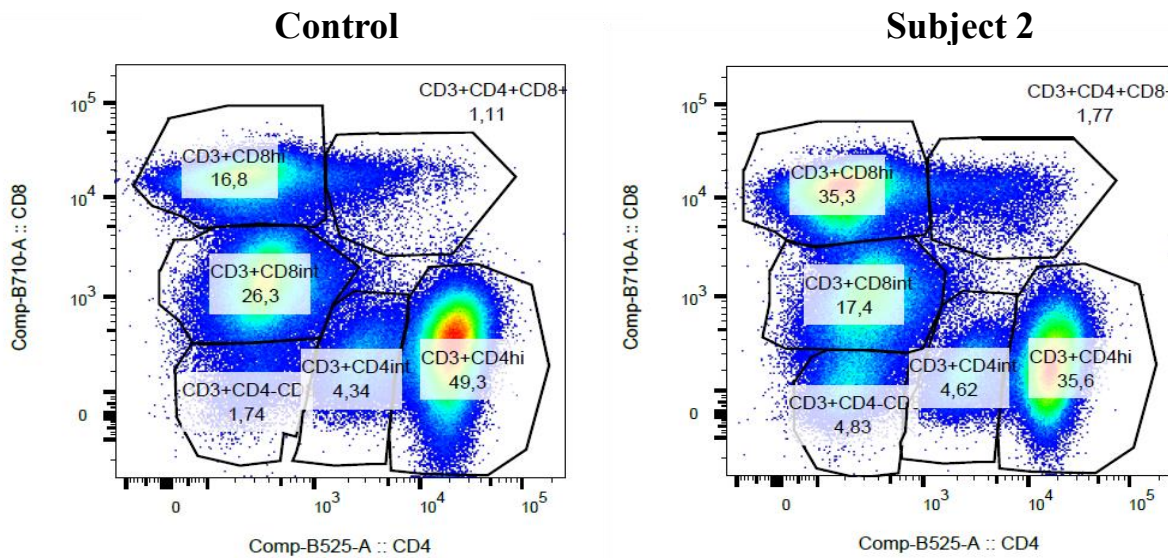


**Figure 21. The p.(Arg201Trp) *PSMC5* variant alters T cell subpopulations in Subject 2.** Dot plots based on flow cytometric results depicting the T cell subpopulations of the examined subjects. The figure in the right panel represents Subject 2 with the p.(Arg201Trp) *PSMC5* variant, while the related control is depicted in the left panel. The numbers within the gates correspond to the percentage of included cells. The gating strategy is described in the Materials & Methods section.

Most importantly, besides the CD4/CD8 ratio which differed between patients, a detailed analysis of the acquired data revealed common T cell features in both Subject 1 and 2. Indeed, the frequency of double-negative (DN, i.e. CD4- CD8-) T cells was increased in both patients (**Fig. 22**), as these constituted 4.37 % and 4.83% of the overall CD3 + T cell populations, when compared to 1.07% and 1.74% in their respective related controls.

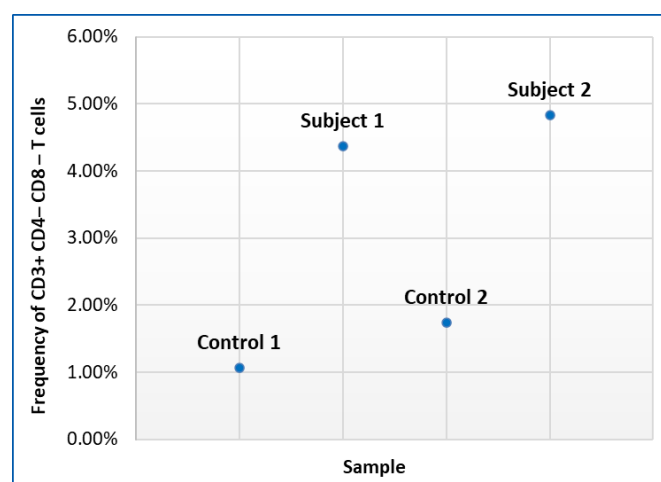


**Figure 22. The *PSMC5* variants augment the frequency of CD4/CD8-double negative (DN) T cells.** The graph depicts the proportion of DN CD3+ CD4- CD8- cells among CD3+ cells in Subject 1 (p.(Pro320Arg) *PSMC5* variant), Subject 2 (p.(Arg201Trp) *PSMC5* variant) and their respective controls, as indicated, based on flow cytometric results and data analysis.

## 5. Discussion

### 5.1. Patient T cells with *PSMC5* variants exhibit severe signs of proteasome dysfunction

Recent studies have shown that mutations in proteasome subunit encoding genes might have an impact on proteasome composition, as first described for *PSMB8* (encoding  $\beta 8$  subunit of the 20S core particle) or lately for *PSMA3* (encodes  $\alpha 7$ ), *PSMB4* (encodes  $\beta 7$ ), *PSMB9* (encodes  $\beta 1i$ ) [161; 162]. Our SDS-PAGE /western-blotting analysis of patient T cells carrying the p.(Pro320Arg) or p.(Arg201Trp) *PSMC5* variants show that the expression steady-state level of most of the 19S and 20S proteasome subunits was not affected by either one of the *PSMC5* missense mutations (**Fig. 14**). These data imply that both *PSMC5* variants escape nonsense-mediated mRNA decay and do not cause haploinsufficiency. In spite of the fact that the p.(Pro320Arg) and p.(Arg201Trp) *PSMC5* variants are translated at the protein level, these fail to assemble into proteasomes, as evidenced by the reduced amounts of 26S complexes detected in patient T cells (**Fig. 15**). Consequently, T cells with *PSMC5* variants were less able to degrade the Suc-LLVY substrate than their control counterparts (**Fig. 16**). Altogether, these data unambiguously demonstrate that both of the p.(Pro320Arg) and p.(Arg201Trp) *PSMC5* substitutions are loss-of-function mutations. Considering the critical role of proteasomes in many essential cellular processes, such as cell cycle and division, differentiation and development, morphogenesis of neuronal networks, modulation of cell surface receptors, ion channels and the secretory pathway, DNA repair, replication, transcriptional regulation, transcriptional silencing, signal transduction, long-term memory, circadian rhythms, regulation of the immune and inflammatory responses, and biogenesis of organelles, it is highly likely that such *PSMC5* variants actively contribute to disease pathogenesis and severity of clinical manifestation of the syndrome in the investigated subjects [29; 44; 157].

### 5.2. *PSMC5* variants dysregulate mTORC1 signalling in patient T cells

Surprisingly, proteasome dysfunction in T cells with *PSMC5* variants was not accompanied by increased ER stress, as determined by the expression levels of HSPA8 and GRP94 which did not substantially vary between control and patient cells (**Fig. 17**). This observation is intriguing but might be partially explained by the potential engagement of compensatory mechanisms. One major pathway rescuing proteasome dysfunction is the

TCF11/Nrf1-NGLY1-DDI2 axis, whereby TCF11/Nrf1 acts as transcription factor and induces proteasome genes following de-glycosylation and cleavage by the NGLY1 and DDI2 proteins, respectively [118]. In this regard, the activation of TCF11/Nrf1 is particularly well exemplified by other proteasomes loss-of-function mutations including *PSMC3* in patients suffering from neurodevelopmental syndromes [143]. Nonetheless, our data show that, in spite of an upregulation of NGLY1 in both subjects, no substantial differences in the expression and/or processing of TCF11/Nrf1 could be observed between control and patient cells (**Fig. 18**). This, however, does not preclude that TCF11/Nrf1 does not undergo activation in other cells types. The observation that NGLY1 is increased in T cells carrying *PSMC5* variants is interesting and suggests that its steady-state expression level is actively regulated by proteasomes. This finding is even more relevant considering the fact that NGLY1 deficiency has been reported to cause developmental delay and intellectual disability [166; 175], namely clinical features which are highly similar to those of Subjects 1 and 2 carrying *PSMC5* variants (**Table 1**). Herein, our data suggest that both deficiency and excess of NGLY1 might result in the acquisition of neuronal phenotypes. The potential contribution of elevated NGLY1 to the pathogenesis of the neurodevelopmental syndrome detected in subjects with *PSMC5* loss-of-function mutations remains, however, to be fully determined.

Interestingly, our data show that proteasome dysfunction in T cells carrying *PSMC5* variants is perceived by mTORC1 whose activity is dramatically changed in both subjects. Indeed, phosphorylation of mTOR at Ser2448 and 4E-BP1 indicative of increased mTORC1 signalling was detected in Subject 1 by western-blotting (**Fig. 19**). This observation is in line with the assumption that defective proteasomes deprive cells of intracellular peptides and a fortiori free amino acids which normally activate mTORC1 [169]. This notion is however challenged by the fact that both phospho-mTOR and -4E-BP1 are decreased in Subject 2, indicating that mTORC1 activity is reduced under these conditions. These contrasting results are difficult to explain but may reflect distinct abilities of the *PSMC5* variants to unfold protein substrates before degradation. It is conceivable that, in contrast to the p.(Pro320Arg) variant, the p.(Arg201Trp) variant is more efficient at denaturing arginine- and/or leucine-rich proteins, thereby facilitating their degradation and supplying free arginine and/or leucine, two potent activators of mTORC1 [169]. On the other hand, mTORC1 may be activated by additional stimuli including signalling cascades initiated by growth factors [168] and one cannot exclude that the *PSMC5* variants might differentially affect any of these pathways. In any case, the mechanisms by which *PSMC5* loss-of-function mutations impact mTORC1 warrants further



investigations, notably through the investigations of further patients carrying variants in this gene.

### **5.3. Both *PSMC5* variants promote receptor-mediated mitophagy in patient T cells**

As a central regulator of important physiological cellular functions such as growth and proliferation, metabolism, death, and survival, mTORC1 represses autophagy [170; 176; 177]. In agreement with their respective mTORC1 activation patterns, autophagy was decreased in Subject 1 and increased in Subject 2, as determined by monitoring the steady-state expression levels of LC3b-II (**Fig. 19**). Noteworthy, autophagy is also implicated in the removal of damaged intracellular organelles, including mitochondria, in a process referred to as mitophagy. It is widely known that the process of mitophagy is critical for maintaining proper cellular functions [172]. Moreover, there is increasing evidence that mitophagy is significantly impaired in several human pathologies, including ageing and age-related diseases such as neurodegenerative disorders, cardiovascular pathologies, and cancer [178].

Importantly, the transmembrane LIR-motif containing protein Bnip3L/NIX was consistently up-regulated in Subjects 1 and 2 with *PSMC5* variants, as determined by western-blotting (**Fig. 19**). These data suggest that receptor-mediated mitophagy is increased in these cells. This observation is fully in line with the fact that the *BNIP3L* gene is transcriptionally induced by the hypoxia-inducible transcription factor HIF-1 $\alpha$ , a well-known substrate of the 26S proteasome [179]. As such, these data also imply that any proteasome dysfunction would lead to HIF-1 $\alpha$  accumulation and subsequent transcription of BNIP3L. The observation that BNIP3L is increased in response to proteasome impairment is interesting and likely to contribute to the pathogenesis of the neurodevelopmental delay in patients with *PSMC5* variants, especially considered the fact that more and more studies support the central role of mitochondrial dysfunction in the (still widely unclear) pathogenesis of a myriad neurodegenerative disorders [180; 181] and interferonopathies [182]. For instance, mitochondrial impairment in the form of distorted mitochondrial morphology, impaired respiratory chain function, and altered mitochondrial DNA, was found to be one of the main disease drivers of Alzheimer disease (AD) [180]. As mitochondrial calcium signalling is a key regulator of both metabolic dysfunction and progressive neuronal loss, it is also linked to AD progression [183]. Furthermore, amyloid pathology and mitochondrial dysfunction appear to be bi-directionally correlated, with growing

body of evidence presenting mitochondrial dysfunction as a common pathomechanism involved in many of the hallmark features of the AD brain, such as amyloid-beta (A $\beta$ ) aggregates (amyloid plaques), neurofibrillary tangles, cholinergic system dysfunction, impaired synaptic transmission and plasticity, oxidative stress, and neuroinflammation, all of which leading to neurodegeneration and cognitive dysfunction [184; 185].

Interestingly, mitochondria play an even more substantial role in the pathology of the Parkinson's disease (PD), as close connection between alpha-synuclein accumulation and mitochondrial dysfunction has been observed [180]. Additionally, several studies demonstrate the impairment of the respiratory chain activity. However, in contrast to AD, where misfolded amyloid beta peptide 1-42 (Abeta) accumulates in the neuronal ER and extracellularly as plaques, in PD there is abnormal accumulation of alpha-synuclein in neuronal cell bodies, axons, and synapses [186]. This is also the case in dementia with Lewy bodies (DLB), where Abeta 1-42 may additionally promote alpha-synuclein accumulation and neurodegeneration [187]. Synaptic damage and mitochondrial dysfunction have also been associated with early events in the pathogenesis of atypical parkinsonisms, in particular multiple system atrophy, and other neurodegenerative disorders, such as Huntington disease [188].

To sum up, available knowledge is still not sufficient to clearly state whether mitochondrial dysfunction plays a primary role in the initial stages of these diseases or is secondary to other phenomena [180]. Nevertheless, translocation of misfolded proteins to the mitochondrial membrane might play a key role in both triggering and perpetuating neurodegeneration, and mitochondrial impairment remains critical for maintaining and fostering the neurodegenerative processes. In this light, increased receptor-mediated mitophagy in response to proteasome impairment with high probability contributes to the pathogenesis of the neurodevelopmental delay in patients with *PSMC5* variants. However, this awareness brings also prospect of new targeted therapy approaches, as research has shown that by activating autophagy, symptoms of neurodegenerative disorders may be significantly relieved [189].

#### **5.4. *PSMC5* gene mutations in the context of interferonopathies**

Interferonopathies are a group of hereditary autoinflammatory diseases, characterized by a dysregulation of the interferon pathway. Clinically heterogeneous, they share some peculiar clinical features, such as neutrophilic dermatosis, panniculitis with progressive

lipodystrophy and muscle atrophy, joint contractures with extremity deformity, sometimes hepatosplenomegaly and hypochromic or haemolytic anaemia, and in many cases also an early-onset metabolic syndrome, with systemic hypertension and dyslipidaemia [31; 190; 191; 192]. As demonstrated in **Table 1** and in the detailed description before it, both investigated subjects were found to manifest some of these specific clinical features, and especially to share some of the neurological findings common for interferonopathies, among which leukodystrophy, spasticity, demyelination, seizures, microcephaly associated to skin manifestations or glaucoma, subacute encephalopathy with basal ganglia calcifications in the first years of life, and microcephaly, were described [193].

Neurological involvement is a prominent feature of nearly all interferonopathies, which may result from the fact that IFN type I is involved in regulating microglial function, both during development and in response to ischaemia, neurodegeneration, and neuroinflammation [193; 194]. The microglia is the local component of the CNS innate immune system and plays a pivotal role in the modulation of CNS inflammatory homeostasis. It is essential for the phagocytosis of myelin debris and provides support to oligodendrocytes and axons, also during synaptogenesis, overall protecting the white matter [195]. Hence, a disruption in the fine balance between necessary clearance and excessive phagocytosis is the basis of neurodegenerative pathologies, while type I IFN plays a substantial role in regulating this balance. It cannot be excluded that it constitutes one of the mechanisms contributing to the intellectual disability also in the investigated subjects.

Definition of type I interferonopathies indicates that autoinflammation can be both interferon and non-interferon related, and that a primary disturbance of the innate immune system in some cases can turn into autoimmunity [196]. The type I interferonopathy should be suspected especially if an autoimmune disease presents a very early onset or is resistant to standard treatment, or when it appears in several members of the same family [197].

The IFN family includes two main classes of related cytokines: type I IFNs and type II IFN [198]. Type I IFNs are potent inflammatory polypeptides, ubiquitously expressed by immune and non-immune cells, including macrophages, lymphocytes, dendritic cells, fibroblasts, and hematopoietic plasmacytoid dendritic cells. On the other hand, type II IFN, represented solely by IFN- $\gamma$ , is an important component of the innate antiviral response and is predominantly produced by NK [199]. Being aware of the impact of IFNs on both antiviral and immunomodulatory functions, as well as of the fact that Mendelian mutations may cause a

disturbance of the homeostatic control of this system [182], the hypothesis that the *PSMC5* gene mutations may affect the IFN levels is worth shedding light on, but requires further investigation. Concurrently, characterization of these molecular pathogenetic mechanisms is a critical step forward to discovering more effective target therapies [193].

## 5.5. Conclusion and outlook

In conclusion, in our study we have characterised the p.(Pro320Arg) and p.(Arg201Trp) *de novo* heterozygous missense mutations in the *PSMC5* gene carried by the patients with the syndromic form of intellectual disability and given new potential insights into the pathophysiological mechanisms and molecular basis of these syndromes. We have shown that both investigated mutations exhibit an impact on proteasome composition. Although the steady-state expression level of PSMC5/Rpt6 was not affected, analysis of the control and patient T cells under non-reducing conditions revealed that PSMC5/Rpt6 mutants were less efficiently incorporated than their wild-type counterparts. This failure to assemble PSMC5/Rpt6 into fully mature proteasomes is the most probable reason for the significantly reduced proteasome chymotrypsin-like activity in patient T cells that we determined by in-plate assays. These data unambiguously show that both of the investigated *PSMC5* mutations are loss-of-function mutations.

Interestingly, our results have revealed that the investigated *PSMC5* gene mutations induce UPR only in a limited manner but may disturb the functioning of the ER quality control systems and T cell differentiation. Sustained expression of ATF6 was observed solely in the p.(Pro320Arg) mutant and, considering its role in proteostasis and neuroembryogenesis, could hypothetically be one of the mechanisms leading to the intellectual disability. Besides, activated mTOR pathway in this subject suggests a perturbation of free amino acid homeostasis. Lower levels of BiP chaperone that we observed in both mutants may be one of the UPR driving mechanisms. The failure to phosphorylate and thereby activate eIF2 $\alpha$  as a key translation regulator in both p.(Pro320Arg) and p.(Arg201Trp) subjects may result in the inability to regulate protein translation and worsen the already present protein overload. Furthermore, in view of the lower expression of GRP94 chaperone, our studies suggest that the functioning of the ER control systems is disturbed in the *PSMC5* gene mutants.

In addition, our studies show that the *PSMC5* gene mutations do not affect ERAD directly through TCF11/Nrf1 expression but via NGLY1 downregulation which prohibits TCF11/Nrf1 from maintaining its proper cellular function. The resulting inability to enter cell nucleus prevents activation of proteasome gene expression, downregulates mitophagy and anti-inflammatory response. Moreover, due to the NGLY1 downregulation and resulting limited deglycosylation of misfolded proteins, they are not sufficiently directed to the cytoplasmic proteasomal degradation. Given the significant role of NGLY1, its decreased levels may be one of the leading pathomechanisms of global developmental delay in the *PSMC5* gene mutants.

Additionally, our data have proven that in the *PSMC5* gene mutant structural proteins of both mitochondrial and autophagosomal membranes differ from their related controls. The impairment of mitophagy and subsequent accumulation of dysfunctional mitochondria in the mutants not only contributes to oxidative damage, but also because of its vital role in maintaining the normal function of neurons may represent one of the possible mechanisms of neuronal dysfunction and a driver of the intellectual disability in the investigated subjects.

Moreover, the specific clinical features of the examined subjects, such as developmental regression, abnormal behaviour and psychosomatic disorders, as well as neurological deviations, together with the awareness of the early disease onset, led us to suspect that the *PSMC5* mutants may belong to the broad family of interferonopathies. Though confirming this hypothesis requires more profound molecular investigation, type I IFN response could be one of the pathways contributing to the etiopathology of the syndromic intellectual disability. If that would be the case, targeting microglia by modulating brain levels of IFNs could constitute a novel therapeutic strategy for the disorder.

In addition, we have demonstrated that both mutations unambiguously impact T-cell differentiation. Significantly increased CD4/CD8 ratio observed in p.(Pro320Arg) mutant seems to be a clear sign of the ongoing autoimmune process. Contrary tendency observed in p.(Arg201Trp) subject, with inverted CD4/CD8 ratio, suggests chronic inflammation. Observed increased frequency of undifferentiated double-negative T cells in both *PSMC5* gene mutants may be one of the crucial factors in autoimmunity and inflammation. Accordingly, we noted decreased percentage of CD62L<sup>+</sup> CD3<sup>+</sup> CD4<sup>+</sup> lymphocytes which serves as a clinical marker in inflammatory diseases and is typically decreased in autoinflammatory syndromes.

Altogether, our data identified for the first time *PSMC5* as a disease-causing gene for a syndromic form of intellectual disability. How proteasome dysfunction caused by *PSMC5* variants contributes to disease pathogenesis, remains to be fully determined.

## 6. Bibliography

- [1] G. Goldstein, M. Scheid, U. Hammerling, D.H. Schlesinger, H.D. Niall, and E.A. Boyse, Isolation of a polypeptide that has lymphocyte-differentiating properties and is probably represented universally in living cells. *Proc Natl Acad Sci U S A* 72 (1975) 11-5.
- [2] C.M. Pickart, and D. Fushman, Polyubiquitin chains: polymeric protein signals. *Curr Opin Chem Biol* 8 (2004) 610-6.
- [3] A. Varshavsky, Ubiquitin, Academic Press, Encyclopedia of Genetics, 2001.
- [4] S. Vijay-Kumar, C.E. Bugg, and W.J. Cook, Structure of ubiquitin refined at 1.8 Å resolution. *J Mol Biol* 194 (1987) 531-44.
- [5] D. Komander, M.J. Clague, and S. Urbe, Breaking the chains: structure and function of the deubiquitinases. *Nat Rev Mol Cell Biol* 10 (2009) 550-63.
- [6] J.S. Thrower, L. Hoffman, M. Rechsteiner, and C.M. Pickart, Recognition of the polyubiquitin proteolytic signal. *EMBO J* 19 (2000) 94-102.
- [7] M. Miranda, and A. Sorkin, Regulation of receptors and transporters by ubiquitination: new insights into surprisingly similar mechanisms. *Mol Interv* 7 (2007) 157-67.
- [8] S.M. Mali, S.K. Singh, E. Eid, and A. Brik, Ubiquitin Signaling: Chemistry Comes to the Rescue. *J Am Chem Soc* 139 (2017) 4971-4986.
- [9] F. Ohtake, H. Tsuchiya, Y. Saeki, and K. Tanaka, K63 ubiquitylation triggers proteasomal degradation by seeding branched ubiquitin chains. *Proc Natl Acad Sci U S A* 115 (2018) E1401-E1408.
- [10] J.R. Morris, and E. Solomon, BRCA1 : BARD1 induces the formation of conjugated ubiquitin structures, dependent on K6 of ubiquitin, in cells during DNA replication and repair. *Hum Mol Genet* 13 (2004) 807-17.
- [11] H. Nishikawa, S. Ooka, K. Sato, K. Arima, J. Okamoto, R.E. Klevit, M. Fukuda, and T. Ohta, Mass spectrometric and mutational analyses reveal Lys-6-linked polyubiquitin chains catalyzed by BRCA1-BARD1 ubiquitin ligase. *J Biol Chem* 279 (2004) 3916-24.
- [12] A.E. Elia, A.P. Boardman, D.C. Wang, E.L. Huttlin, R.A. Everley, N. Dephoure, C. Zhou, I. Koren, S.P. Gygi, and S.J. Elledge, Quantitative Proteomic Atlas of Ubiquitination and Acetylation in the DNA Damage Response. *Mol Cell* 59 (2015) 867-81.
- [13] A. Ordureau, S.A. Sarraf, D.M. Duda, J.M. Heo, M.P. Jedrychowski, V.O. Sviderskiy, J.L. Olszewski, J.T. Koerber, T. Xie, S.A. Beausoleil, J.A. Wells, S.P. Gygi, B.A. Schulman, and J.W. Harper, Quantitative proteomics reveal a feedforward mechanism for mitochondrial PARKIN translocation and ubiquitin chain synthesis. *Mol Cell* 56 (2014) 360-375.
- [14] M.L. Matsumoto, K.E. Wickliffe, K.C. Dong, C. Yu, I. Bosanac, D. Bustos, L. Phu, D.S. Kirkpatrick, S.G. Hymowitz, M. Rape, R.F. Kelley, and V.M. Dixit, K11-linked polyubiquitination in cell cycle control revealed by a K11 linkage-specific antibody. *Mol Cell* 39 (2010) 477-84.
- [15] M. Gatti, S. Pinato, A. Maiolica, F. Rocchio, M.G. Prato, R. Aebbersold, and L. Penengo, RNF168 promotes noncanonical K27 ubiquitination to signal DNA damage. *Cell Rep* 10 (2015) 226-38.
- [16] Q. Wang, X. Liu, Y. Cui, Y. Tang, W. Chen, S. Li, H. Yu, Y. Pan, and C. Wang, The E3 ubiquitin ligase AMFR and INSIG1 bridge the activation of TBK1 kinase by modifying the adaptor STING. *Immunity* 41 (2014) 919-33.
- [17] H. Huang, M.S. Jeon, L. Liao, C. Yang, C. Elly, J.R. Yates, 3rd, and Y.C. Liu, K33-linked polyubiquitination of T cell receptor-zeta regulates proteolysis-independent T cell signaling. *Immunity* 33 (2010) 60-70.

- [18] A.K. Al-Hakim, A. Zagorska, L. Chapman, M. Deak, M. Peggie, and D.R. Alessi, Control of AMPK-related kinases by USP9X and atypical Lys(29)/Lys(33)-linked polyubiquitin chains. *Biochem J* 411 (2008) 249-60.
- [19] W.C. Yuan, Y.R. Lee, S.Y. Lin, L.Y. Chang, Y.P. Tan, C.C. Hung, J.C. Kuo, C.H. Liu, M.Y. Lin, M. Xu, Z.J. Chen, and R.H. Chen, K33-Linked Polyubiquitination of Coronin 7 by Cul3-KLHL20 Ubiquitin E3 Ligase Regulates Protein Trafficking. *Mol Cell* 54 (2014) 586-600.
- [20] H. Clevers, and R. Nusse, Wnt/beta-catenin signaling and disease. *Cell* 149 (2012) 1192-205.
- [21] Y. Shimizu, L. Taraborrelli, and H. Walczak, Linear ubiquitination in immunity. *Immunol Rev* 266 (2015) 190-207.
- [22] M. Karin, and Y. Ben-Neriah, Phosphorylation meets ubiquitination: the control of NF-[kappa]B activity. *Annu Rev Immunol* 18 (2000) 621-63.
- [23] M. Akutsu, I. Dikic, and A. Bremm, Ubiquitin chain diversity at a glance. *J Cell Sci* 129 (2016) 875-80.
- [24] M.J. Lee, B.H. Lee, J. Hanna, R.W. King, and D. Finley, Trimming of ubiquitin chains by proteasome-associated deubiquitinating enzymes. *Mol Cell Proteomics* 10 (2011) R110003871.
- [25] C.T. Neu, Regulation of proteasomal gene expression via the DDI-2/Nrf1 axis, Institute of Medical Biochemistry and Molecular Biology, University of Greifswald, 2019.
- [26] T. Csizmadia, and P. Low, The Role of Deubiquitinating Enzymes in the Various Forms of Autophagy. *Int J Mol Sci* 21 (2020).
- [27] D. Komander, The emerging complexity of protein ubiquitination. *Biochem Soc Trans* 37 (2009) 937-53.
- [28] Y. Li, and D. Reverter, Molecular Mechanisms of DUBs Regulation in Signaling and Disease. *Int J Mol Sci* 22 (2021).
- [29] M.H. Glickman, and A. Ciechanover, The ubiquitin-proteasome proteolytic pathway: destruction for the sake of construction. *Physiol Rev* 82 (2002) 373-428.
- [30] I. Amm, T. Sommer, and D.H. Wolf, Protein quality control and elimination of protein waste: the role of the ubiquitin-proteasome system. *Biochim Biophys Acta* 1843 (2014) 182-96.
- [31] F. Ebstein, M.C. Poli Harlowe, M. Studencka-Turski, and E. Kruger, Contribution of the Unfolded Protein Response (UPR) to the Pathogenesis of Proteasome-Associated Autoinflammatory Syndromes (PRAAS). *Front Immunol* 10 (2019) 2756.
- [32] A.W. Murray, Recycling the cell cycle: cyclins revisited. *Cell* 116 (2004) 221-34.
- [33] F. Bernassola, A. Ciechanover, and G. Melino, The ubiquitin proteasome system and its involvement in cell death pathways. *Cell Death Differ* 17 (2010) 1-3.
- [34] R.Z. Orłowski, The role of the ubiquitin-proteasome pathway in apoptosis. *Cell Death Differ* 6 (1999) 303-13.
- [35] B. Dahlmann, Mammalian proteasome subtypes: Their diversity in structure and function. *Arch Biochem Biophys* 591 (2016) 132-40.
- [36] K. Tanaka, The proteasome: overview of structure and functions. *Proc Jpn Acad Ser B Phys Biol Sci* 85 (2009) 12-36.
- [37] T. Jung, Grune, T., The proteasome and the degradation of oxidized proteins: Part I—structure of proteasomes, 2013.
- [38] Y. Hirano, H. Hayashi, S. Iemura, K.B. Hendil, S. Niwa, T. Kishimoto, M. Kasahara, T. Natsume, K. Tanaka, and S. Murata, Cooperation of multiple chaperones required for the assembly of mammalian 20S proteasomes. *Mol Cell* 24 (2006) 977-84.



- [39] Y. Hirano, K.B. Hendil, H. Yashiroda, S. Iemura, R. Nagane, Y. Hioki, T. Natsume, K. Tanaka, and S. Murata, A heterodimeric complex that promotes the assembly of mammalian 20S proteasomes. *Nature* 437 (2005) 1381-5.
- [40] S. Murata, H. Yashiroda, and K. Tanaka, Molecular mechanisms of proteasome assembly. *Nat Rev Mol Cell Biol* 10 (2009) 104-15.
- [41] W. Heinemeyer, M. Fischer, T. Krimmer, U. Stachon, and D.H. Wolf, The active sites of the eukaryotic 20 S proteasome and their involvement in subunit precursor processing. *J Biol Chem* 272 (1997) 25200-9.
- [42] R.J. Tomko, Jr., and M. Hochstrasser, Order of the proteasomal ATPases and eukaryotic proteasome assembly. *Cell Biochem Biophys* 60 (2011) 13-20.
- [43] R. Verma, L. Aravind, R. Oania, W.H. McDonald, J.R. Yates, 3rd, E.V. Koonin, and R.J. Deshaies, Role of Rpn11 metalloprotease in deubiquitination and degradation by the 26S proteasome. *Science* 298 (2002) 611-5.
- [44] J.A.M. Bard, E.A. Goodall, E.R. Greene, E. Jonsson, K.C. Dong, and A. Martin, Structure and Function of the 26S Proteasome. *Annu Rev Biochem* 87 (2018) 697-724.
- [45] G.A. Collins, and A.L. Goldberg, The Logic of the 26S Proteasome. *Cell* 169 (2017) 792-806.
- [46] M. Aki, N. Shimbara, M. Takashina, K. Akiyama, S. Kagawa, T. Tamura, N. Tanahashi, T. Yoshimura, K. Tanaka, and A. Ichihara, Interferon-gamma induces different subunit organizations and functional diversity of proteasomes. *J Biochem* 115 (1994) 257-69.
- [47] K. Tanaka, Role of proteasomes modified by interferon-gamma in antigen processing. *J Leukoc Biol* 56 (1994) 571-5.
- [48] B. Strehl, U. Seifert, E. Kruger, S. Heink, U. Kuckelkorn, and P.M. Kloetzel, Interferon-gamma, the functional plasticity of the ubiquitin-proteasome system, and MHC class I antigen processing. *Immunol Rev* 207 (2005) 19-30.
- [49] F. Ebstein, N. Lange, S. Urban, U. Seifert, E. Kruger, and P.M. Kloetzel, Maturation of human dendritic cells is accompanied by functional remodelling of the ubiquitin-proteasome system. *Int J Biochem Cell Biol* 41 (2009) 1205-15.
- [50] U. Seifert, L.P. Bialy, F. Ebstein, D. Bech-Otschir, A. Voigt, F. Schroter, T. Prozorovski, N. Lange, J. Steffen, M. Rieger, U. Kuckelkorn, O. Aktas, P.M. Kloetzel, and E. Kruger, Immunoproteasomes preserve protein homeostasis upon interferon-induced oxidative stress. *Cell* 142 (2010) 613-24.
- [51] E. Kruger, and P.M. Kloetzel, Immunoproteasomes at the interface of innate and adaptive immune responses: two faces of one enzyme. *Curr Opin Immunol* 24 (2012) 77-83.
- [52] M. Groettrup, C.J. Kirk, and M. Basler, Proteasomes in immune cells: more than peptide producers? *Nat Rev Immunol* 10 (2010) 73-8.
- [53] A. Angeles, G. Fung, and H. Luo, Immune and non-immune functions of the immunoproteasome. *Front Biosci (Landmark Ed)* 17 (2012) 1904-16.
- [54] F. Ebstein, P.M. Kloetzel, E. Kruger, and U. Seifert, Emerging roles of immunoproteasomes beyond MHC class I antigen processing. *Cell Mol Life Sci* 69 (2012) 2543-58.
- [55] N. Klare, M. Seeger, K. Janek, P.R. Jungblut, and B. Dahlmann, Intermediate-type 20 S proteasomes in HeLa cells: "asymmetric" subunit composition, diversity and adaptation. *J Mol Biol* 373 (2007) 1-10.
- [56] S. Murata, K. Sasaki, T. Kishimoto, S. Niwa, H. Hayashi, Y. Takahama, and K. Tanaka, Regulation of CD8+ T cell development by thymus-specific proteasomes. *Science* 316 (2007) 1349-53.
- [57] B. Guillaume, J. Chapiro, V. Stroobant, D. Colau, B. Van Holle, G. Parvizi, M.P. Bousquet-Dubouch, I. Theate, N. Parmentier, and B.J. Van den Eynde, Two abundant

- proteasome subtypes that uniquely process some antigens presented by HLA class I molecules. *Proc Natl Acad Sci U S A* 107 (2010) 18599-604.
- [58] B. Guillaume, V. Stroobant, M.P. Bousquet-Dubouch, D. Colau, J. Chapiro, N. Parmentier, A. Dalet, and B.J. Van den Eynde, Analysis of the processing of seven human tumor antigens by intermediate proteasomes. *J Immunol* 189 (2012) 3538-47.
- [59] B. Dahlmann, Proteasomes. *Essays Biochem* 41 (2005) 31-48.
- [60] M. Keller, F. Ebstein, E. Burger, K. Textoris-Taube, X. Gorny, S. Urban, F. Zhao, T. Dannenberg, A. Sucker, C. Keller, L. Saveanu, E. Kruger, H.J. Rothkotter, B. Dahlmann, P. Henklein, A. Voigt, U. Kuckelkorn, A. Paschen, P.M. Kloetzel, and U. Seifert, The proteasome immunosubunits, PA28 and ER-aminopeptidase 1 protect melanoma cells from efficient MART-126-35 -specific T-cell recognition. *Eur J Immunol* 45 (2015) 3257-68.
- [61] D. Respondek, M. Voss, I. Kuhlewindt, K. Klingel, E. Kruger, and A. Beling, PA28 modulates antigen processing and viral replication during coxsackievirus B3 infection. *PLoS One* 12 (2017) e0173259.
- [62] Y. Yu, and G.S. Hayward, The ubiquitin E3 ligase RAUL negatively regulates type I interferon through ubiquitination of the transcription factors IRF7 and IRF3. *Immunity* 33 (2010) 863-77.
- [63] S.C. Ling, E.K. Lau, A. Al-Shabeeb, A. Nikolic, A. Catalano, H. Iland, N. Horvath, P.J. Ho, S. Harrison, S. Fleming, D.E. Joshua, and J.D. Allen, Response of myeloma to the proteasome inhibitor bortezomib is correlated with the unfolded protein response regulator XBP-1. *Haematologica* 97 (2012) 64-72.
- [64] H. Xu, M. You, H. Shi, and Y. Hou, Ubiquitin-mediated NFkappaB degradation pathway. *Cell Mol Immunol* 12 (2015) 653-5.
- [65] J. Zhao, G.A. Garcia, and A.L. Goldberg, Control of proteasomal proteolysis by mTOR. *Nature* 529 (2016) E1-2.
- [66] C.P. Ma, C.A. Slaughter, and G.N. DeMartino, Identification, purification, and characterization of a protein activator (PA28) of the 20 S proteasome (macropain). *J Biol Chem* 267 (1992) 10515-23.
- [67] C. Wojcik, K. Tanaka, N. Paweletz, U. Naab, and S. Wilk, Proteasome activator (PA28) subunits, alpha, beta and gamma (Ki antigen) in NT2 neuronal precursor cells and HeLa S3 cells. *Eur J Cell Biol* 77 (1998) 151-60.
- [68] N. Tanahashi, K. Yokota, J.Y. Ahn, C.H. Chung, T. Fujiwara, E. Takahashi, G.N. DeMartino, C.A. Slaughter, T. Toyonaga, K. Yamamura, N. Shimbara, and K. Tanaka, Molecular properties of the proteasome activator PA28 family proteins and gamma-interferon regulation. *Genes Cells* 2 (1997) 195-211.
- [69] J.R. Knowlton, S.C. Johnston, F.G. Whitby, C. Realini, Z. Zhang, M. Rechsteiner, and C.P. Hill, Structure of the proteasome activator REGalpha (PA28alpha). *Nature* 390 (1997) 639-43.
- [70] A. Ciechanover, N-terminal Ubiquitination, *Protein Science Encyclopedia*, 2008, pp. 10-20.
- [71] J.R. Schoenborn, and C.B. Wilson, Regulation of interferon-gamma during innate and adaptive immune responses. *Adv Immunol* 96 (2007) 41-101.
- [72] C. Oikonomou, and L. Hendershot, Disposing of misfolded ER proteins: A troubled substrate's way out of the ER. *Molecular and Cellular Endocrinology* 500 (2019) 110630.
- [73] L. Qi, B. Tsai, and P. Arvan, New Insights into the Physiological Role of Endoplasmic Reticulum-Associated Degradation. *Trends Cell Biol* 27 (2017) 430-440.
- [74] J.A. Olzmann, R.R. Kopito, and J.C. Christianson, The mammalian endoplasmic reticulum-associated degradation system. *Cold Spring Harb Perspect Biol* 5 (2013).

- [75] J.L. Brodsky, and R.J. Wojcikiewicz, Substrate-specific mediators of ER associated degradation (ERAD). *Curr Opin Cell Biol* 21 (2009) 516-21.
- [76] A. Helenius, and M. Aebi, Roles of N-linked glycans in the endoplasmic reticulum. *Annu Rev Biochem* 73 (2004) 1019-49.
- [77] M. Aebi, R. Bernasconi, S. Clerc, and M. Molinari, N-glycan structures: recognition and processing in the ER. *Trends Biochem Sci* 35 (2010) 74-82.
- [78] D.N. Hebert, R. Bernasconi, and M. Molinari, ERAD substrates: which way out? *Semin Cell Dev Biol* 21 (2010) 526-32.
- [79] G.Z. Lederkremer, Glycoprotein folding, quality control and ER-associated degradation. *Curr Opin Struct Biol* 19 (2009) 515-23.
- [80] H. Byun, Y. Gou, A. Zook, M.M. Lozano, and J.P. Dudley, ERAD and how viruses exploit it. *Front Microbiol* 5 (2014) 330.
- [81] C.L. Ward, S. Omura, and R.R. Kopito, Degradation of CFTR by the ubiquitin-proteasome pathway. *Cell* 83 (1995) 121-7.
- [82] R. Verma, S. Chen, R. Feldman, D. Schieltz, J. Yates, J. Dohmen, and R.J. Deshaies, Proteasomal proteomics: identification of nucleotide-sensitive proteasome-interacting proteins by mass spectrometric analysis of affinity-purified proteasomes. *Mol Biol Cell* 11 (2000) 3425-39.
- [83] P. Walter, and D. Ron, The unfolded protein response: from stress pathway to homeostatic regulation. *Science* 334 (2011) 1081-6.
- [84] S.A. Oakes, and F.R. Papa, The role of endoplasmic reticulum stress in human pathology. *Annu Rev Pathol* 10 (2015) 173-94.
- [85] J.F. Diaz-Villanueva, R. Diaz-Molina, and V. Garcia-Gonzalez, Protein Folding and Mechanisms of Proteostasis. *Int J Mol Sci* 16 (2015) 17193-230.
- [86] C. Hetz, and F.R. Papa, The Unfolded Protein Response and Cell Fate Control. *Mol Cell* 69 (2018) 169-181.
- [87] J.H. Lin, P. Walter, and T.S. Yen, Endoplasmic reticulum stress in disease pathogenesis. *Annu Rev Pathol* 3 (2008) 399-425.
- [88] C. Hetz, K. Zhang, and R.J. Kaufman, Mechanisms, regulation and functions of the unfolded protein response. *Nat Rev Mol Cell Biol* 21 (2020) 421-438.
- [89] J.E. Chambers, and S.J. Marciniak, Cellular Mechanisms of Endoplasmic Reticulum Stress Signaling in Health and Disease. 2. Protein misfolding and ER stress. *American Journal of Physiology-Cell Physiology* 307 (2014) C657-C670.
- [90] J.S. Cox, C.E. Shamu, and P. Walter, Transcriptional induction of genes encoding endoplasmic reticulum resident proteins requires a transmembrane protein kinase. *Cell* 73 (1993) 1197-206.
- [91] J.J. Credle, J.S. Finer-Moore, F.R. Papa, R.M. Stroud, and P. Walter, On the mechanism of sensing unfolded protein in the endoplasmic reticulum. *Proc Natl Acad Sci U S A* 102 (2005) 18773-84.
- [92] X. Shen, R.E. Ellis, K. Lee, C.Y. Liu, K. Yang, A. Solomon, H. Yoshida, R. Morimoto, D.M. Kurnit, K. Mori, and R.J. Kaufman, Complementary signaling pathways regulate the unfolded protein response and are required for *C. elegans* development. *Cell* 107 (2001) 893-903.
- [93] M. Calton, H. Zeng, F. Urano, J.H. Till, S.R. Hubbard, H.P. Harding, S.G. Clark, and D. Ron, IRE1 couples endoplasmic reticulum load to secretory capacity by processing the XBP-1 mRNA. *Nature* 415 (2002) 92-6.
- [94] D.S. Coelho, and P.M. Domingos, Physiological roles of regulated Ire1 dependent decay. *Front Genet* 5 (2014) 76.
- [95] A.B. Tam, A.C. Koong, and M. Niwa, Ire1 has distinct catalytic mechanisms for XBP1/HAC1 splicing and RIDD. *Cell Rep* 9 (2014) 850-8.

- [96] M. Maurel, E. Chevet, J. Tavernier, and S. Gerlo, Getting RIDD of RNA: IRE1 in cell fate regulation. *Trends Biochem Sci* 39 (2014) 245-54.
- [97] H.P. Harding, Y. Zhang, and D. Ron, Protein translation and folding are coupled by an endoplasmic-reticulum-resident kinase. *Nature* 397 (1999) 271-4.
- [98] R. Sano, and J.C. Reed, ER stress-induced cell death mechanisms. *Biochim Biophys Acta* 1833 (2013) 3460-3470.
- [99] K.M. Vattem, and R.C. Wek, Reinitiation involving upstream ORFs regulates ATF4 mRNA translation in mammalian cells. *Proc Natl Acad Sci U S A* 101 (2004) 11269-74.
- [100] H.P. Harding, Y. Zhang, A. Bertolotti, H. Zeng, and D. Ron, Perk is essential for translational regulation and cell survival during the unfolded protein response. *Mol Cell* 5 (2000) 897-904.
- [101] S. Deegan, S. Saveljeva, A.M. Gorman, and A. Samali, Stress-induced self-cannibalism: on the regulation of autophagy by endoplasmic reticulum stress. *Cell Mol Life Sci* 70 (2013) 2425-41.
- [102] K. Ameri, and A.L. Harris, Activating transcription factor 4. *Int J Biochem Cell Biol* 40 (2008) 14-21.
- [103] H. Zinszner, M. Kuroda, X. Wang, N. Batchvarova, R.T. Lightfoot, H. Remotti, J.L. Stevens, and D. Ron, CHOP is implicated in programmed cell death in response to impaired function of the endoplasmic reticulum. *Genes Dev* 12 (1998) 982-95.
- [104] M.H. Brush, D.C. Weiser, and S. Shenolikar, Growth arrest and DNA damage-inducible protein GADD34 targets protein phosphatase 1 alpha to the endoplasmic reticulum and promotes dephosphorylation of the alpha subunit of eukaryotic translation initiation factor 2. *Mol Cell Biol* 23 (2003) 1292-303.
- [105] H.Y. Jiang, S.A. Wek, B.C. McGrath, D. Lu, T. Hai, H.P. Harding, X. Wang, D. Ron, D.R. Cavener, and R.C. Wek, Activating transcription factor 3 is integral to the eukaryotic initiation factor 2 kinase stress response. *Mol Cell Biol* 24 (2004) 1365-77.
- [106] E. Kojima, A. Takeuchi, M. Haneda, A. Yagi, T. Hasegawa, K. Yamaki, K. Takeda, S. Akira, K. Shimokata, and K. Isobe, The function of GADD34 is a recovery from a shutoff of protein synthesis induced by ER stress: elucidation by GADD34-deficient mice. *FASEB J* 17 (2003) 1573-5.
- [107] S.J. Marciniak, C.Y. Yun, S. Oyadomari, I. Novoa, Y. Zhang, R. Jungreis, K. Nagata, H.P. Harding, and D. Ron, CHOP induces death by promoting protein synthesis and oxidation in the stressed endoplasmic reticulum. *Genes Dev* 18 (2004) 3066-77.
- [108] Y. Ma, and L.M. Hendershot, Delineation of a negative feedback regulatory loop that controls protein translation during endoplasmic reticulum stress. *J Biol Chem* 278 (2003) 34864-73.
- [109] J.M. Farook, J. Shields, A. Tawfik, S. Markand, T. Sen, S.B. Smith, D. Brann, K.M. Dhandapani, and N. Sen, GADD34 induces cell death through inactivation of Akt following traumatic brain injury. *Cell Death Dis* 4 (2013) e754.
- [110] K. Pakos-Zebrucka, I. Koryga, K. Mnich, M. Ljujic, A. Samali, and A.M. Gorman, The integrated stress response. *EMBO Rep* 17 (2016) 1374-1395.
- [111] S.B. Cullinan, and J.A. Diehl, PERK-dependent activation of Nrf2 contributes to redox homeostasis and cell survival following endoplasmic reticulum stress. *J Biol Chem* 279 (2004) 20108-17.
- [112] A.J. Schindler, and R. Schekman, In vitro reconstitution of ER-stress induced ATF6 transport in COPII vesicles. *Proc Natl Acad Sci U S A* 106 (2009) 17775-80.
- [113] K. Haze, H. Yoshida, H. Yanagi, T. Yura, and K. Mori, Mammalian transcription factor ATF6 is synthesized as a transmembrane protein and activated by proteolysis in response to endoplasmic reticulum stress. *Mol Biol Cell* 10 (1999) 3787-99.

- [114] J. Ye, R.B. Rawson, R. Komuro, X. Chen, U.P. Dave, R. Prywes, M.S. Brown, and J.L. Goldstein, ER stress induces cleavage of membrane-bound ATF6 by the same proteases that process SREBPs. *Mol Cell* 6 (2000) 1355-64.
- [115] J. Shen, X. Chen, L. Hendershot, and R. Prywes, ER stress regulation of ATF6 localization by dissociation of BiP/GRP78 binding and unmasking of Golgi localization signals. *Dev Cell* 3 (2002) 99-111.
- [116] H. Yamazaki, N. Hiramatsu, K. Hayakawa, Y. Tagawa, M. Okamura, R. Ogata, T. Huang, S. Nakajima, J. Yao, A.W. Paton, J.C. Paton, and M. Kitamura, Activation of the Akt-NF-kappaB pathway by subtilase cytotoxin through the ATF6 branch of the unfolded protein response. *J Immunol* 183 (2009) 1480-7.
- [117] M.S. Brown, and J.L. Goldstein, A proteolytic pathway that controls the cholesterol content of membranes, cells, and blood. *Proc Natl Acad Sci U S A* 96 (1999) 11041-8.
- [118] J. Steffen, M. Seeger, A. Koch, and E. Kruger, Proteasomal degradation is transcriptionally controlled by TCF11 via an ERAD-dependent feedback loop. *Mol Cell* 40 (2010) 147-58.
- [119] A.B. Dirac-Svejstrup, J. Walker, P. Faull, V. Encheva, V. Akimov, M. Puglia, D. Perkins, S. Kumper, S.S. Hunjan, B. Blagoev, A.P. Snijders, D.J. Powell, and J.Q. Svejstrup, DDI2 Is a Ubiquitin-Directed Endoprotease Responsible for Cleavage of Transcription Factor NRF1. *Mol Cell* 79 (2020) 332-341 e7.
- [120] S. Meiners, D. Heyken, A. Weller, A. Ludwig, K. Stangl, P.M. Klotzel, and E. Kruger, Inhibition of proteasome activity induces concerted expression of proteasome genes and de novo formation of Mammalian proteasomes. *J Biol Chem* 278 (2003) 21517-25.
- [121] M. Laplante, and D.M. Sabatini, mTOR signaling at a glance. *J Cell Sci* 122 (2009) 3589-94.
- [122] M. Laplante, and D.M. Sabatini, mTOR signaling in growth control and disease. *Cell* 149 (2012) 274-93.
- [123] D.A. Guertin, and D.M. Sabatini, Defining the role of mTOR in cancer. *Cancer Cell* 12 (2007) 9-22.
- [124] L. Ciuffreda, C. Di Sanza, U.C. Incani, and M. Milella, The mTOR pathway: a new target in cancer therapy. *Curr Cancer Drug Targets* 10 (2010) 484-95.
- [125] K. Inoki, J. Kim, and K.L. Guan, AMPK and mTOR in cellular energy homeostasis and drug targets. *Annu Rev Pharmacol Toxicol* 52 (2012) 381-400.
- [126] P. Baldo, S. Cecco, E. Giacomini, R. Lazzarini, B. Ros, and S. Marastoni, mTOR pathway and mTOR inhibitors as agents for cancer therapy. *Curr Cancer Drug Targets* 8 (2008) 647-65.
- [127] J.O. Lipton, and M. Sahin, The neurology of mTOR. *Neuron* 84 (2014) 275-91.
- [128] C. Garza-Lombo, and M.E. Gonsebatt, Mammalian Target of Rapamycin: Its Role in Early Neural Development and in Adult and Aged Brain Function. *Front Cell Neurosci* 10 (2016) 157.
- [129] H.G.S. Liddell, R.; Jones, H.S.; McKenzie, R., *A Greek-English Lexicon*, Oxford University Press, 2018.
- [130] D.J. Klionsky, The molecular machinery of autophagy: unanswered questions. *J Cell Sci* 118 (2005) 7-18.
- [131] M. Kundu, and C.B. Thompson, Autophagy: basic principles and relevance to disease. *Annu Rev Pathol* 3 (2008) 427-55.
- [132] P. Starokadomskyy, and K.V. Dmytruk, A bird's-eye view of autophagy. *Autophagy* 9 (2013) 1121-6.
- [133] D.J. Klionsky, F.C. Abdalla, H. Abeliovich, R.T. Abraham, A. Acevedo-Arozena, K. Adeli, L. Agholme, M. Agnello, P. Agostinis, J.A. Aguirre-Ghiso, H.J. Ahn, O. Ait-Mohamed, S. Ait-Si-Ali, T. Akematsu, S. Akira, H.M. Al-Younes, M.A. Al-Zeer, M.L.

- Albert, R.L. Albin, J. Alegre-Abarrategui, M.F. Aleo, M. Alirezaei, A. Almasan, M. Almonte-Becerril, A. Amano, R. Amaravadi, S. Amarnath, A.O. Amer, N. Andrieu-Abadie, V. Anantharam, D.K. Ann, S. Anoopkumar-Dukie, H. Aoki, N. Apostolova, G. Arancia, J.P. Aris, K. Asanuma, N.Y. Asare, H. Ashida, V. Askanas, D.S. Askew, P. Auberger, M. Baba, S.K. Backues, E.H. Baehrecke, B.A. Bahr, X.Y. Bai, Y. Bailly, R. Baiocchi, G. Baldini, W. Balduini, A. Ballabio, B.A. Bamber, E.T. Bampton, G. Banhegyi, C.R. Bartholomew, D.C. Bassham, R.C. Bast, Jr., H. Batoko, B.H. Bay, I. Beau, D.M. Bechet, T.J. Begley, C. Behl, C. Behrends, S. Bekri, B. Bellaire, L.J. Bendall, L. Benetti, L. Berliocchi, H. Bernardi, F. Bernassola, S. Besteiro, I. Bhatia-Kissova, X. Bi, M. Biard-Piechaczyk, J.S. Blum, L.H. Boise, P. Bonaldo, D.L. Boone, B.C. Bornhauser, K.R. Bortoluci, I. Bossis, F. Bost, J.P. Bourquin, P. Boya, M. Boyer-Guittaut, P.V. Bozhkov, N.R. Brady, C. Brancolini, A. Brech, J.E. Brenman, A. Brennan, E.H. Bresnick, P. Brest, D. Bridges, M.L. Bristol, P.S. Brookes, E.J. Brown, J.H. Brumell, et al., Guidelines for the use and interpretation of assays for monitoring autophagy. *Autophagy* 8 (2012) 445-544.
- [134] C. He, M.C. Bassik, V. Moresi, K. Sun, Y. Wei, Z. Zou, Z. An, J. Loh, J. Fisher, Q. Sun, S. Korsmeyer, M. Packer, H.I. May, J.A. Hill, H.W. Virgin, C. Gilpin, G. Xiao, R. Bassel-Duby, P.E. Scherer, and B. Levine, Exercise-induced BCL2-regulated autophagy is required for muscle glucose homeostasis. *Nature* 481 (2012) 511-5.
- [135] N. Mizushima, and B. Levine, Autophagy in mammalian development and differentiation. *Nat Cell Biol* 12 (2010) 823-30.
- [136] Focusing on autophagy. *Nat Cell Biol* 12 (2010) 813.
- [137] P. Codogno, and A.J. Meijer, Autophagy and signaling: their role in cell survival and cell death. *Cell Death Differ* 12 Suppl 2 (2005) 1509-18.
- [138] Q. Zheng, T. Huang, L. Zhang, Y. Zhou, H. Luo, H. Xu, and X. Wang, Dysregulation of Ubiquitin-Proteasome System in Neurodegenerative Diseases. *Front Aging Neurosci* 8 (2016) 303.
- [139] T.A. Thibaudeau, and D.M. Smith, A Practical Review of Proteasome Pharmacology. *Pharmacol Rev* 71 (2019) 170-197.
- [140] A. Brehm, and E. Kruger, Dysfunction in protein clearance by the proteasome: impact on autoinflammatory diseases. *Semin Immunopathol* 37 (2015) 323-33.
- [141] M.S. Brehme, A.; Voisine, C., Proteostasis network deregulation signatures as biomarkers for pharmacological disease intervention. *Current Opinion in Systems Biology* , 2019, pp. 74-81.
- [142] A. Hoischen, N. Krumm, and E.E. Eichler, Prioritization of neurodevelopmental disease genes by discovery of new mutations. *Nat Neurosci* 17 (2014) 764-72.
- [143] A. Kroll-Hermi, F. Ebstein, C. Stoetzel, V. Geoffroy, E. Schaefer, S. Scheidecker, S. Bar, M. Takamiya, K. Kawakami, B.A. Zieba, F. Studer, V. Pelletier, C. Eyermann, C. Speeg-Schatz, V. Laugel, D. Lipsker, F. Sandron, S. McGinn, A. Boland, J.F. Deleuze, L. Kuhn, J. Chicher, P. Hammann, S. Friant, C. Etard, E. Kruger, J. Muller, U. Strahle, and H. Dollfus, Proteasome subunit PSMC3 variants cause neurosensory syndrome combining deafness and cataract due to proteotoxic stress. *EMBO Mol Med* 12 (2020) e11861.
- [144] M. Ansar, F. Ebstein, H. Ozkoc, S.A. Paracha, J. Iwaszkiewicz, M. Gesemann, V. Zoete, E. Ranza, F.A. Santoni, M.T. Sarwar, J. Ahmed, E. Kruger, R. Bachmann-Gagescu, and S.E. Antonarakis, Biallelic variants in PSMB1 encoding the proteasome subunit beta6 cause impairment of proteasome function, microcephaly, intellectual disability, developmental delay and short stature. *Hum Mol Genet* 29 (2020) 1132-1143.
- [145] Y. Liu, Y. Ramot, A. Torrelo, A.S. Paller, N. Si, S. Babay, P.W. Kim, A. Sheikh, C.C. Lee, Y. Chen, A. Vera, X. Zhang, R. Goldbach-Mansky, and A. Zlotogorski, Mutations

- in proteasome subunit beta type 8 cause chronic atypical neutrophilic dermatosis with lipodystrophy and elevated temperature with evidence of genetic and phenotypic heterogeneity. *Arthritis Rheum* 64 (2012) 895-907.
- [146] R. Goldbach-Mansky, Immunology in clinic review series; focus on autoinflammatory diseases: update on monogenic autoinflammatory diseases: the role of interleukin (IL)-1 and an emerging role for cytokines beyond IL-1. *Clin Exp Immunol* 167 (2012) 391-404.
- [147] G.H. Calamandrei, F.; van den Hazel, P.; Koppe, J.; Nick, L.; Ray, D.; Steffens, W. Technical working group on priority diseases, subgroup neurodevelopmental disorders., Draft Baseline Report on neurodevelopmental disorders in the framework of the European Environment and Health Strategy, 2003.
- [148] I. Parenti, L.G. Rabaneda, H. Schoen, and G. Novarino, Neurodevelopmental Disorders: From Genetics to Functional Pathways. *Trends Neurosci* 43 (2020) 608-621.
- [149] C. Gilissen, J.Y. Hehir-Kwa, D.T. Thung, M. van de Vorst, B.W. van Bon, M.H. Willemsen, M. Kwint, I.M. Janssen, A. Hoischen, A. Schenck, R. Leach, R. Klein, R. Tearle, T. Bo, R. Pfundt, H.G. Yntema, B.B. de Vries, T. Kleefstra, H.G. Brunner, L.E. Vissers, and J.A. Veltman, Genome sequencing identifies major causes of severe intellectual disability. *Nature* 511 (2014) 344-7.
- [150] S.R. Schroeder, Mental retardation and developmental disabilities influenced by environmental neurotoxic insults. *Environ Health Perspect* 108 Suppl 3 (2000) 395-9.
- [151] A.A.o.I.a.D. Disabilities, FAQ on Intellectual Disability. , 2009.
- [152] D.K. Daily, H.H. Ardinger, and G.E. Holmes, Identification and evaluation of mental retardation. *Am Fam Physician* 61 (2000) 1059-67, 1070.
- [153] J. Flint, and A.O. Wilkie, The genetics of mental retardation. *Br Med Bull* 52 (1996) 453-64.
- [154] C. Murphy, C. Boyle, D. Schendel, P. Decoufle , and M. Yeargin-Allsopp, Epidemiology of mental retardation in children. *Mental Retardation and Developmental Disabilities Research Reviews* 4 (1998) 6-13.
- [155] F. Hormozdiari, O. Penn, E. Borenstein, and E.E. Eichler, The discovery of integrated gene networks for autism and related disorders. *Genome Res* 25 (2015) 142-54.
- [156] A.S. Cristino, S.M. Williams, Z. Hawi, J.Y. An, M.A. Bellgrove, C.E. Schwartz, F. Costa Lda, and C. Claudianos, Neurodevelopmental and neuropsychiatric disorders represent an interconnected molecular system. *Mol Psychiatry* 19 (2014) 294-301.
- [157] T. Santiago-Sim, L.C. Burrage, F. Ebstein, M.J. Tokita, M. Miller, W. Bi, A.A. Braxton, J.A. Rosenfeld, M. Shahrou, A. Lehmann, B. Cogne, S. Kury, T. Besnard, B. Isidor, S. Bezieau, I. Hazart, H. Nagakura, L.L. Immken, R.O. Littlejohn, E. Roeder, S.H.C. EuroEpinomics Res Consortium Autosomal Recessive working group, B. Kara, K. Hardies, S. Weckhuysen, P. May, J.R. Lemke, O. Elpeleg, B. Abu-Libdeh, K.N. James, J.L. Silhavy, M.Y. Issa, M.S. Zaki, J.G. Gleeson, J.R. Seavitt, M.E. Dickinson, M.C. Ljungberg, S. Wells, S.J. Johnson, L. Teboul, C.M. Eng, Y. Yang, P.M. Kloetzel, J.D. Heaney, and M.A. Walkiewicz, Biallelic Variants in OTUD6B Cause an Intellectual Disability Syndrome Associated with Seizures and Dysmorphic Features. *Am J Hum Genet* 100 (2017) 676-688.
- [158] M. Hirota, M. Kitagaki, H. Itagaki, and S. Aiba, Quantitative measurement of spliced XBP1 mRNA as an indicator of endoplasmic reticulum stress. *J Toxicol Sci* 31 (2006) 149-56.
- [159] A. van Schadewijk, E.F. van't Wout, J. Stolk, and P.S. Hiemstra, A quantitative method for detection of spliced X-box binding protein-1 (XBP1) mRNA as a measure of endoplasmic reticulum (ER) stress. *Cell Stress Chaperones* 17 (2012) 275-9.

- [160] J.R. MacDonald, R. Ziman, R.K. Yuen, L. Feuk, and S.W. Scherer, The Database of Genomic Variants: a curated collection of structural variation in the human genome. *Nucleic Acids Res* 42 (2014) D986-92.
- [161] K.L. Shanley, C.L. Hu, and O.A. Bizzozero, Proteasome Composition in Cytokine-Treated Neurons and Astrocytes is Determined Mainly by Subunit Displacement. *Neurochem Res* 45 (2020) 860-871.
- [162] A. Brehm, Y. Liu, A. Sheikh, B. Marrero, E. Omoyinmi, Q. Zhou, G. Montealegre, A. Biancotto, A. Reinhardt, A.A. de Jesus, M. Pelletier, W.L. Tsai, E.F. Remmers, L. Kardava, S. Hill, H. Kim, H.J. Lachmann, A. Megarbane, J.J. Chae, J. Brady, R.D. Castillo, D. Brown, A.V. Casano, L. Gao, D. Chapelle, Y. Huang, D. Stone, Y. Chen, F. Sotzny, C.C. Lee, D.L. Kastner, A. Torreló, A. Zlotogorski, S. Moir, M. Gadina, P. McCoy, R. Wesley, K.I. Rother, P.W. Hildebrand, P. Brogan, E. Kruger, I. Aksentijevich, and R. Goldbach-Mansky, Additive loss-of-function proteasome subunit mutations in CANDLER/PRAAS patients promote type I IFN production. *J Clin Invest* 126 (2016) 795.
- [163] B.M. Gardner, and P. Walter, Unfolded proteins are Ire1-activating ligands that directly induce the unfolded protein response. *Science* 333 (2011) 1891-4.
- [164] F.M. Tomlin, U.I.M. Gerling-Driessen, Y.C. Liu, R.A. Flynn, J.R. Vangala, C.S. Lentz, S. Clauder-Muenster, P. Jakob, W.F. Mueller, D. Ordonez-Rueda, M. Paulsen, N. Matsui, D. Foley, A. Rafalko, T. Suzuki, M. Bogyo, L.M. Steinmetz, S.K. Radhakrishnan, and C.R. Bertozzi, Inhibition of NGLY1 Inactivates the Transcription Factor Nrf1 and Potentiates Proteasome Inhibitor Cytotoxicity. *ACS Cent Sci* 3 (2017) 1143-1155.
- [165] A. Koch, J. Steffen, and E. Kruger, TCF11 at the crossroads of oxidative stress and the ubiquitin proteasome system. *Cell Cycle* 10 (2011) 1200-7.
- [166] A.O. Caglayan, S. Comu, J.F. Baranoski, Y. Parman, H. Kaymakcalan, G.T. Akgumus, C. Caglar, D. Dolen, E.Z. Erson-Omay, A.S. Harmanci, K. Mishra-Gorur, H.H. Freeze, K. Yasuno, K. Bilguvar, and M. Gunel, NGLY1 mutation causes neuromotor impairment, intellectual disability, and neuropathy. *Eur J Med Genet* 58 (2015) 39-43.
- [167] H. Ge, Q. Wu, H. Lu, Y. Huang, T. Zhou, D. Tan, and ZhongqinJin, Two novel compound heterozygous mutations in NGLY1 as a cause of congenital disorder of deglycosylation: a case presentation. *BMC Med Genet* 21 (2020) 135.
- [168] R.A. Saxton, and D.M. Sabatini, mTOR Signaling in Growth, Metabolism, and Disease. *Cell* 169 (2017) 361-371.
- [169] D.C. Goberdhan, C. Wilson, and A.L. Harris, Amino Acid Sensing by mTORC1: Intracellular Transporters Mark the Spot. *Cell Metab* 23 (2016) 580-9.
- [170] J. Zhao, and A.L. Goldberg, Coordinate regulation of autophagy and the ubiquitin proteasome system by MTOR. *Autophagy* 12 (2016) 1967-1970.
- [171] C.T. Chu, Mechanisms of selective autophagy and mitophagy: Implications for neurodegenerative diseases. *Neurobiol Dis* 122 (2019) 23-34.
- [172] W.X. Ding, and X.M. Yin, Mitophagy: mechanisms, pathophysiological roles, and analysis. *Biol Chem* 393 (2012) 547-64.
- [173] G. Bellot, R. Garcia-Medina, P. Gounon, J. Chiche, D. Roux, J. Pouyssegur, and N.M. Mazure, Hypoxia-induced autophagy is mediated through hypoxia-inducible factor induction of BNIP3 and BNIP3L via their BH3 domains. *Mol Cell Biol* 29 (2009) 2570-81.
- [174] J.A. McBride, and R. Striker, Imbalance in the game of T cells: What can the CD4/CD8 T-cell ratio tell us about HIV and health? *PLoS Pathog* 13 (2017) e1006624.
- [175] D.M. Panneman, S.B. Wortmann, C.A. Haaxma, P.M. van Hasselt, N.I. Wolf, Y. Hendriks, B. Kusters, S. van Emst-de Vries, E. van de Westerloo, W.J.H. Koopman, L.



- Wintjes, F. van den Brandt, M. de Vries, D.J. Lefeber, J.A.M. Smeitink, and R.J. Rodenburg, Variants in NGLY1 lead to intellectual disability, myoclonus epilepsy, sensorimotor axonal polyneuropathy and mitochondrial dysfunction. *Clin Genet* 97 (2020) 556-566.
- [176] T. Takahara, Y. Amemiya, R. Sugiyama, M. Maki, and H. Shibata, Amino acid-dependent control of mTORC1 signaling: a variety of regulatory modes. *J Biomed Sci* 27 (2020) 87.
- [177] L. Bar-Peled, and D.M. Sabatini, Regulation of mTORC1 by amino acids. *Trends Cell Biol* 24 (2014) 400-6.
- [178] G. Chen, G. Kroemer, and O. Kepp, Mitophagy: An Emerging Role in Aging and Age-Associated Diseases. *Front Cell Dev Biol* 8 (2020) 200.
- [179] P. Jaakkola, D.R. Mole, Y.M. Tian, M.I. Wilson, J. Gielbert, S.J. Gaskell, A. von Kriegsheim, H.F. Hebestreit, M. Mukherji, C.J. Schofield, P.H. Maxwell, C.W. Pugh, and P.J. Ratcliffe, Targeting of HIF-alpha to the von Hippel-Lindau ubiquitylation complex by O2-regulated prolyl hydroxylation. *Science* 292 (2001) 468-72.
- [180] G. Monzio Compagnoni, A. Di Fonzo, S. Corti, G.P. Comi, N. Bresolin, and E. Masliah, The Role of Mitochondria in Neurodegenerative Diseases: the Lesson from Alzheimer's Disease and Parkinson's Disease. *Mol Neurobiol* 57 (2020) 2959-2980.
- [181] Y. Wang, N. Liu, and B. Lu, Mechanisms and roles of mitophagy in neurodegenerative diseases. *CNS Neurosci Ther* 25 (2019) 859-875.
- [182] E.F. Isidor B., Hurst A., et al., Stankiewicz-Isidor syndrome: expanding the clinical and molecular phenotype. *Genetics in Medicine*, Elsevier Inc. (2021).
- [183] P. Jadiya, D.W. Kolmetzky, D. Tomar, A. Di Meco, A.A. Lombardi, J.P. Lambert, T.S. Luongo, M.H. Ludtmann, D. Pratico, and J.W. Elrod, Impaired mitochondrial calcium efflux contributes to disease progression in models of Alzheimer's disease. *Nat Commun* 10 (2019) 3885.
- [184] C. Sharma, S. Kim, Y. Nam, U.J. Jung, and S.R. Kim, Mitochondrial Dysfunction as a Driver of Cognitive Impairment in Alzheimer's Disease. *Int J Mol Sci* 22 (2021).
- [185] W. Wang, F. Zhao, X. Ma, G. Perry, and X. Zhu, Mitochondria dysfunction in the pathogenesis of Alzheimer's disease: recent advances. *Mol Neurodegener* 15 (2020) 30.
- [186] L. King, and H. Plun-Favreau, *Mitophagy*, 2017, pp. 139-177.
- [187] M. Hashimoto, E. Rockenstein, L. Crews, and E. Masliah, Role of protein aggregation in mitochondrial dysfunction and neurodegeneration in Alzheimer's and Parkinson's diseases. *Neuromolecular Med* 4 (2003) 21-36.
- [188] V. Nicoletti, G. Palermo, E. Del Prete, M. Mancuso, and R. Ceravolo, Understanding the Multiple Role of Mitochondria in Parkinson's Disease and Related Disorders: Lesson From Genetics and Protein-Interaction Network. *Front Cell Dev Biol* 9 (2021) 636506.
- [189] V. Schaeffer, I. Lavenir, S. Ozcelik, M. Tolnay, D.T. Winkler, and M. Goedert, Stimulation of autophagy reduces neurodegeneration in a mouse model of human tauopathy. *Brain* 135 (2012) 2169-77.
- [190] A.A. de Jesus, A. Brehm, R. VanTries, P. Pillet, A.S. Parentelli, G.A. Montealegre Sanchez, Z. Deng, I.K. Paut, R. Goldbach-Mansky, and E. Kruger, Novel proteasome assembly chaperone mutations in PSMG2/PAC2 cause the autoinflammatory interferonopathy CANDLE/PRAAS4. *J Allergy Clin Immunol* 143 (2019) 1939-1943 e8.
- [191] A. Torreló, S. Patel, I. Colmenero, D. Gurbindo, F. Lendinez, A. Hernandez, J.C. Lopez-Robledillo, A. Dadban, L. Requena, and A.S. Paller, Chronic atypical neutrophilic dermatosis with lipodystrophy and elevated temperature (CANDLE) syndrome. *J Am Acad Dermatol* 62 (2010) 489-95.

- [192] A. Garg, M.D. Hernandez, A.B. Sousa, L. Subramanyam, L. Martinez de Villarreal, H.G. dos Santos, and O. Barboza, An autosomal recessive syndrome of joint contractures, muscular atrophy, microcytic anemia, and panniculitis-associated lipodystrophy. *J Clin Endocrinol Metab* 95 (2010) E58-63.
- [193] D.M. d'Angelo, P. Di Filippo, L. Breda, and F. Chiarelli, Type I Interferonopathies in Children: An Overview. *Front Pediatr* 9 (2021) 631329.
- [194] A. McDonough, R.V. Lee, and J.R. Weinstein, Microglial Interferon Signaling and White Matter. *Neurochem Res* 42 (2017) 2625-2638.
- [195] S.R. Anderson, and M.L. Vetter, Developmental roles of microglia: A window into mechanisms of disease. *Dev Dyn* 248 (2019) 98-117.
- [196] M.P. Rodero, and Y.J. Crow, Type I interferon-mediated monogenic autoinflammation: The type I interferonopathies, a conceptual overview. *J Exp Med* 213 (2016) 2527-2538.
- [197] S. Volpi, P. Picco, R. Caorsi, F. Candotti, and M. Gattorno, Type I interferonopathies in pediatric rheumatology. *Pediatr Rheumatol Online J* 14 (2016) 35.
- [198] S. Pestka, C.D. Krause, and M.R. Walter, Interferons, interferon-like cytokines, and their receptors. *Immunol Rev* 202 (2004) 8-32.
- [199] A.J. Lee, and A.A. Ashkar, The Dual Nature of Type I and Type II Interferons. *Front Immunol* 9 (2018) 2061.

## **Affidavit**

I hereby declare that I have written this dissertation independently and have not used any auxiliary materials other than those indicated.

The dissertation has not yet been submitted to any other faculty or scientific institution.

I declare that I have not yet unsuccessfully completed a doctoral examination and that I have not been deprived of a doctoral degree which I have already obtained.

01.12.2021    Anna Marta Hajdukowicz



Yearning for knowledge and self-development, willingly undertaking challenges and sustainably working to achieve my dreams. Professionally a young Medical Doctor, privately a curious, creative and open-minded Renaissance woman, with multiple interests in both scientific and non-scientific fields. Communicative, ambitious, reliable, and initiative-taking. Gladly participating in international exchanges, local and global events and conferences.

## LANGUAGE SKILLS

Polish	mother tongue
English	C2
German	C2
Italian	B2
Spanish	B1
Latin	A2

## Curriculum Vitae

# Anna Marta Hajdukowicz, MD

## EDUCATION

### University of Greifswald, Germany

10.2018 – 08.2022

Doctoral Studies in the field of Medicine at the Institute of Molecular Biology and Medical Biochemistry; laboratory work and scientific research on *Functional characterisation of de novo mutations in the PSMC5 gene carried by patients with the syndromic form of intellectual disability*

### Pomeranian Medical University in Szczecin, Poland

10.2013 – 07.2019

Medicine, finished among the best graduates

### University of Greifswald, Germany

09.2016 – 06.2019

Medicine, double Erasmus+ scholar

### University of Szczecin, Poland

10.2015 – 06.2016

Scandinavian studies

### XIII Grammar School in Szczecin, Poland

09.2010 – 06.2013

Olympic class of the best secondary school in Poland, finished among the best graduates, Finalist of the Polish Language and Literature Olympiad, scholar of Individual Study Programmes

## WORKING EXPERIENCE IN THE FIELD OF MEDICINE

### General Practice and Night Medical Assistance as well as COVID-19 vaccination centres in Myślibórz and in Szczecin, Poland

03.2021 – 08.2022

### Voivodship Hospital in Szczecin, Poland – Medical Doctor Foundation Programme

10.2019 – 10.2020

Clinical rotations among diverse clinical departments, successfully completed and awarded **full medical license** on the 21<sup>st</sup> Oct. 2020

### Polish Ministry of Health – internship

09.2019

Insight to health management on a national and global scale

### Department of Biochemistry and Molecular Biology in Suzhou, China – research scholarship

07.2018

Insight to laboratory work and scientific research, additionally short internships in clinical departments such as ER and TCM

### Clinical Hospital in Split, Croatia – clinical internship in the Paediatrics and Paediatric Surgery Departments

08.2016

Observation, MD work, assisting to surgeries

### Clinical internships in the in- and out-patient care and ER in Szczecin, Poland 2014, 2015, 2016, 2018

## INTERPERSONAL SKILLS

- communicativeness
- active listening and curiosity
- ability to work in multicultural environments
- public speaking
- leadership
- reliability
- creativity

## ORGANIZATIONAL SKILLS

- ability to organize the workload to meet deadlines
- initiative-taking
- problem-solving

## DIGITAL SKILLS

- Microsoft Word, Excel, PowerPoint
- Adobe Creative Cloud
- Canva
- Social Media

## HOBBIES & INTERESTS

- travel and culture
- art, dance, music and sport
- languages
- psychology

## CONTACT DETAILS

| Anna Hajdukowicz  
✉ [aniah6@poczta.onet.pl](mailto:aniah6@poczta.onet.pl)

## NON-MEDICAL WORKING EXPERIENCE

### European Solidarity Corps volunteering projects

10.2020 – 12.2020, 06.2021 – 07.2021

Voluntary work in the fields of education, health and well-being, sports, culture and arts, media, promotion and active citizenship

### Translation, interpretation, language tutorials

(Polish/English/German), international groups coordinator

2012 – 2022

## EXTRACURRICULAR ACTIVITIES

### EU Youth Exchanges and Training Courses

09.2020 – in due

Non-formal education, developing hard- and soft-skills

### IFMSA – International Federation of Medical Students' Associations

09.2013 – 06.2019

Voluntary work in the fields of medical education, human rights and peace, public health, sexual and reproductive health, professional exchange, research exchange

### Participation in multiple national and international scientific conferences and projects

09.2013 – 06.2019

### Polish Cup in Surgical Sewing 2018 & 2019

**Involvement and leadership in numerous student research groups,** such as Paediatric Scientific Club, *Study on calcium- phosphate metabolism disorders among children with type 1 diabetes*, Dept. of Paediatrics, Szczecin, Poland, 2014-2016; Chairwoman of the Neurosurgical Scientific Club, Dept. of Neurosurgery and Paediatric Neurosurgery, Szczecin, Poland, 2015-2016

## LANGUAGE CERTIFICATES

### Certificate of Proficiency in English (CEFR C2 level)

06.2012

### Deutsches Sprachdiplom II (CEFR C1 level)

12.2012

## PUBLICATIONS AND CONFERENCES

*Protéasomopathies neurodéveloppementales causées par des altérations des gènes de sous-unités de la particule régulatrice 19S* – National French Meeting of Human Genetics, Tours, France, 2020

*Neurodevelopmental Proteasomopathies Caused by Alterations of Genes Encoding Subunits of the 19S Regulatory Particle* – Annual Meeting of the American Society of Human Genetics, Houston, USA, 2019

Informative brochure on type 1 diabetes implemented as part of the National Program for Prevention and Diabetes Education, in cooperation with the Ministry of Health, the University Clinical Centre and the Paediatric Section of the Polish Diabetes Association, Poland, 2012

## Acknowledgments

I would like to thank all the people who I have had on my side throughout the past four years of my work, and whose presence and support contributed in different ways to its finalisation.

First of all, I would like to thank the Director of the Institute of Medical Biochemistry and Molecular Biology of the University of Greifswald, Prof. Elke Krüger, PhD, for the trust expressed by allowing me to conduct my doctoral training in the extraordinary circumstances, as an exchange student, and flexibility that connecting the clinical rotations with laboratory work required, as well as for providing me with an interesting scientific topic for my thesis, enabling to do the experimental work in her laboratories and showing understanding for time that my remote writing due to the simultaneous exams, post-diploma foundation programme and numerous projects abroad required.

Secondly, I would like to express gratitude to my supervisor, PD Frédéric Ebstein, PhD, for outstanding guidance and meticulous introduction to the secrets of laboratory work, for showing me a proper way of conducting diverse experiments and their explanations, for patience in answering my endless questions, for assistance in writing the thesis and bringing it to its final form, as well as for all thought-provoking and stimulating conversations that we had, would it be in person during my time in the laboratory or remotely later on. The sharpness of your mind, hard-working attitude and high vulnerability lead you to have insights and understanding that go far beyond what the eyes can see, and make you a true authority in my eyes.

Moreover, I would like to thank my colleague, Barbara Zięba, PhD, for the laboratory guidance and introducing me to the subtleties of the PCR method, as well as for all the helpful advice and support; Maja Studencka-Turski, PhD, for all helpful suggestions both during the laboratory work and while writing the thesis, together with answering both basic and more complex questions coming to my mind, as well as for support and entertainment; and Daniel Mrochen, PhD, for agreeing to host me in the Department of Immunology and help in assessing the flow cytometric data and their analysis. I also want to thank Gonca Çetin, for all helpful suggestions, and Robert Beyer, for technical advice while conducting my experiments. Furthermore, I would like to thank the whole research group, for making the time spent in the laboratory not only a significant step and occasion for my professional and scientific, but also personal development.

In addition, I would like to thank all our collaborators: our partners from Boston Children's Hospital, Harvard, USA and the UPMC Children's Hospital of Pittsburgh, for the assessment of the cryopreserved peripheral blood mononuclear cells (PBMCs); our geneticist collaborators from the Dept. of Genetics of the University of Nantes, France, for the comparative examination of the entire exome in various patients diagnosed with syndromic ID using next-generation sequencing (NGS); Siddharth Srivastava from Boston Children's Hospital, Harvard, USA, for performing the clinical anamnesis and examination of Subject 1, and Damara Ortiz from the UPMC Children's Hospital of Pittsburgh, USA, of Subject 2.

Finally, I wish to thank all my friends that supported me in diverse phases of my work. To my Greifswald mates – Mirinka, Helena, Daniel, Philipp, Robert, Shehla, for encouragement and comfort during my stay in Germany. To my old dear friends – Natalia H.-B., Karina, Kamila, Asia, Grzesiek, Oliwia, Ola, who believed in me even, or especially, in the times when I doubted myself. To later, but no less important acquaintances, whose friendship I deeply value, Agata – for the emotional support and deep understanding of the hurdles of the doctoral training, Ewa – for the loyal companionship and caring on the daily-basis, Kasia K. – for your endless amounts of good energy and believing in me. To Pooya – esp. for your words ‘Anna, with your personality and inner strength your wings when clipped will only grow stronger’, and to Paweł, Piotr, Natalia M., Natalia K., Liz, Caro – for all encouragement and support. To Mr. Skowroński, whose secondary school words ‘I believe in you’ resonated in me for years and whose precious ways of stimulating creativity and critical thinking brought me further in life. To Gastón, for questions that stayed in my mind for long. To Andrea – for probably the most motivating letter I have ever received and numerous inspiring dialogues throughout the years. To Federico, for the support during the pandemic time. To my volunteering team in Romania, especially Barbara, for being a loyal companion in my internal development, and for huge emotional support overtime. To all my mentors in my IFMSA traineeships in Split, Croatia, in Suzhou, China, and in all further EU volunteering projects, youth exchanges and training courses in Romania, Italy, Greece, the Netherlands and Poland, for the contribution to the raise of my knowledge, skills and self-awareness. To my singing and dance instructors, for the impact on freeing my voice and increase of public-speaking skills. To Elwira, for accompanying me independent on time and place I was physically and mentally in, and for all the support received, as well as to Magda, for the motivating coaching sessions. To aunt Gosia, for the support throughout my life. Last but not least, to my parents, grandma, aunt Mirka and Renia, for raising me up with open development possibilities and contributing in this way to who I have become.